

FOR REFERENCE

NOT TO BE TAKEN FROM THIS ROOM

CALCULATION OF
STRESS INTENSITY FACTOR
IN AN ORTHOTROPIC STRIP AND PLATE
USING
STRESS FIELDS OF EDGE DISLOCATIONS

by

Timuçin Gürer

B.S. in M.E., Boğaziçi University, 1980

Bogazici University Library



14

39001100315962

Submitted to the Institute for Graduate Studies in
Science and Engineering in partial fulfillment of
the requirements for the degree of
Master of Science
in
Mechanical Engineering

Boğaziçi University

1983

CALCULATION OF
STRESS INTENSITY FACTOR
IN AN ORTHOTROPIC STRIP AND A PLATE
USING
STRESS FIELDS OF EDGE DISLOCATIONS

APPROVED BY

Doç.Dr.Sabri Altıntaş
(Co-Supervisor)

S. Altıntaş...

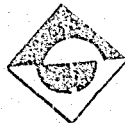
Doç.Dr.M.Başar Civelek
(Co-Supervisor)

M. Başar Civelek...

Doç.Dr.Öktem Vardar

Öktem Vardar.....

DATE OF APPROVAL



ACKNOWLEDGEMENTS

The author wishes to express his gratitude to Doç. Dr.M.Başar Civelek and Doç.Dr.Sabri Altıntaş for their valuable guiding help during the course of this study.

Thanks are also due to Doç.Dr.Öktem Vardar for his valuable comments and suggestions.

Special thanks are due to Müge Gürer, Semih Sökmen and Sencan Derebeyoğlu for their interest, help with the technical details of the study and patience.

The author is also indebted to the technical staff of the computer center.

ABSTRACT

In this study the general elastostatic problem for an orthotropic strip containing cracks perpendicular to its boundaries is considered.

Appropriate superposition of stress field solutions of edge dislocations together with the Fourier integral transform technique made it possible to solve the field equations in terms of new material parameters for an elastic homogenous, orthotropic strip.

Two specific problems of interest are then studied in detail. First problem involves the investigation of a single transverse crack in an orthotropic strip subjected to uniform tension or uniform shear, the latter being unavailable in literature. The second problem of interest is a rectangular orthotropic plate containing an edge crack and subjected to uniform tension by the help of which it is possible to simulate the Standard Compact Tension Specimen for an orthotropic material; which is not available in literature either.

The singular integral equations of these problems are derived then they are solved numerically and the stress intensity factors are obtained. Numerical results are presented for isotropic and orthotropic materials with various crack geometries.

ÖZET

Bu çalışmada, içinde kenarlara dik çatlaklar bulunan ortotropik bir şeritin elastostatik problemi incelenmiştir.

Kenar dislokasyon çözümlerinin uygun bir şekilde süperpozisyonu ve Fourier integral dönüşüm tekniği kullanılarak, elastik ve homojen bir şerit için alan denklemleri bulunmuştur.

İki özel durum ayrıntılı olarak incelenmiştir. Birincisi üniform çekme veya kayma kuvvetlerinin etkisi altında kalan enine bir çatlak dğeriyse dikdörtgen bir levhada yer alan ve yüzeylerine üniform çekme kuvveti uygulanan bir kenar çatlağıdır. Ayrıca, ikinci problemin yardımıyla, deneysel araştırmalarda kullanılan standart numunelerin benzetlenmesine çalışılmıştır.

Bu problemlerin tekil integral denklemleri çıkarılmış, bilgisayar programları hazırlanmış ve gerilme şiddeti faktörleri sayısal olarak bulunmuştur. Çeşitli çatlak geometrileri için izotropik ve ortotropik malzemelerde bu faktörün alacağı sayısal değerler bulunmuş ve değişim incelenmiştir.

TABLE OF CONTENTS

	Page
ACKNOWLEDGEMENTS	iii
ABSTRACT	iv
OZET.....	v
LIST OF FIGURES	viii
LIST OF TABLES	x
LIST OF SYMBOLS	xi
I. INTRODUCTION	1
II. PLANE PROBLEMS OF AN ANISOTROPIC ELASTIC BODY.	
A. The Equilibrium Equations.....	5
B. Strain Displacement Relations.....	5
C. Stress Strain Relations	6
D. Field Equation for an Orthotropic Body.....	9
E. New Material Parameters	11
III. STRESS FIELDS OF EDGE DISLOCATIONS IN AN ORTHOTROPIC BODY	14
A. A Pair of Edge Dislocations in an Infinite Orthotropic Plane	15
B. A Pair of Edge Dislocations in an Orthotropic Strip	18
IV. REPRESENTATION OF CRACKS IN TERMS OF DISLOCATIONS	26
V. FORMULATION OF THE PROBLEMS	31
A. Crack in an Orthotropic Strip Subjected to Uniform Tension	31
B. Crack in an Orthotropic Strip Subjected to Uniform Shear.....	34
C. Orthotropic Rectangular Plate with an Edge Crack	36
VI. NUMERICAL SOLUTION OF INTEGRAL EQUATIONS	43
VII. RESULTS AND DISCUSSION	49
VIII. CONCLUSIONS	79
APPENDIX A	82
APPENDIX B	83
APPENDIX C	85
APPENDIX D	87

	Page
APPENDIX E	89
APPENDIX F	90
APPENDIX G	92
APPENDIX H	93
APPENDIX I	94
APPENDIX J	96
APPENDIX K	98
REFERENCES	114

LIST OF FIGURES

	Page
FIGURE 1. A pair of edge dislocations at the position $(t,0)$ with Burgers vector \vec{b}_x and \vec{b}_y in an infinite orthotropic plane.	14
FIGURE 2. (a) A crack along the x-axis extending from b to c. (b) A pair of edge dislocations at position $(t,0)$.	16
FIGURE 3. A pair of edge dislocations in an orthotropic strip $0 < x < H$ parallel to y-axis.	18
FIGURE 4. An edge dislocation at the position $(t,0)$ with Burgers vector \vec{b}_x in an orthotropic strip.	22
FIGURE 5. An edge dislocation at the position $(t,0)$ with Burgers vector \vec{b}_y in an orthotropic strip.	25
FIGURE 6. Griffith type crack in a homogenous orthotropic strip.	26
FIGURE 7. Basic modes of crack extension.	27
FIGURE 8. Representation of a normally loaded crack in terms of edge dislocations with Burgers vector \vec{b}_y .	28
FIGURE 9. Representation of an inplane shear crack in terms of edge dislocations with Burgers vector \vec{b}_x .	29
FIGURE 10. Coordinate system of crack front stress components.	30
FIGURE 11. Schematic representation of the superposition problem which yields the strip solution.	32
FIGURE 12. The basic crack geometry for an infinite orthotropic strip containing three line cracks.	36
FIGURE 13. Schematic representation of the superimposed stress state.	38
FIGURE 14. Stress intensity factors for an internal and edge crack in an orthotropic strip.	47
FIGURE 15. Loading conditions considered in the analysis.	50
FIGURE 16. Stress intensity factor (SIF) versus crack length (c/H) for an internal crack $(b/H=0.2)$ in an orthotropic strip of material I, subjected to uniform shear.	61
FIGURE 17. SIF versus c/H for an internal crack $(b/H=0.2)$ in an orthotropic strip of material I, uniform shear.	62
FIGURE 18. Comparison of the SIF values for symmetric internal cracks subjected to uniform tension for three different materials (Ortho.I, Ortho.II, Isotropic).	64

- FIGURE 19. Comparison of the SIF values for symmetric internal cracks subjected to uniform shear for two different materials(Ortho.I,Isotropic). 65
- FIGURE 20. SIF versus crack length c/H for an edge crack in an isotropic strip of material III subjected to uniform tension and uniform shear. 68
- FIGURE 21. SIF versus crack length c/H for an edge crack in an orthotropic strip of material I subjected to uniform tension and uniform shear. 69
- FIGURE 22. Comparison of the SIF values with respect to the shear parameter K for an edge crack in a strip of different materials. 71
- FIGURE 23. SIF versus crack length c/H in a uniformly stressed orthotropic plate of material I containing an edge crack for a fixed half length to width ratio of 0.5 73
- FIGURE 24. SIF versus half length to width ratio(B/H) for an orthotropic plate of material I containing an edge crack of length $0.1H$ 74
- FIGURE 25. Comparison of the experimental data points and the finite element solution of Mandell et.al.⁽³²⁾ with the present study for the SIF values in a Double Cantilever Beam Specimen subjected to a concentrated force P . 76
- FIGURE 26. Notation for the standard compact tension specimen (CTS). 55

LIST OF TABLES

	Page
TABLE 1. The material elastic constants.	56
TABLE 2. The stress intensity factors in an orthotropic strip of material I subjected to uniform tension and uniform shear(SIF versus c/H) :	
a) $b/H=0.1$	57
b) $b/H=0.2$	58
c) $b/H=0.3$	59
d) $b/H=0.4$	60
TABLE 3. Comparison of the SIF values for a symmetric internal crack subjected to uniform tension or uniform shear for three different materials.	63
TABLE 4. SIF versus c/H for an edge crack in an isotropic strip of material III subjected to uniform tension and uniform shear.	66
TABLE 5. SIF versus c/H for an edge crack in an orthotropic strip of material I subjected to uniform tension and uniform shear.	67
TABLE 6. Comparison of the SIF values for an edge crack in a strip of different materials subjected to uniform tension and uniform shear(SIF versus K).	70
TABLE 7. SIF values in a uniformly stressed orthotropic plate of material I containing an edge crack($B/H=0.5$).	72
TABLE 8. The effect of half length-to-width ratio, B/H , on the SIF values for an orthotropic plate of material I containing an edge crack ($c/H=0.1$).	72
TABLE 9. SIF values for an orthotropic Double Centilever Beam specimen subjected to a concentrated force P .	75
TABLE 10. Comparison of the SIF values in an isotropic compact tension specimen(CTS) with that found by Civelek and Erdoğan ⁽²⁵⁾ for two crack lengths.	77
TABLE 11. SIF versus c/H for the orthotropic compact tension specimen of material I.	77

LIST OF SYMBOLS

\vec{b}_x	Burgers vector of an edge dislocation parallel to x-axis.
\vec{b}_y	Burgers vector of an edge dislocation parallel to y-axis.
B	Half length of a rectangular plate in y-direction.
b, c	End points of a single transverse crack in a strip or of the inner crack in a rectangular plate.
d, e	End points of the outer cracks in a rectangular plate.
$c_{ij} \quad i, j=1, \dots, 6$	Material elastic constants.
E	Effective stiffness.
E_{11}, E_{22}, E_{33}	Young's Moduli along principal directions.
$f(x), g(x), h(x)$	Dislocation density functions.
$G_{ij} \quad i, j=1, \dots, 6$	Shear Moduli
H	Strip or plate width.
K	Shear Parameter.
$k_1(x), k_2(x), k_3(x)$	Stress intensity factors corresponding to opening, sliding and tearing modes of fracture.
$k(x, t), \bar{k}(x, t)$	Kernels of the singular integral equations for a crack in an orthotropic strip subjected to uniform tension and uniform shear.
$k_{ij}(x, t) \quad i, j=1, 2, 3$	Kernels of the singular integral equations for a system of cracks in an orthotropic rectangular plate subjected to uniform tension.
l	Half crack length.
$p_1(x), p_2(x), p_3(x)$	Crack surface tractions.
t	Horizontal distance of the edge dislocation.

$U(x,y)$	Airy Stress function.
u_1, u_2, u_3	Displacement components in cartesian coordinates.
u, v, w	Transformed displacements.
w_1, w_2	Roots of the characteristic equation.
x_1, x_2, x_3	Cartesian coordinate system.
x, y, z	Transformed coordinates.
δ	Stiffness ratio.
$\epsilon_{ij} \quad i=j=1,2,3$	Strain components
$\gamma_{ij} \quad i \neq j=1,2,3$	
$\mu_{ij} \quad i, j=1,2,3$	Poisson ratios.
μ	Effective stiffness ratio.
$\Phi(x,y)$	Fourier Transform of the Airy Stress function U.
$\sigma_{ij} \quad i, j=1, \dots, 6$	Stress components in cartesian coordinates.
$\sigma_{ij} \quad i, j=x, y, z$	Transformed stress components.
$\sigma_{ij}^d \quad i, j=x, y, z$	Stress components due to a pair of edge dislocations in an infinite orthotropic plane.
$\sigma_{ij}^1 \quad i, j=x, y, z$	Stress components due to an edge dislocation with Burgers vector \vec{b}_x (Strip).
$\sigma_{ij}^2 \quad i, j=x, y, z$	Stress components due to an edge dislocation with Burgers vector \vec{b}_y (Strip).
$\sigma(x)$	Uniform tension applied at crack faces.
$\tau(x)$	Uniform shear applied at crack faces.

I. INTRODUCTION

Depending on the mechanical behavior of the material, nature of the loading and environmental conditions, fracture is considered as an important problem for safe and economical design of structures although it may not always mean total failure.

Failure analysis, using the principles of fracture mechanics deals with initial flaws or certain types of imperfections which exist in the material. Such defects are treated as "cracks" which act as fracture nuclei that may propagate under fluctuating or stationary external loads. Thus, it is obvious that the existence of defects which may lead to fracture initiation and propagation is unavoidable and therefore one must take them into consideration during the design process and select the appropriate material and dimensions.

There are two main problems in studying the fracture of structures: The development of an appropriate failure criterion and a mathematical model for the calculation of a load factor which reflects the geometrical and physical properties of the medium.

It is the failure criterion which determines the physical quantities that one should compute (such as the stress intensity factor, the strain energy release rate, crack opening displacement, etc.)

There are many failure criteria or failure theories which are used to predict the failure of structures. In Linear Elastic Fracture Mechanics where only small scale yielding is allowed, $K \leq K_{IC}$ is the accepted criterion⁽¹⁾. In this case failure occurs when the calculated value of the stress intensity factor, K , reaches a critical value, K_{IC} , which can be determined experimentally as a material property. There are also other failure criteria such as critical plastic stress intensity factor K_{pc} or the J-Integral which have been proposed to predict failure from elastic to fully plastic range.

All the structures require the most economical utilization of materials in terms of stiffness-to-weight, strength-to-weight and cost-to-weight ratios. These requirements are the basic motivations for the development of composite materials which have introduced new and useful combinations of mechanical properties.

The advantage of composites is that during the process of manufacturing they can be directionally strengthened so that their structural resistance to unstable crack propagation is very high.

Most common engineering materials are homogenous and isotropic. In contrast, composite materials are in general non-homogenous and anisotropic. Properties are functions of both position and orientation at a point in the body. Since the non-homogeneity and anisotropy make it difficult to apply linear elastic fracture mechanics to composite materials, they are usually treated as being homogenous and orthotropic.

In linear elastic fracture mechanics, problems related to cracks in a strip or half plane have been widely studied. In some of these studies the medium is assumed to be isotropic⁽²⁻¹⁵⁾. Because of the fact that some of the most important structural applications of composites have been in sheet form and also for analytical reasons, the crack problems in orthotropic materials have been studied mostly for plane stress or plane strain conditions. Depending on the values of elastic constants, orthotropic materials are classified in two groups⁽¹⁶⁻¹⁸⁾: Materials of type I and of type II. (See Appendix I). A different formulation is needed for each combination.

In plane problems of orthotropic materials, if the medium is infinite, containing a line crack or a series of collinear cracks, it has been shown that⁽¹⁹⁻²²⁾ orthotropy does not affect the stress intensity factor and the results are identical to the isotropic case with the same crack geometry. However, if the medium is bounded, stress intensity factor is highly dependent on the material orthotropy and it is greater or smaller than the corresponding isotropic values.

To study this dependence one may refer to a number of previous studies. For example Delale and Erdoğan investigated the problem of periodically arranged orthotropic strip containing cracks⁽¹⁶⁾ and an orthotropic strip containing an internal or edge crack⁽¹⁷⁾ for material types I and II. Lately the problem of an inclined crack in an orthotropic strip is solved by Delale et.al.⁽²³⁾ where the stress state in an infinite plane is taken as one of the two constituents of the superposition problem.

In the case of plane isotropic elasticity, the study of stress problems is greatly facilitated by the fact that only one of the material properties, namely the Poisson ratio ν , can influence the stress field^(15,24). However, when studying the fracture problem of anisotropic materials the situation is very different and solutions of practical interest involve complicated combinations of material properties. Therefore it is desirable to describe anisotropic materials in terms of new parameters which simplifies the solution procedure. Instead of a direct use of four independent elastic constants introducing the new material properties and a variable transformation proposed by Krenk⁽²⁴⁾ not only simplifies the solution procedure but also enables a straightforward transition from orthotropic to isotropic problems depending upon a single parameter, namely the shear parameter K . On the other hand the solution procedure is further simplified when a crack is represented by a continuous distribution of dislocations. This way, once the infinite plane solution due to a pair of edge dislocations are obtained, one may get the strip solution in a straightforward manner imposing the boundary conditions at strip edges. Civelek and Erdoğan⁽²⁵⁾ solved various crack problems in an infinite strip and rectangular plate using the stress field solutions of a pair of edge dislocations where the material is assumed to be isotropic. Stress intensity factors are obtained for strip, plate and compact tension specimen geometries subjected to various loading conditions.

In the present study a similar procedure will be used to formulate the strip and plate problems of interest in an orthotropic medium. For this purpose, first the stress field of an infinite orthotropic plane due to a pair of edge dislocations will be obtained from the existing crack solution⁽²³⁾ in terms of the new material properties⁽²⁴⁾. Using this solution together with the boundary conditions of the residual loading problem, the stress state due to each separate kind of dislocation in an orthotropic strip will be derived by the help of the standard Fourier Transform Technique. To simulate a line crack along an axis, stress solutions due to edge dislocations will be converted to the corresponding crack solutions replacing the Burger's vectors by dislocation densities and integrating these density functions along the crack. Finally the problem of an edge crack in an orthotropic plate will be formulated superimposing the stress distributions due to three line cracks in a strip, keeping the middle one and letting the outer ones meet the edges. Then one may simulate the orthotropic compact tension specimen which is of practical interest in many applications.

Singular integral equations for a single crack in a strip and a system of integral equations for the plate problem will be obtained using the crack surface boundary conditions. The resulting integral equations are solved numerically using the Gauss-Chebyshev integration formulas (15,26) and the stress intensity factors are calculated for various crack geometries and materials.

II. PLANE PROBLEMS OF AN ANISOTROPIC ELASTIC BODY

A. The Equilibrium Equations

In the absence of body forces, the stress components in a continuous body which is in equilibrium must satisfy the equilibrium equations, which in Cartesian coordinates (x_1, x_2, x_3) are:

$$\frac{\partial \sigma_{11}}{\partial x_1} + \frac{\partial \sigma_{12}}{\partial x_2} + \frac{\partial \sigma_{13}}{\partial x_3} = 0$$

$$\frac{\partial \sigma_{12}}{\partial x_1} + \frac{\partial \sigma_{22}}{\partial x_2} + \frac{\partial \sigma_{23}}{\partial x_3} = 0$$

$$\frac{\partial \sigma_{13}}{\partial x_1} + \frac{\partial \sigma_{23}}{\partial x_2} + \frac{\partial \sigma_{33}}{\partial x_3} = 0 \quad (1a-c)$$

B. Strain Displacement Relations

The state of deformation in the neighborhood of a given point in a continuous body is characterized by six components of deformation:

$$\epsilon_{ij} \quad (i=j=1,2,3)$$

$$\gamma_{ij} \quad (i \neq j, \quad i, j=1,2,3)$$

In the Cartesian system, the components ϵ_{ij} represents the relative elongations of infinitely small line segments which in the undeformed body are parallel to axis x_1, x_2, x_3 ; and the components γ_{ij} represent the relative shears or changes in angles between indicated line segments which are previously perpendicular to each other.

The components of deformation can be expressed in terms of displacements. In the case of small deformations the strain-displacement relations are:

$$\begin{aligned}
 \epsilon_{11} &= \frac{\partial u_1}{\partial x_1} & , & & \gamma_{23} &= \frac{\partial u_2}{\partial x_3} + \frac{\partial u_3}{\partial x_2} \\
 \epsilon_{22} &= \frac{\partial u_2}{\partial x_2} & , & & \gamma_{13} &= \frac{\partial u_3}{\partial x_1} + \frac{\partial u_1}{\partial x_3} \\
 \epsilon_{33} &= \frac{\partial u_3}{\partial x_3} & , & & \gamma_{12} &= \frac{\partial u_1}{\partial x_2} + \frac{\partial u_2}{\partial x_1}
 \end{aligned} \tag{2a-f}$$

where u_1, u_2, u_3 are the displacements in directions x_1, x_2, x_3 respectively.

C. Stress Strain Relations, Generalized Hooke's Law

The equations (1a-c) and (2a-f) are not sufficient to solve the problems of equilibrium, motion or stability of an elastic body. Additional relations are necessary between the components of stress and deformation. For small deformations an elastic body is taken to be a continuous body which obeys the generalized Hooke's Law that means the components of deformation are linear functions of the components of stress if the body is elastic (reverse is also true).

If we consider a homogenous elastic body in arbitrarily chosen orthogonal coordinates x_1, x_2, x_3 ; Generalized Hooke's Law can be written as:

$$\begin{bmatrix} \epsilon_{11} \\ \epsilon_{22} \\ \epsilon_{33} \\ \gamma_{23} \\ \gamma_{13} \\ \gamma_{12} \end{bmatrix} = [c_{ij}] \begin{bmatrix} \sigma_{11} \\ \sigma_{22} \\ \sigma_{33} \\ \sigma_{23} \\ \sigma_{13} \\ \sigma_{12} \end{bmatrix} \tag{3}$$

where c_{ij} $i, j=1, \dots, 6$ are the elastic constants and $c_{ij} = c_{ji}$
 In this general case the number of independent constants is 21.

When a body possesses symmetry of internal structure, its elastic properties would show the symmetry. This elastic symmetry means that each point of a body has symmetrical directions in each of which the elastic properties are identical. These directions are called equivalent directions. Equations of Hooke's Law are simplified in the presence of elastic symmetry. Some of the constants c_{ij} become equal to zero and dependencies appear between some others.

1. Orthotropy, three planes of elastic symmetry

A homogenous body with three mutually perpendicular planes of elastic symmetry passing through every point is called orthogonal-anisotropic or orthotropic. In this case the matrix $[c_{ij}]$ as referred to coordinate system x_1, x_2, x_3 with axes normal to these planes will be:

$$[c_{ij}] = \begin{bmatrix} c_{11} & c_{12} & c_{13} & 0 & 0 & 0 \\ c_{12} & c_{22} & c_{23} & 0 & 0 & 0 \\ c_{13} & c_{23} & c_{33} & 0 & 0 & 0 \\ 0 & 0 & 0 & c_{44} & 0 & 0 \\ 0 & 0 & 0 & 0 & c_{55} & 0 \\ 0 & 0 & 0 & 0 & 0 & c_{66} \end{bmatrix} \quad (4)$$

When engineering constants are introduced instead of elastic constants c_{ij} , generalized Hooke's Law for an orthotropic body may be expressed as⁽¹⁾:

$$\epsilon_{11} = \frac{1}{E_{11}} \sigma_{11} - \frac{\nu_{21}}{E_{22}} \sigma_{22} - \frac{\nu_{31}}{E_{33}} \sigma_{33}$$

$$\epsilon_{22} = \frac{\nu_{12}}{E_{11}} \sigma_{11} + \frac{1}{E_{22}} \sigma_{22} - \frac{\nu_{32}}{E_{33}} \sigma_{33}$$

$$\epsilon_{33} = \frac{\nu_{13}}{E_{11}} \sigma_{11} - \frac{\nu_{23}}{E_{22}} \sigma_{22} + \frac{1}{E_{33}} \sigma_{33}$$

$$\gamma_{12} = \frac{1}{G_{12}} \sigma_{12}$$

.....

where E_{ii} are the Young's Moduli along principal directions,
 ν_{ij} are the Poisson's ratios characterizing the decrease in j direction during tension in i direction,
 G_{ij} are shear moduli characterizing the changes of angles between directions i and j ($i, j=1, 2, 3$).

Due to symmetry of equations (5a-f) the following relation exist between Young's Moduli and Poisson ratios:

$$E_{ii} \nu_{ji} = E_{jj} \nu_{ij} \quad i, j=1, 2, 3 \quad (6)$$

The number of independent elastic constants in this case is nine.

2. Isotropy, complete symmetry

Every plane of an isotropic body is a plane of elastic symmetry, and every direction is a principal direction. The generalized Hooke's Law for an isotropic body may be expressed as:

$$\begin{aligned} \epsilon_{11} &= \frac{1}{E} [\sigma_{11} - \nu(\sigma_{22} + \sigma_{33})] \\ \epsilon_{22} &= \frac{1}{E} [\sigma_{22} - \nu(\sigma_{11} + \sigma_{33})] \\ \epsilon_{33} &= \frac{1}{E} [\sigma_{33} - \nu(\sigma_{11} + \sigma_{22})] \\ \gamma_{23} &= \frac{1}{G} \sigma_{23} \\ \gamma_{13} &= \frac{1}{G} \sigma_{13} \\ \gamma_{12} &= \frac{1}{G} \sigma_{12} \end{aligned} \quad (7a-f)$$

where E is the Young's modulus, ν is the Poisson ratio and G is the shear modulus ($G = E/2(1+\nu)$).

The number of independent elastic constants here is only two. It is important to note that for isotropic bodies, when any system of coordinates x'_1, x'_2, x'_3 is used instead of x_1, x_2, x_3 , equations (7a-f) will not change and elastic constants E and ν will preserve their numerical values. However, for anisotropic bodies new elastic constants c'_{ij} are required which can be expressed in terms of the old ones.

D. Field Equation for an Orthotropic Body

The state of stress of an elastic body is known if the stress components at every point are known on three planes which are normal to the coordinate directions. The state of deformation is determined by the components of deformation which depend on three displacements in the coordinate directions. Therefore in order to have a complete picture about the state of stress and deformation of an elastic body which is subjected to external forces, it is necessary to determine six stress components and three displacements. In order to determine them nine independent equations are necessary.

Furthermore, the plane problem of the theory of elasticity is reduced to determination of a stress function $U(x_1, x_2)$ on plane $x_1 x_2$, which satisfies a differential equation of fourth order and the boundary conditions. This differential equation is called the 'field equation' or the 'compatibility condition' of the problem. In the case of generalized plane stress, $\sigma_{33} = \sigma_{13} = \sigma_{23} = 0$ and for average stresses and strains equilibrium equations (1a-c) becomes:

$$\frac{\partial \sigma_{11}}{\partial x_1} + \frac{\partial \sigma_{12}}{\partial x_2} = 0$$

$$\frac{\partial \sigma_{12}}{\partial x_1} + \frac{\partial \sigma_{22}}{\partial x_2} = 0$$

(8a-b)

Hooke's Law (5a-f) changes to;

$$\begin{bmatrix} \epsilon_{11} \\ \epsilon_{22} \\ 2\gamma_{12} \end{bmatrix} = \begin{bmatrix} \frac{1}{E_{11}} & -\frac{\nu_{12}}{E_{22}} & 0 \\ -\frac{\nu_{21}}{E_{11}} & \frac{1}{E_{22}} & 0 \\ 0 & 0 & \frac{1}{G_{12}} \end{bmatrix} \begin{bmatrix} \sigma_{11} \\ \sigma_{22} \\ \sigma_{12} \end{bmatrix} \quad (9)$$

and the strain-displacement relations (2a-f) turn out to be:

$$\epsilon_{11} = \frac{\partial u}{\partial x_1}, \quad \epsilon_{22} = \frac{\partial u}{\partial x_2}, \quad \gamma_{12} = \frac{\partial u}{\partial x_2} + \frac{\partial u}{\partial x_1} \quad (10)$$

By differentiation of displacements u and v in (10) one may obtain the condition of compatibility of deformation as:

$$\frac{\partial^2 \epsilon_{11}}{\partial x_2^2} + \frac{\partial^2 \epsilon_{22}}{\partial x_1^2} = 2 \frac{\partial^2 \gamma_{12}}{\partial x_1 \partial x_2} \quad (11)$$

In the absence of body forces the equilibrium equations (8a-b) are satisfied by the introduction of a stress function $U(x_1, x_2)$ and assuming that:

$$\sigma_{11} = \frac{\partial^2 U}{\partial x_2^2}, \quad \sigma_{22} = \frac{\partial^2 U}{\partial x_1^2}, \quad \sigma_{12} = -\frac{\partial^2 U}{\partial x_1 \partial x_2} \quad (12)$$

Thus, substituting the expressions ϵ_{11} , ϵ_{22} , ϵ_{12} from equation (9) in equation (11) and expressing the stress components through $U(x_1, x_2)$ one may obtain the fourth order differential equation which must be satisfied by the stress function. Therefore; in the absence of body forces, for a two dimensional elastic, homogenous, orthotropic body in generalized plane stress, if $U(x_1, x_2)$ is the stress function, the solution of the equations of equilibrium reduces to the solution of the following field equation:

$$\frac{E_{11}}{E_{22}} \frac{\partial^4 U}{\partial x_1^4} + \left(\frac{E_{11}}{G_{12}} - 2\nu_{12} \right) \frac{\partial^4 U}{\partial x_1^2 \partial x_2^2} + \frac{\partial^4 U}{\partial x_2^4} = 0 \quad (13)$$

To study the stresses and deformations of such a body, it is sufficient to know only four elastic constants from the total number of nine: E_{11} , E_{22} , G_{12} and ν_{12} .

Note that for an isotropic plate; $E_{11} = E_{22} = E$ and $G_{12} = E/2(1+\nu)$, thus equation (13) reduces to:

$$\nabla^4 U = 0 \quad (14)$$

which is the biharmonic equation.

E. New Material Parameters for Plane Orthotropy

Instead of a direct use of four independent elastic constants $E_{11}, E_{22}, G_{12}, \nu_{12}$ we introduce the following parameters as proposed by Krenk⁽²⁴⁾ for generalized plane stress case,

$$\begin{aligned} E &= [E_{11}E_{22}]^{1/2} \\ \nu &= [\nu_{12}\nu_{21}]^{1/2} \\ \delta^4 &= \frac{E_{11}}{E_{22}} = \frac{\nu_{12}}{\nu_{21}} \\ K &= \frac{1}{2}[E_{11}E_{22}]^{1/2} \left(\frac{1}{G_{12}} - \frac{\nu_{12}}{E_{11}} - \frac{\nu_{21}}{E_{22}} \right) \end{aligned} \quad (15a-d)$$

and for plane strain case,

$$\begin{aligned} E &= \left[\frac{E_{11}E_{22}}{(1-\nu_{13}\nu_{31})(1-\nu_{23}\nu_{32})} \right]^{1/2} \\ \nu &= \left[\frac{(\nu_{12}+\nu_{13}\nu_{32})(\nu_{21}+\nu_{23}\nu_{31})}{(1-\nu_{13}\nu_{31})(1-\nu_{23}\nu_{32})} \right]^{1/2} \\ \delta^4 &= \frac{E_{11}}{E} \frac{1-\nu_{23}\nu_{32}}{1-\nu_{13}\nu_{31}} \\ K &= \frac{1}{2} \left[\frac{E_{11}E_{22}}{(1-\nu_{13}\nu_{31})(1-\nu_{23}\nu_{32})} \right]^{1/2} \left(\frac{1}{G_{12}} - \frac{\nu_{12}+\nu_{13}\nu_{32}}{E_{11}} - \frac{\nu_{21}+\nu_{23}\nu_{31}}{E_{22}} \right) \end{aligned} \quad (16a-d)$$

where E is the effective stiffness, ν is the effective Poisson ratio, δ is the stiffness ratio, K is the shear parameter. Then Hooke's Law for an orthotropic body both for generalized plane stress and plane strain cases become:

$$\begin{bmatrix} \epsilon_{11} \\ \epsilon_{22} \\ 2\gamma_{12} \end{bmatrix} = \frac{1}{E} \begin{bmatrix} \delta^{-2} & -\nu & 0 \\ -\nu & \delta^2 & 0 \\ 0 & 0 & 2(K+\nu) \end{bmatrix} \begin{bmatrix} \sigma_{11} \\ \sigma_{22} \\ \sigma_{12} \end{bmatrix} \quad (17)$$

By a suitable variable transformation it is possible to eliminate the dependence on δ either. Introducing the new coordinates,

$$x = x_1 / \sqrt{\delta} \quad y = x_2 \sqrt{\delta} \quad (18)$$

the new displacements,

$$u = u_1 \sqrt{\delta} \quad v = u_2 / \sqrt{\delta} \quad (19)$$

the new stresses,

$$\sigma_{xx} = \sigma_{11} / \delta \quad \sigma_{yy} = \sigma_{22} \delta \quad \sigma_{xy} = \sigma_{12} \quad (20)$$

and the corresponding new strains,

$$\epsilon_{xx} = \epsilon_{11} \delta \quad \epsilon_{yy} = \epsilon_{22} / \delta \quad \gamma_{xy} = \gamma_{12}$$

finally Hooke's Law takes the form:

$$\begin{bmatrix} \epsilon_{xx} \\ \epsilon_{yy} \\ 2\gamma_{xy} \end{bmatrix} = \frac{1}{E} \begin{bmatrix} 1 & -\nu & 0 \\ -\nu & 1 & 0 \\ 0 & 0 & 2(K+\nu) \end{bmatrix} \begin{bmatrix} \sigma_{xx} \\ \sigma_{yy} \\ \sigma_{xy} \end{bmatrix} \quad (21)$$

Remembering the stress expressions through the stress function (12) in terms of the original variables; if U is the Airy's stress function of a problem formulated in the original variables, it will also be the stress function of the transformed problem due to equations (18) and (20). Thus, stresses may still be expressed as:

$$\sigma_{xx} = \frac{\partial^2 U}{\partial y^2}, \quad \sigma_{yy} = \frac{\partial^2 U}{\partial x^2}, \quad \sigma_{xy} = -\frac{\partial^2 U}{\partial x \partial y} \quad (22)$$

By a similar procedure as in Section D., it can be easily shown that the field equation in terms of the new material parameters come out to be:

$$\frac{\partial^4 U}{\partial x^4} + 2K \frac{\partial^4 U}{\partial x^2 \partial y^2} + \frac{\partial^4 U}{\partial y^4} = 0 \quad (23)$$

where K is the shear parameter. It should be noted that for an isotropic material $K = 1$ and equation (23) turns out

to be the biharmonic equation again. For an isotropic material with E_{ii} and ν_i also note that:

$\delta = \kappa = 1$ for generalized plane stress and plane strain,

$E = E_{ii}$, $\nu = \nu_i$ for generalized plane stress,

$E = \frac{E_{ii}}{1-\nu_i^2}$, $\nu = \frac{\nu_i}{(1-\nu_i)}$ for plane stress cases.

As seen from equation (23), in terms of the new variables (17-20) the field equation and the solution of the problem are independent of the stiffness ratio δ .

III. STRESS FIELDS OF EDGE DISLOCATIONS IN AN ORTHOTROPIC BODY

In this section, first the stress field of an elastic orthotropic infinite plane due to a pair of edge dislocations with burger's vectors \vec{b}_x (parallel to x-axis) and \vec{b}_y (parallel to y-axis) located at the point $x=t$, $y=0$ will be determined (Figure 1).

From the infinite plane solution together with the boundary conditions of the residual loading program, the stress state due to edge dislocations in an infinite strip $0 < x < H$ parallel to y-axis will be derived using the standard Fourier transform technique.

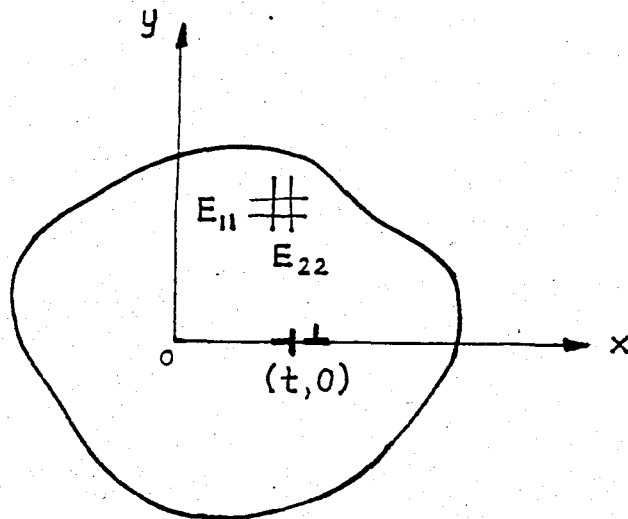


Figure 1. A pair of edge dislocations at the position $(t, 0)$ with burger's vectors \vec{b}_x and \vec{b}_y in an infinite orthotropic plane.

The same procedure is applied in the study of Civelek and Erdoğan⁽²⁵⁾ for the solution of the isotropic case.

A. A Pair of Edge Dislocations in an Infinite Orthotropic Plane

The problem of an inclined crack in an orthotropic strip is considered by Delale et.al.⁽²³⁾ and the solution is expressed as the sum of two states of stress: Crack in an infinite plane and an infinite strip with no cracks. The governing equations are solved separately for these two cases and then the solutions are superimposed.

however, their solution procedure is greatly facilitated when a crack is represented by a continuous array of dislocations. Once the infinite plane solution due to a pair of edge dislocations are obtained, one may get the strip solution in a straightforward manner imposing the boundary conditions at the strip edges and using the standard Fourier transform technique. Then, since the dislocations are 'point functions'⁽²⁵⁾, replacing the Burger's vectors of the dislocations with the density functions and integrating the solution found for the dislocations; the solution for any number of cracks may be obtained through a system of integral equations for the unknown density functions.

Therefore it is quite useful to begin the present formulation by obtaining the dislocation solutions for an infinite orthotropic plane from the existing crack solution of Delale et.al.⁽²³⁾.

It is known that a crack along the x-axis can be represented by continuous distribution of edge dislocations with density functions

$$f(x) = \frac{\partial}{\partial x} [v(x, 0^+) - v(x, 0^-)]$$

$$g(x) = \frac{\partial}{\partial x} [u(x, 0^+) - u(x, 0^-)] \quad (24a-b)$$

where u, v are the displacement components in the (x, y) coordinate system⁽²⁷⁾. As the crack extends from b to c , it is obvious that:

$$f(x) = g(x) = 0 \quad \text{for } x > c, \quad x < b$$

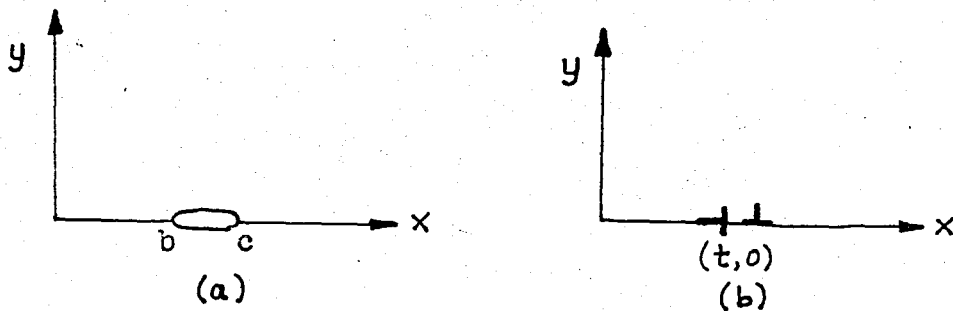


Figure 2. (a) A crack along the x-axis extending from b to c, (b) A pair of edge dislocations at the position (t, 0)

As seen in Figure 2, to obtain the stresses due to a pair of edge dislocations with Burger's vectors \vec{b}_x and \vec{b}_y , the integrations over the density functions f and g within the crack solution should be replaced by the 'relative displacements' at a single point $(t, 0)$. Thus:

$$\begin{aligned} \int_b^c f(t) dt & \quad \text{by} \quad v(t, 0^+) - v(t, 0^-) = -b_y \\ \text{and} \quad \int_b^c g(t) dt & \quad \text{by} \quad u(t, 0^+) - u(t, 0^-) = -b_x \end{aligned} \quad (25a-b)$$

where b_x and b_y are the magnitudes of the Burger's vectors \vec{b}_x and \vec{b}_y and the minus sign comes from a conventional assumption that the negative of the relative displacement is called the Burger's vector of the dislocation (RH/FS, namely, Right Hand Frank Sign convention⁽¹⁾).

At this stage, the desired infinite orthotropic plane solution due to edge dislocations may be obtained as follows.

Consider an infinite orthotropic plane containing a pair of edge dislocations with Burger's vectors \vec{b}_x (parallel to x-axis) and \vec{b}_y (parallel to y-axis) located at the point $x=t, y=0$. Introducing the new material parameters (15a-d) and the variable transformations (18-20), the stresses may be expressed as:

$$\begin{aligned}\sigma_{xx}^d(x,y) &= \frac{Dx}{\Pi} G_{xx}^d(x,y,t) + \frac{Dy}{\Pi} F_{xx}^d(x,y,t) \\ \sigma_{yy}^d(x,y) &= \frac{Dx}{\Pi} G_{yy}^d(x,y,t) + \frac{Dy}{\Pi} F_{yy}^d(x,y,t) \\ \sigma_{xy}^d(x,y) &= \frac{Dx}{\Pi} G_{xy}^d(x,y,t) + \frac{Dy}{\Pi} F_{xy}^d(x,y,t)\end{aligned}\quad (26a-c)$$

and the influence functions are given by,

$$\begin{aligned}G_{xx}^d(x,y,t) &= y \left[\frac{w_1^3}{(t-x)^2 + w_1^2 y^2} - \frac{w_2^3}{(t-x)^2 + w_2^2 y^2} \right] \\ F_{xx}^d(x,y,t) &= (t-x) \left[\frac{w_1}{(t-x)^2 + w_1^2 y^2} - \frac{w_2}{(t-x)^2 + w_2^2 y^2} \right] \\ G_{yy}^d(x,y,t) &= y \left[\frac{-w_1}{(t-x)^2 + w_1^2 y^2} + \frac{w_2}{(t-x)^2 + w_2^2 y^2} \right] \\ F_{yy}^d(x,y,t) &= (t-x) \left[\frac{-1/w_1}{(t-x)^2 + w_1^2 y^2} + \frac{1/w_2}{(t-x)^2 + w_2^2 y^2} \right] \\ G_{xy}^d(x,y,t) &= (t-x) \left[\frac{w_1}{(t-x)^2 + w_1^2 y^2} - \frac{w_2}{(t-x)^2 + w_2^2 y^2} \right] \\ F_{xy}^d(x,y,t) &= y \left[\frac{-w_1}{(t-x)^2 + w_1^2 y^2} + \frac{w_2}{(t-x)^2 + w_2^2 y^2} \right]\end{aligned}\quad (27a-f)$$

where $Dx = \frac{-E}{4\sqrt{K^2-1}} b_x$, $Dy = \frac{-E}{4\sqrt{K^2-1}} b_y$,

and E is the effective stiffness ,

K is the shear parameter ,

b_x, b_y are the magnitudes of the Burger's vectors.

B. A Pair of Edge Dislocations in an Orthotropic Strip

To determine the stress state due to a pair of edge dislocations in an infinite orthotropic strip $0 < x < H$ parallel to the y -axis as in Figure 3, the two kinds of dislocations will be treated separately and the stresses corresponding to each one will be obtained.

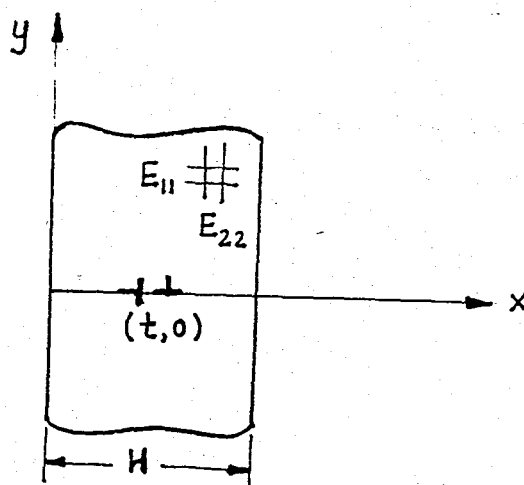


Figure 3. A pair of edge dislocations in an orthotropic strip $0 < x < H$ parallel to y -axis.

A single edge dislocation with Burger's vector \vec{b}_x (parallel to x -axis) corresponds to the case $D_x \neq 0, D_y = 0$ whereas the other kind with Burger's vector \vec{b}_y (parallel to y -axis) can be represented by $D_x = 0, D_y \neq 0$.

Depending upon the loading conditions, a crack may be represented by the distribution of a specific kind of dislocation. Thus it is sufficient to obtain the stress state due to each kind of dislocations and use the simple superposition technique to formulate various problems of interest. The details of the representation of cracks in terms of dislocations will be given in Section IV.

1. An edge dislocation with Burger's vector \vec{b}_x

The residual loading problem for the infinite strip is formulated in terms of the Airy's stress function U which satisfies the field equation (23)

$$\frac{\partial^4 U}{\partial x^4} + 2K \frac{\partial^4 U}{\partial x^2 \partial y^2} + \frac{\partial^4 U}{\partial y^4} = 0$$

For the case $Dx \neq 0$, $Dy = 0$ it is convenient to express,

$$U(x, y) = \frac{2}{\pi} \int_0^{\infty} \bar{\Phi}(x, \alpha) \sin \alpha y d\alpha \quad (28)$$

Substitution of (28) in the field equation yields,

$$\left(\frac{d^4}{dx^4} - 2K\alpha^2 \frac{d^2}{dx^2} + \alpha^4 \right) \bar{\Phi} = 0 \quad (29)$$

which has the solution (see Appendix I),

$$\bar{\Phi}(x, \alpha) = A_1 e^{-w_1 \alpha |x|} + B_1 e^{-w_2 \alpha |x|} + A_2 e^{w_1 \alpha |x|} + B_2 e^{w_2 \alpha |x|} \quad (30)$$

Thus the Airy's stress function can be expressed as,

$$U(x, y) = \frac{2}{\pi} \int_0^{\infty} [A_1 e^{-w_1 \alpha x} + B_1 e^{-w_2 \alpha x} + A_2 e^{w_1 \alpha x} + B_2 e^{w_2 \alpha x}] \sin \alpha y d\alpha \quad (31)$$

where $A_1(\alpha)$, $A_2(\alpha)$, $B_1(\alpha)$ and $B_2(\alpha)$ are unknown functions to be determined from the boundary conditions.

The stress components will be expressed by using the relations,

$$\sigma_{xx} = \frac{\partial^2 U}{\partial y^2}, \quad \sigma_{yy} = \frac{\partial^2 U}{\partial x^2}, \quad \sigma_{xy} = -\frac{\partial^2 U}{\partial x \partial y} \quad (32)$$

Upon differentiation one may obtain,

$$\begin{aligned}\sigma_{xx} &= \frac{-2}{\pi} \int_0^{\infty} \alpha^2 \left[A_1 e^{-w_1 \alpha x} + B_1 e^{-w_2 \alpha x} \right. \\ &\quad \left. + A_2 e^{+w_1 \alpha x} + B_2 e^{+w_2 \alpha x} \right] \sin \alpha y d\alpha \\ \sigma_{yy} &= \frac{2}{\pi} \int_0^{\infty} \alpha^2 \left[w_1^2 A_1 e^{-w_1 \alpha x} + w_2^2 B_1 e^{-w_2 \alpha x} \right. \\ &\quad \left. + w_1^2 A_2 e^{+w_1 \alpha x} + w_2^2 B_2 e^{+w_2 \alpha x} \right] \sin \alpha y d\alpha \\ \sigma_{xy} &= \frac{-2}{\pi} \int_0^{\infty} \alpha^2 \left[-w_1 A_1 e^{-w_1 \alpha x} - w_2 B_1 e^{-w_2 \alpha x} \right. \\ &\quad \left. + w_1 A_2 e^{+w_1 \alpha x} + w_2 B_2 e^{+w_2 \alpha x} \right] \cos \alpha y d\alpha\end{aligned}\quad (33a-c)$$

Boundary conditions of the residual loading problem at the strip edges $x=0$ and $x=H$ are:

$$\begin{aligned}\sigma_{xx}(0,y) &= -\sigma_{xx}^d(0,y) \\ \sigma_{xy}(0,y) &= -\sigma_{xy}^d(0,y) \\ \sigma_{xx}(H,y) &= -\sigma_{xx}^d(H,y) \\ \sigma_{xy}(H,y) &= -\sigma_{xy}^d(H,y)\end{aligned}\quad (34a-d)$$

Applying the above boundary conditions, taking transforms of the resulting equations and evaluating the infinite integrals on the right hand side,

$$\begin{aligned}A_1 + B_1 + A_2 + B_2 &= \frac{-Dx}{2\alpha^2} \left\{ w_1 e^{-\alpha t w_2} - w_2 e^{-\alpha t w_1} \right\} \\ -w_1 A_1 - w_2 B_1 + w_1 A_2 + w_2 B_2 &= \frac{-Dx}{2\alpha^2} \left\{ e^{-\alpha t w_2} - e^{-\alpha t w_1} \right\} \\ A_1 e^{-w_1 \alpha H} + B_1 e^{-w_2 \alpha H} + A_2 e^{w_1 \alpha H} + B_2 e^{w_2 \alpha H} \\ &= \frac{-Dx}{2\alpha^2} \left\{ w_1 e^{-\alpha(H-t)w_2} - w_2 e^{-\alpha(H-t)w_1} \right\} \\ -w_1 A_1 e^{-w_1 \alpha H} - w_2 B_1 e^{-w_2 \alpha H} + w_1 A_2 e^{w_1 \alpha H} + w_2 B_2 e^{w_2 \alpha H} \\ &= \frac{-Dx}{2\alpha^2} \left\{ -e^{-\alpha(H-t)w_2} + e^{-\alpha(H-t)w_1} \right\}\end{aligned}$$

In evaluating the transforms σ_{xx}^d , σ_{xy}^d which take place at

the right hand sides of the equations (34a-d), it is helpful to note that,

$$\left. \begin{aligned} \int_0^{\infty} \frac{1}{n^2+y^2} \cos \alpha y dy &= \frac{\pi}{2n} e^{-\alpha n} \\ \int_0^{\infty} \frac{y}{n^2+y^2} \sin \alpha y dy &= \frac{\pi}{2} e^{-\alpha n} \end{aligned} \right\} \text{ for } n > 0$$

After a few steps of long but straightforward algebra, the functions A_1, B_1, A_2 and B_2 can be expressed as follows:

$$A_1 = \frac{-Dx}{2\alpha^2 D(\alpha)} \left\{ w_2 r_1 e^{-\alpha w_1 t} + w_1 r_2 e^{-\alpha w_2 t} - w_2 r_3 e^{\alpha w_1 t} - w_1 r_4 e^{\alpha w_2 t} \right\}$$

$$B_1 = \frac{-Dx}{2\alpha^2 D(\alpha)} \left\{ w_1 r_5 e^{-\alpha w_2 t} + w_2 r_6 e^{-\alpha w_1 t} - w_1 r_7 e^{\alpha w_2 t} - w_2 r_8 e^{\alpha w_1 t} \right\}$$

$$A_2 = \frac{-Dx}{2\alpha^2 D(\alpha)} \left\{ w_2 r_9 e^{-\alpha w_1 t} + w_1 r_{10} e^{-\alpha w_2 t} - w_2 r_{11} e^{\alpha w_1 t} - w_1 r_{12} e^{\alpha w_2 t} \right\}$$

$$B_2 = \frac{-Dx}{2\alpha^2 D(\alpha)} \left\{ w_1 r_{13} e^{-\alpha w_2 t} + w_2 r_{14} e^{-\alpha w_1 t} - w_1 r_{15} e^{\alpha w_2 t} - w_2 r_{16} e^{\alpha w_1 t} \right\}$$

(35a-d)

where $Dx = \frac{-Eb_x}{4\sqrt{K^2-1}}$, $D(\alpha)$ and $r_i(\alpha)$ are given in Appendix A.

substituting A_1, B_1, A_2 and B_2 in the stress expressions (33a-c) and adding the infinite plane solution (26a-c) one obtains the stress state at any point within the strip (for the case of $Dx \neq 0, Dy = 0$).

At this stage, σ_{xx} expression is omitted from the formulation procedure since not only for strip but also for plate solutions the crack surface boundary conditions will be either of normal type (in y-direction) or tangential type. Thus σ_{yy} and σ_{xy} expressions are sufficient to formulate the problem.

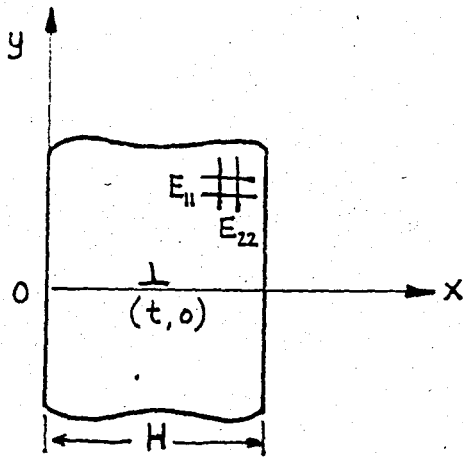


Figure 4. An edge dislocation at the position $(t,0)$ with Burger's vector \vec{b}_x in an orthotropic strip.

Thus, using the equations (26a-c), (33a-c) and (35a-d) one may obtain the stress expressions for an edge dislocation with Burger's vector \vec{b}_x (for the case $Dx \neq 0, Dy = 0$) in an orthotropic strip as seen in Figure 4. Denoting the stresses corresponding to this kind of dislocation by a superscript '1', the stresses are:

$$\begin{aligned} \sigma_{yy}^1(x,y,t) &= \frac{-Dx}{\Pi} \left\{ G_{yy}^d(x,y,t) + \bar{k}_{11}(x,y,t) \right\} \\ \sigma_{xy}^1(x,y,t) &= \frac{-Dx}{\Pi} \left\{ G_{xy}^d(x,y,t) + \bar{k}_{12}(x,y,t) \right\} \end{aligned} \quad (36a-b)$$

where the kernels \bar{k}_{11} and \bar{k}_{12} are given in Appendix B.

After the asymptotic examination of the kernels (see Appendix D), the stresses may finally be expressed as:

$$\begin{aligned} \sigma_{yy}^1(x,y,t) &= \frac{-Dx}{\Pi} \left\{ G_{yy}^d(x,y,t) + Q_4(x,y,t) + Q_4(H-x,y,H-t) \right\} \\ &\quad - \frac{Dx}{\Pi} \int_0^{\infty} \frac{-1}{D(\alpha)} \sum_{i=1}^8 [S_i(x,t,\alpha) + S_i(H-x,H-t,\alpha)] \sin \alpha y d\alpha \\ \sigma_{xy}^1(x,y,t) &= \frac{-Dx}{\Pi} \left\{ G_{xy}^d(x,y,t) + Q_8(x,y,t) - Q_8(H-x,y,H-t) \right\} \\ &\quad - \frac{Dx}{\Pi} \int_0^{\infty} \frac{-1}{D(\alpha)} \sum_{i=1}^8 [U_i(x,t,\alpha) - U_i(H-x,H-t,\alpha)] \cos \alpha y d\alpha \end{aligned} \quad (37a-b)$$

where $Dx = \frac{-E}{4\sqrt{K^2-1}} b_x$, see Appendix E for Q_4 and Q_8 and Appendix F for U_i and S_i $i:1, \dots, 8$

2. An edge dislocation with Burger's vector \vec{b}_y

Again the residual loading problem for the infinite strip will be formulated in terms of the Airy's stress function U which satisfies the governing field equation (23). But for the present case of $D_x=0$, $D_y \neq 0$; this time it is convenient to express,

$$U(x,y) = \frac{2}{\pi} \int_0^{\infty} \bar{\Phi}(x,\alpha) \cos \alpha y d\alpha \quad (38)$$

Substituting in the field equation and solving for $\bar{\Phi}$ yields,

$$U(x,y) = \frac{2}{\pi} \int_0^{\infty} [A_1 e^{-w_1 \alpha x} + B_1 e^{-w_2 \alpha x} + A_2 e^{w_1 \alpha x} + B_2 e^{w_2 \alpha x}] \cos \alpha y d\alpha \quad (39)$$

and the stress components can be expressed through the relations (32) as:

$$\begin{aligned} \sigma_{xx} &= \frac{-2}{\pi} \int_0^{\infty} \alpha^2 [A_1 e^{-w_1 \alpha x} + B_1 e^{-w_2 \alpha x} + A_2 e^{w_1 \alpha x} + B_2 e^{w_2 \alpha x}] \cos \alpha y d\alpha \\ \sigma_{yy} &= \frac{2}{\pi} \int_0^{\infty} \alpha^2 [w_1^2 A_1 e^{-w_1 \alpha x} + w_2^2 B_1 e^{-w_2 \alpha x} + w_1^2 A_2 e^{w_1 \alpha x} + w_2^2 B_2 e^{w_2 \alpha x}] \cos \alpha y d\alpha \\ \sigma_{xy} &= \frac{2}{\pi} \int_0^{\infty} \alpha^2 [-w_1 A_1 e^{-w_1 \alpha x} - w_2 B_1 e^{-w_2 \alpha x} + w_1 A_2 e^{w_1 \alpha x} + w_2 B_2 e^{w_2 \alpha x}] \sin \alpha y d\alpha \end{aligned} \quad (40a-c)$$

Applying the boundary conditions (34a-d) and following a similar procedure as in the previous section,

$$\begin{aligned} A_1 + B_1 + A_2 + B_2 &= \frac{-Dy}{2\alpha^2} \left\{ e^{-\alpha t w_2} - e^{-\alpha t w_1} \right\} \\ w_1 A_1 + w_2 B_1 - w_1 A_2 - w_2 B_2 &= \frac{-Dy}{2\alpha^2} \left\{ -w_2 e^{-\alpha t w_2} + w_1 e^{-\alpha t w_1} \right\} \end{aligned}$$

$$\begin{aligned}
& A_1 e^{-w_1 \alpha H} + B_1 e^{-w_2 \alpha H} + A_2 e^{+w_1 \alpha H} + B_2 e^{+w_2 \alpha H} \\
&= \frac{-Dy}{2\alpha^2} \left\{ -e^{-\alpha(H-t)w_2} + e^{-\alpha(H-t)w_1} \right\} \\
& w_1 A_1 e^{-w_1 \alpha H} + w_2 B_1 e^{-w_2 \alpha H} - w_1 A_2 e^{+w_1 \alpha H} - w_2 B_2 e^{+w_2 \alpha H} \\
&= \frac{-Dy}{2\alpha^2} \left\{ -w_2 e^{-\alpha(H-t)w_2} + w_1 e^{-\alpha(H-t)w_1} \right\}
\end{aligned}$$

After a few steps of long but straightforward algebra, A_1, B_1, A_2 and B_2 can be expressed as follows:

$$\begin{aligned}
A_1 &= \frac{-Dy}{2\alpha^2 D(\alpha)} \left\{ r_1 e^{-\alpha w_1 t} + r_2 e^{-\alpha w_2 t} + r_3 e^{\alpha w_1 t} + r_4 e^{\alpha w_2 t} \right\} \\
B_1 &= \frac{-Dy}{2\alpha^2 D(\alpha)} \left\{ r_5 e^{-\alpha w_2 t} + r_6 e^{-\alpha w_1 t} + r_7 e^{\alpha w_2 t} + r_8 e^{\alpha w_1 t} \right\} \\
A_2 &= \frac{-Dy}{2\alpha^2 D(\alpha)} \left\{ r_9 e^{-\alpha w_1 t} + r_{10} e^{-\alpha w_2 t} + r_{11} e^{\alpha w_1 t} + r_{12} e^{\alpha w_2 t} \right\} \\
B_2 &= \frac{-Dy}{2\alpha^2 D(\alpha)} \left\{ r_{13} e^{-\alpha w_2 t} + r_{14} e^{-\alpha w_1 t} + r_{15} e^{\alpha w_2 t} + r_{16} e^{\alpha w_1 t} \right\}
\end{aligned} \tag{41a-d}$$

where $Dy = \frac{-Eb_y}{4\sqrt{K^2-1}}$, $D(\alpha)$ and $r_i(\alpha)$ are given in appendix A.

Substitution of the above functions in the stress expressions (33a-c) adding the infinite plane solution (26a-c), yields the stresses due to an edge dislocation with Burger's vector \vec{b}_y (the case $D_x=0, D_y \neq 0$) in an orthotropic strip as seen in Figure 5. Denoting the stresses corresponding to this kind of dislocation by a superscript '2', the stresses may be expressed as:

$$\begin{aligned}
\sigma_{yy}^2(x,y,t) &= \frac{-Dy}{\pi} \left\{ F_{yy}^d(x,y,t) + k_{11}(x,y,t) \right\} \\
\sigma_{xy}^2(x,y,t) &= \frac{-Dy}{\pi} \left\{ F_{xy}(x,y,t) + k_{12}(x,y,t) \right\}
\end{aligned} \tag{42a-b}$$

where the kernels k_{11} and k_{12} are given in Appendix B.

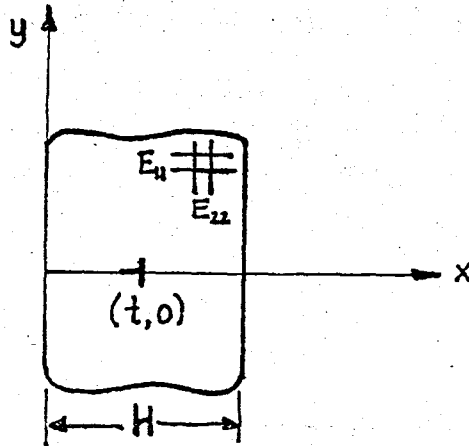


Figure 5. An edge dislocation at the position $(t, 0)$ with Burger's vector \vec{b}_y in an orthotropic strip.

Examination of the asymptotic behavior of the kernels this time yields (see Appendix D),

$$\sigma_{yy}^2(x, y, t) = \frac{-Dy}{\pi} \left\{ F_{yy}^d(x, y, t) + Q_2(x, y, t) - Q_2(H-x, y, H-t) \right\} \\ - \frac{Dy}{\pi} \int_0^\infty \frac{1}{D(\alpha)} \sum_{i=1}^8 \left[R_i(x, t, \alpha) - R_i(H-x, H-t, \alpha) \right] \cos \alpha y d\alpha$$

$$\sigma_{xy}^2(x, y, t) = \frac{-Dy}{\pi} \left\{ F_{xy}^d(x, y, t) + Q_6(x, y, t) + Q_6(H-x, y, H-t) \right\} \\ - \frac{Dy}{\pi} \int_0^\infty \frac{1}{D(\alpha)} \sum_{i=1}^8 \left[T_i(x, t, \alpha) + T_i(H-x, H-t, \alpha) \right] \sin \alpha y d\alpha \quad (43a-b)$$

where $Dy = \frac{-E}{4\sqrt{K^2-1}} b_y$, see Appendix E for Q_2 and Q_6 and Appendix F for R_i and T_i $i=1, \dots, 8$

IV. CRACKS IN TERMS OF DISLOCATIONS

The stress fields created in isotropic, homogenous elastic media by applying loads to the surfaces of cracks of Griffith type have been studied extensively as discussed in Section I.

Either exact or approximate solutions to these problems have been obtained using integral transform technique. The application of this technique to crack problems in anisotropic materials is quite complicated.

However, as stated by Tupholme⁽²⁷⁾; in 1948 Zener⁽²⁸⁾ and later Friedel⁽²⁹⁾ pointed out that many straight cracks can be represented by continuous distribution of dislocations. Several authors have used this simple but powerful technique and summaries of such works are included in reference(1).

The stress field of dislocations in homogenous, anisotropically elastic solids for a 3-Dimensional state of stress has been developed by Eshelby et.al.⁽³⁰⁾ and later generalized by Stroh⁽³¹⁾. Finally Tupholme⁽²⁷⁾ examined the dislocation layer approach for various crack surface tractions.

Depending on the results of the above studies, the basic principles of dislocation layer approach at different modes can be summarized as follows:

Consider a plane, stationary, Griffith-type crack of width $2l$ in a homogenous, orthotropic strip $0 < x < H$. The material is assumed to be initially everywhere at rest and stress free and situated so that its three mutually perpendicular planes of symmetry (axes of orthotropy) coincides with the cartesian coordinates x, y, z .

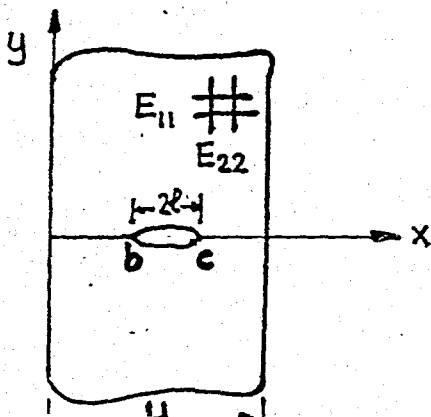


Fig.6 Griffith type crack in a homogenous, orthotropic strip.

The crack is assumed to occupy the region $b < x < c$, $y = 0$, $-\infty < z < \infty$ of the x - z plane.

As stated in reference(1), regarding the cracks in solids as surfaces of discontinuity of the displacement vector, Irwin observed that there are three independent kinematic movements of the upper and lower crack surfaces with respect to each other. These three basic type of deformation are illustrated in Figure 7, which shows the displacement of a small element containing the crack front. For a crack lying in the xz plane, the types of motion are as follows:

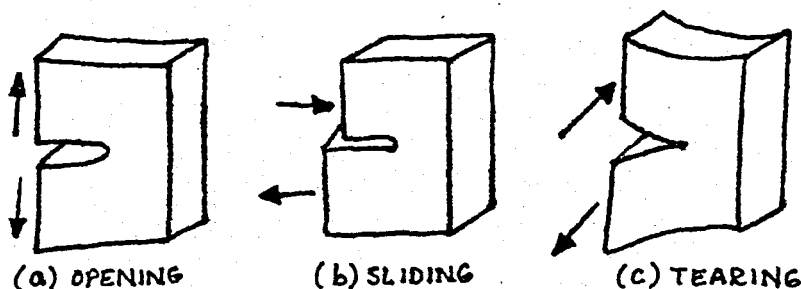


Figure 7. Basic modes of crack extension

Opening Mode , Normally Loaded Crack

The opening mode, Figure 7a, is characterized by the motions of the crack surfaces that tend to separate symmetrically with respect to the plane occupied by the crack before the deformation. Crack surface tractions for such a normally loaded crack is given by

$$\sigma_{yy}(x,0) = p_1(x)$$

$$\sigma_{xy}(x,0) = 0 \quad (44a-b)$$

where σ_{yy} , σ_{xy} are the stress components and $p_1(x)$ is the prescribed function.

According to the general procedure of the dislocation layer method, a loaded crack can be discussed by replacing it by a continuous distribution of dislocations. For this opening mode crack, it is appropriate to use stationary straight edge dislocations with dislocation line

in x direction and Burger's vector \vec{b}_y in y direction (27).

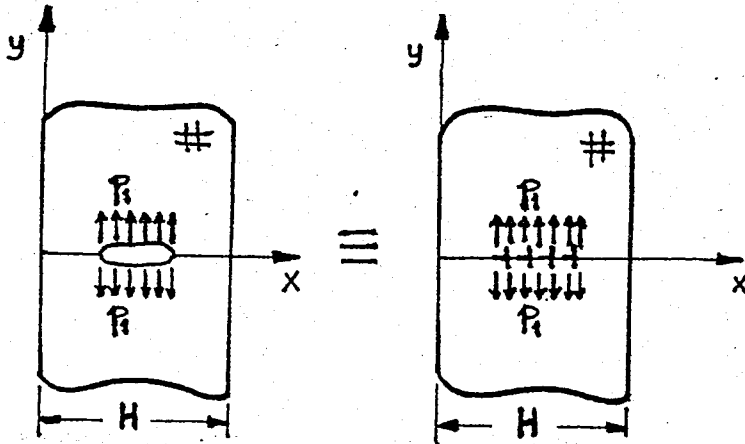


Figure 8. Representation of a normally loaded crack in terms of edge dislocations with Burger's vector \vec{b}_y .

A dislocation of this type corresponds to a displacement discontinuity across the plane $y=0$ given by:

$$v(x,0^+) - v(x,0^-) = -b_y \quad (45)$$

where b_y is the magnitude of the Burger's vector \vec{b}_y and the minus sign comes from a conventional assumption stated before (in Section III.A)

Sliding Mode , Inplane Shear Crack

The sliding mode, Figure 7b, concerns a local deformation in which the crack surfaces glide over one another in opposite directions but in the same plane. For such an inplane shear crack, crack surface tractions are as follows:

$$\sigma_{yy}(x,0) = 0$$

$$\sigma_{xy}(x,0) = p_2(x) \quad (46a-b)$$

To satisfy these conditions, this time it is necessary to use edge dislocations whose Burger's vectors, \vec{b}_x , are in x -direction (27).

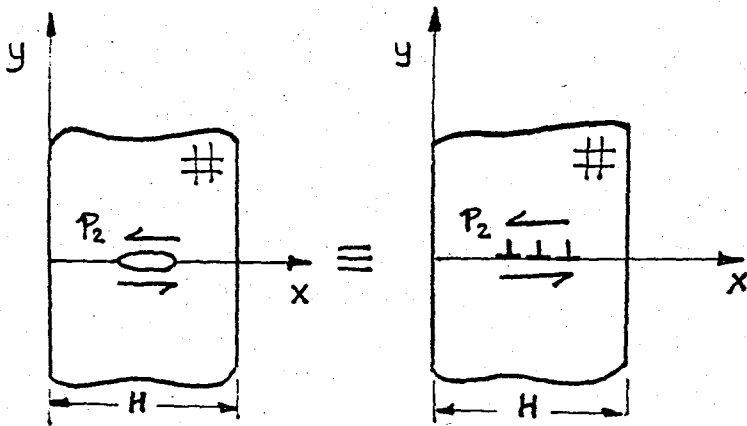


Figure 9. Representation of an inplane shear crack in terms of edge dislocations with Burger's vectors \vec{b}_x .

A dislocation of this type corresponds to a displacement discontinuity across $y=0$, given by:

$$u(x,0^+) - u(x,0^-) = -b_x \quad (47)$$

where b_x is the magnitude of the Burger's vector \vec{b}_y .

Tearing Mode , Anti-plane shear crack

Finally the movement of the crack surfaces associated with the tearing mode of fracture, Figure 7c, can be related to torsion effect in which the material points, initially in the same plane, occupy different planes after deformation. For such an anti-plane shear crack, crack surface tractions are

$$\sigma_{yz}(x,0) = p_3(x) \quad (48)$$

and it can be replaced by a distribution of screw dislocations whose displacement discontinuities are given by:

$$w(x,0^+) - w(x,0^-) = -b_z \quad (49)$$

but this mode of crack extension is not considered in

this study and details may be found in the study by Tupholme⁽²⁷⁾.

It follows that each of the three crack movements in Figure 7 is associated with a stress field in the vicinity of the crack edge. Consider an arbitrary point O on the border of a crack of some general shape and introduce a coordinate system with origin at O as shown in Figure 10.

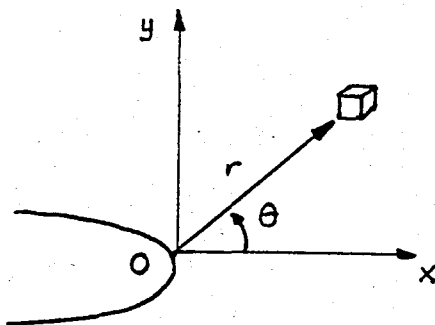


Figure 10. Coordinate system of crack front stress components

The three stress components σ_{yy} , σ_{xy} , and σ_{yz} at points on the x axis close to the origin take the simple forms⁽¹⁾,

$$\sigma_{yy} = \frac{k_1}{(2x)^{1/2}} + o(1)$$

$$\sigma_{xy} = \frac{k_2}{(2x)^{1/2}} + o(1)$$

$$\sigma_{yz} = \frac{k_3}{(2x)^{1/2}} + o(1) \quad (50a-c)$$

where the higher order terms in the variable x have been neglected. The three parameters k_1 , k_2 , k_3 are known as the stress intensity factors corresponding to the opening, sliding and tearing modes of fracture, respectively. As indicated in Equations(50a-c) the k -factors govern the intensity or magnitude of the local stresses and play an important role in the prediction of strength of bodies with cracks.

V. FORMULATION OF THE PROBLEMS (Singular Integral Equations)

A. Crack in an Orthotropic Strip Subjected to Uniform Tension (Opening Mode)

For a uniformly loaded crack in a strip, crack surface tractions are as follows:

$$\begin{aligned}\sigma_{yy}(x,0) &= -\sigma(x) \\ \sigma_{xy}(x,0) &= 0\end{aligned}\quad (51)$$

As stated before, a normally loaded crack can be represented by a distribution of edge dislocations whose Burger's vectors are in the y -direction (see Figure 5.). The stress expressions σ_{yy}^2 and σ_{xy}^2 for an edge dislocation with Burger's vector \vec{b}_y in an orthotropic strip are also given in section IV (equations 43a-b).

If we now define the discontinuity in the displacement derivatives by

$$\begin{aligned}f(x) &= \frac{\partial}{\partial x} [v(x,0^+) - v(x,0^-)] \\ g(x) &= \frac{\partial}{\partial x} [u(x,0^+) - u(x,0^-)]\end{aligned}\quad (52a-b)$$

where u, v are the displacement components in the x, y coordinate system. As the crack extends from b to c we obviously have

$$\begin{aligned}f(x) = g(x) &= 0 \quad \text{for } x > c, x < b \\ \int_b^c f(t) dt &= \int_b^c g(t) dt = 0 \quad \text{for } b < x < c\end{aligned}\quad (53a-b)$$

The singular integral equation of the problem will be obtained from the condition,

$$\sigma_{yy}(x,0) = -\sigma(x) \quad (54)$$

Replacing b_y with $f(t)dt$ and integrating from b to c one may express the integral equation of the problem as:
(See equations 43a-b)

$$\frac{E}{4\pi\sqrt{K^2-1}} \int_b^c f(t) \left\{ F_{yy}^d(x,0,t) + Q_2(0,x,t) - Q_2(0,H-x,H-t) + k_{f1}(x,0,t) \right\} dt = -\sigma(x) \quad (55a)$$

where $k_{f1}(x,0,t) = \int_0^\infty \frac{1}{D(\alpha)} \sum_{i=1}^8 [R_i(x,t,\alpha) - R_i(H-x,H-t,\alpha)] d\alpha$
and F_{yy}^d is previously defined by equation (27d).

Note that in the above integral equation if one takes $n \rightarrow \infty$ the integral equation of the half-plane problem will be obtained. A schematic representation of the superposition problem is given in Figure 11.

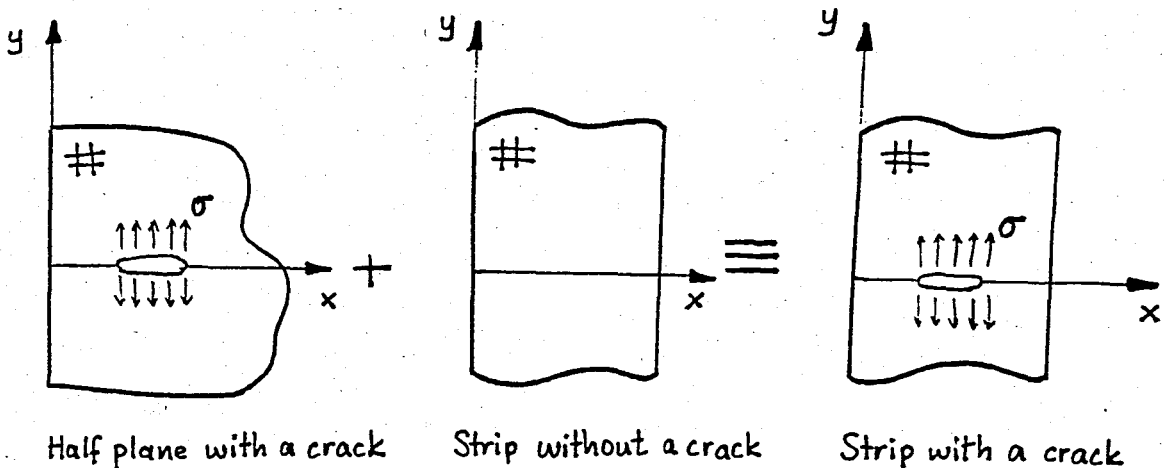


Figure 11. Schematic representation of the superposition problem which yields the strip solution.

As seen in the figure, 'half plane with a crack' part corresponds to the combined contribution,

$$F_{yy}^d(x,0,t) + Q_2(0,x,t)$$

whereas 'strip without a crack' part corresponds to,

$$-Q_2(0,H-x,H-t) + k_{f1}(x,0,t)$$

which becomes zero when H goes to infinity.

Using the Appendices E and F we can write the integral equation (55a) in a simple form as:

$$\frac{E}{\pi\sqrt{8(K+1)}} \int_b^c f(t) \left[\frac{1}{t-x} + k(x,t) \right] dt = -\sigma'(x) \quad (55b)$$

$b < x < c$

where $k(x,t) = \frac{1}{w_1 - w_2} \left[Q_2(0,x,t) - Q_2(0,H-x,H-t) + k_{f1}(x,0,t) \right],$

Q_2 is defined in Appendix E,

k_{f1} is defined in Appendix H,

w_1 and w_2 are the roots of the characteristic equation (29), the solution of which is given in Appendix I.

B. Crack in an Orthotropic Strip Subjected to Uniform Shear (Sliding Mode)

For a crack in a strip subjected to uniform shear, crack surface tractions are:

$$\begin{aligned}\sigma_{yy}(x,0) &= 0 \\ \sigma_{xy}(x,0) &= -\tau(x)\end{aligned}\quad (56a-b)$$

As discussed in Section IV, an inplane shear crack can be represented by a distribution of edge dislocations whose Burger's vectors are in the x-direction (see Fig.4). The stresses σ_{yy}^1 and σ_{xy}^1 for an edge dislocation with Burger's vector b_x in an orthotropic strip are already obtained (equations 37a-b).

Defining the discontinuity in the displacement derivatives as in equations (53a-b) again, replacing b_x by $g(t)dt$ and integrating from b to c , this time the integral equation of the problem will be obtained from the condition,

$$\sigma_{xy}(x,0) = -\tau(x) \quad (57)$$

and we obtain (see equations 37a-b):

$$\frac{E}{4\pi\sqrt{k^2-1}} \int_b^c g(t) \left\{ u_{xy}(x,0,t) + Q_8(0,x,t) - Q_8(0,H-x,H-t) + \bar{K}_{12}(x,0,t) \right\} = -\tau(x)$$

where $\bar{K}_{12}(x,0,t) = \int_0^\infty \frac{1}{D(\alpha)} \sum_{i=1}^8 [U_i(x,t,\alpha) - U_i(H-x,H-t,\alpha)]$

(58a)

and G_{xy}^d is previously defined by equation (27e).

Using the Appendices E and F, one may simplify the integral equation (58a) and get the form,

$$\frac{E}{\pi\sqrt{8(K+1)}} \int_b^c g(t) \left[\frac{1}{t-x} + \bar{k}(x,t) \right] dt = -\zeta(x) \quad (58b)$$

$b < x < c$

where $\bar{k}(x,t) = \frac{1}{w_1 - w_2} \left[Q_8(0,x,t) - Q_8(0,H-x,H-t) + \bar{K}_{12}(x,0,t) \right]$

Q_8 is defined in Appendix E,

w_1 and w_2 are the roots of the characteristic equation (29), the solution of which is given in Appendix I.

c. Orthotropic Rectangular Plate with an Edge Crack

The basic crack geometry under consideration is shown in Figure 12. It is assumed that $y=0$ is a plane of symmetry with respect to loading as well as crack geometry. The problems of the rectangular plate and the compact tension specimen are solved by letting $d=0$ and $e=H$. In this case both ends of the outer cracks are treated as if they are the free ends of an edge crack. In all the problems considered for this geometry, it is assumed that the tractions p_2 and p_3 on the surfaces of the outer cracks are zero.

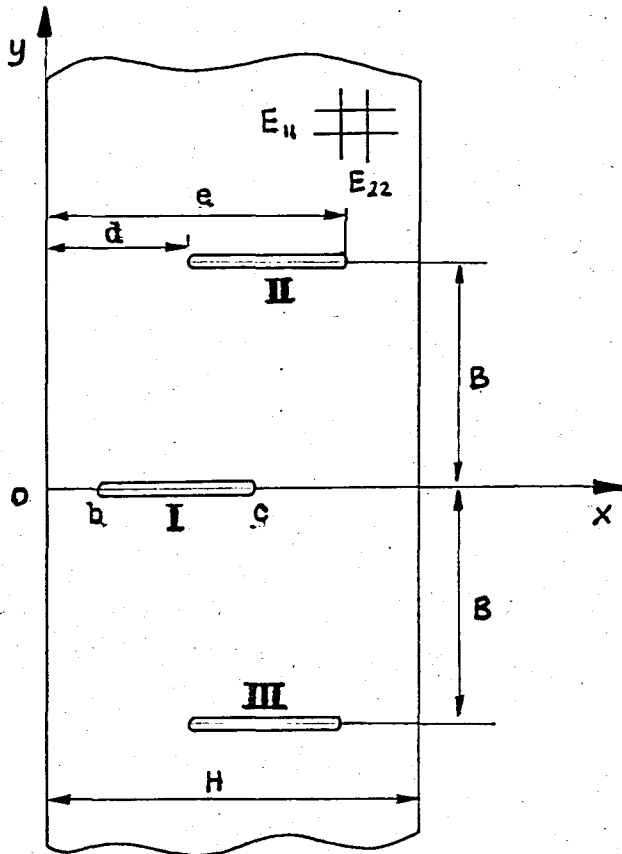


Figure 12. The basic crack geometry for an infinite orthotropic strip containing three line cracks.

For a pair of edge dislocations with densities g and h located at the point (x_0, y_0) , the discontinuity in the displacement derivatives may be expressed as⁽²⁵⁾:

$$\begin{aligned} g(x_0, y_0) &= \frac{\partial}{\partial x} [v(x, y_0^+) - v(x, y_0^-)] \\ h(x_0, y_0) &= \frac{\partial}{\partial x} [u(x, y_0^+) - u(x, y_0^-)] \end{aligned} \quad (59a-b)$$

Referring now to Figure 12. let $g(t), h(t)$ and $g(t), -h(t)$ be the density functions defined by (59a-b) for the cracks II and III, respectively, for which $c < t < e$, $y_0 = \pm B$. The strip also have an additional crack I along $b < x_0 = t < c$, $y_0 = 0$. Considering the symmetry of the problem, for crack I one may write ,

$$\begin{aligned} \frac{\partial}{\partial x} [u(x, 0^+) - u(x, 0^-)] &= h(x) = 0 \\ \frac{\partial}{\partial x} v(x, 0^+) &= -\frac{\partial}{\partial x} v(x, 0^-) = f(x), \quad b < x < c \end{aligned} \quad (60a-b)$$

Let the strip be subjected to the following crack surface tractions:

$$\sigma_{yy}(x, 0) = p_1(x), \quad \sigma_{xy}(x, 0) = 0 \quad (61a-b)$$

$$\sigma_{yy}(x, B) = \sigma_{yy}(x, -B) = p_2(x) \quad (62)$$

$$\sigma_{xy}(x, B) = \sigma_{xy}(x, -B) = p_3(x) \quad (63)$$

Substituting the combined stresses in the strip into the crack surface boundary conditions given above, one may obtain the system of integral equations to determine the functions f, g and h .

stress expressions related with each density function are obtained through the equations (37a-b) and (43a-b) replacing b_x by $h(t)dt$ and b_y by $g(t)dt$ and integrating from b to c or d to e . Stresses in the superimposed state must contain the following contributions:

From crack I : $g=f$ and $h=0$

From crack II : g and h

From crack III : g and $-h$

The schematic representation of the superposition problem is given in Figure 13.

$$\sigma_{yy}(x,0) = \begin{array}{|c|} \hline f \\ \hline \end{array} + \begin{array}{|c|} \hline +g \\ \hline \end{array} + \begin{array}{|c|} \hline +h \\ \hline \end{array} = p_1(x) \quad (64)$$

$$\sigma_{yy}(x,B) = \begin{array}{|c|} \hline +f \\ \hline \end{array} + \begin{array}{|c|} \hline g \\ \hline \end{array} + \begin{array}{|c|} \hline -h \\ \hline \end{array} = p_2(x) \quad (65)$$

$$\sigma_{xy}(x,B) = \begin{array}{|c|} \hline +f \\ \hline \end{array} + \begin{array}{|c|} \hline +g \\ \hline \end{array} + \begin{array}{|c|} \hline h \\ \hline \end{array} + \begin{array}{|c|} \hline -h \\ \hline \end{array} = p_3(x) \quad (66)$$

Figure 13. Schematic representation of the superimposed stress state.

Thus, equations (61a) and (64) yields the first integral equation as follows: (See equations 37a-b and 43a-b)

$$\begin{aligned}
 & \frac{1}{\pi} \int_b^c f(t) \left\{ Q_1(0, x, t) + Q_2(0, x, t) - Q_2(0, H-x, H-t) \right. \\
 & \quad \left. + \int_0^\infty \frac{1}{D(\alpha)} \sum_{i=1}^8 [R_i(x, t, \alpha) - R_i(H-x, H-t, \alpha)] d\alpha \right\} dt \\
 & + \frac{1}{\pi} \int_d^e g(t) \left\{ 2[Q_1(-B, x, t) + Q_2(-B, x, t) - Q_2(-B, H-x, H-t)] \right. \\
 & \quad \left. + \int_0^\infty \frac{1}{D(\alpha)} \sum_{i=1}^8 [R_i(x, t, \alpha) - R_i(H-x, H-t, \alpha)] \cos(\alpha B) d\alpha \right\} dt \\
 & + \frac{1}{\pi} \int_d^e h(t) \left\{ 2[Q_3(-B, x, t) + Q_4(-B, x, t) + Q_4(-B, H-x, H-t)] \right. \\
 & \quad \left. - \int_0^\infty \frac{1}{D(\alpha)} \sum_{i=1}^8 [S_i(x, t, \alpha) + S_i(H-x, H-t, \alpha)] \sin(\alpha B) d\alpha \right\} dt \\
 & = \frac{4\sqrt{K^2-1}}{E} p_1(x)
 \end{aligned}$$

or arranging the terms:

$$\begin{aligned}
 & \frac{1}{\pi} \int_b^c f(t) \left\{ \frac{1}{t-x} + k_{11}(x, t) \right\} dt + \frac{1}{\pi} \int_d^e k_{12}(x, t) g(t) dt \\
 & + \frac{1}{\pi} \int_d^e k_{13}(x, t) h(t) dt = \frac{\sqrt{8(K+1)}}{E} p_1(x)
 \end{aligned}$$

$b < x < c$

(67)

where the kernels $k_{1j}(x, t)$, ($j=1, 2, 3$) are given in App.G

The second integral equation may be derived using equations (62) and (65) as: (See equations 37a-b and 43a-b)

$$\begin{aligned}
 & \frac{1}{\pi} \int_b^c f(t) \left\{ Q_1(B, x, t) + Q_2(B, x, t) - Q_2(B, H-x, H-t) \right. \\
 & \quad \left. + \int_0^\infty \frac{1}{D(\alpha)} \sum_{i=1}^8 [R_i(x, t, \alpha) - R_i(H-x, H-t, \alpha)] \cos(\alpha B) d\alpha \right\} dt \\
 & + \frac{1}{\pi} \int_d^e g(t) \left\{ Q_1(0, x, t) + Q_2(0, x, t) - Q_2(0, H-x, H-t) \right. \\
 & \quad \left. + \int_0^\infty \frac{1}{D(\alpha)} \sum_{i=1}^8 [R_i(x, t, \alpha) - R_i(H-x, H-t, \alpha)] d\alpha \right. \\
 & \quad \left. + Q_1(2B, x, t) - Q_2(2B, x, t) - Q_2(2B, H-x, H-t) \right. \\
 & \quad \left. + \int_0^\infty \frac{1}{D(\alpha)} \sum_{i=1}^8 [R_i(x, t, \alpha) - R_i(H-x, H-t, \alpha)] \cos(2\alpha B) d\alpha \right\} dt \\
 & + \frac{1}{\pi} \int_d^e h(t) \left\{ Q_3(2B, x, t) + Q_4(2B, x, t) + Q_4(2B, H-x, H-t) \right. \\
 & \quad \left. + \int_0^\infty \frac{1}{D(\alpha)} \sum_{i=1}^8 [S_i(x, t, \alpha) + S_i(H-x, H-t, \alpha)] \sin(2\alpha B) d\alpha \right\} dt \\
 & = \frac{4\sqrt{K^2-1}}{E} p_2(x)
 \end{aligned}$$

or, arranging the terms:

$$\begin{aligned}
 & \frac{1}{\pi} \int_b^c k_{21}(x, t) f(t) dt + \frac{1}{\pi} \int_d^e g(t) \left\{ \frac{1}{t-x} + k_{22}(x, t) \right\} dt \\
 & \quad + \frac{1}{\pi} \int_d^e k_{23}(x, t) h(t) dt = \frac{\sqrt{8(K+1)}}{E} p_2(x) \\
 & \quad \quad \quad d < x < e \quad (68)
 \end{aligned}$$

where the kernels $k_{2j}(x, t)$, ($j=1, 2, 3$) are given in App.G

Finally, the third integral equation may be obtained using the equations (63) and (66) as: (See equations 37a-b and 43a-b)

$$\begin{aligned}
 & \frac{1}{\pi} \int_b^c f(t) \left\{ Q_5(B, x, t) + Q_6(B, x, t) + Q_6(B, H-x, H-t) \right. \\
 & \quad \left. + \int_0^\infty \frac{1}{D(\alpha)} \sum_{i=1}^8 [T_i(x, t, \alpha) + T_i(H-x, H-t, \alpha)] \sin(\alpha B) d\alpha \right\} dt \\
 & + \frac{1}{\pi} \int_d^e g(t) \left\{ Q_5(2B, x, t) + Q_6(2B, x, t) + Q_6(2B, H-x, H-t) \right. \\
 & \quad \left. + \int_0^\infty \frac{1}{D(\alpha)} \sum_{i=1}^8 [T_i(x, t, \alpha) + T_i(H-x, H-t, \alpha)] \sin(2\alpha B) d\alpha \right\} dt \\
 & + \frac{1}{\pi} \int_d^e h(t) \left\{ Q_7(0, x, t) + Q_8(0, x, t) + Q_8(0, H-x, H-t) \right. \\
 & \quad + \int_0^\infty \frac{1}{D(\alpha)} \sum_{i=1}^8 [U_i(x, t, \alpha) - U_i(H-x, H-t, \alpha)] d\alpha \\
 & \quad - Q_7(2B, x, t) - Q_8(2B, x, t) + Q_8(2B, H-x, H-t) \\
 & \quad \left. - \int_0^\infty \frac{1}{D(\alpha)} \sum_{i=1}^8 [U_i(x, t, \alpha) - U_i(H-x, H-t, \alpha)] \cos(2\alpha B) d\alpha \right\} dt \\
 & = \frac{4\sqrt{K^2-1}}{E} p_3(x)
 \end{aligned}$$

or, arranging the terms:

$$\begin{aligned}
 & \frac{1}{\pi} \int_b^c k_{31}(x, t) f(t) dt + \frac{1}{\pi} \int_d^e k_{32}(x, t) g(t) dt \\
 & + \frac{1}{\pi} \int_d^e h(t) \left\{ \frac{1}{t-x} + k_{33}(x, t) \right\} dt = \frac{\sqrt{8(K+1)}}{E} p_3(x) \\
 & \qquad \qquad \qquad d < x < e \quad (69)
 \end{aligned}$$

where the kernels $k_{3j}(x, t)$, ($j=1, 2, 3$) are given in App.G

thus, the combined stresses in the strip, the schematic representation of which is given in Figure 13, together with the crack surface boundary conditions (61a), (62) and (63) gives the system of integral equations to determine the functions f, g and h . Bringing together equations 67, 68 and 69; the system of integral equations is:

$$\frac{1}{\pi} \int_b^c f(t) \left\{ \frac{1}{t-x} + k_{11}(x, t) \right\} dt + \frac{1}{\pi} \int_d^e k_{12}(x, t) g(t) dt + \frac{1}{\pi} \int_d^e k_{13}(x, t) h(t) dt = \frac{\sqrt{8(K+1)}}{E} p_1(x), \quad b < x < c$$

$$\frac{1}{\pi} \int_b^c k_{21}(x, t) f(t) dt + \frac{1}{\pi} \int_d^e g(t) \left\{ \frac{1}{t-x} + k_{22}(x, t) \right\} dt + \frac{1}{\pi} \int_d^e k_{23}(x, t) h(t) dt = \frac{\sqrt{8(K+1)}}{E} p_2(x), \quad d < x < e$$

$$\frac{1}{\pi} \int_b^c k_{31}(x, t) f(t) dt + \frac{1}{\pi} \int_d^e k_{32}(x, t) g(t) dt + \frac{1}{\pi} \int_d^e h(t) \left\{ \frac{1}{t-x} + k_{33}(x, t) \right\} dt = \frac{\sqrt{8(K+1)}}{E} p_3(x), \quad d < x < e$$

(70a-c)

where the kernels $k_{ij}(x, t)$, $(i, j=1, 2, 3)$ are defined in Appendix G.

The complete solution of the problem is obtained once the density functions f, g, h are determined.

VI. NUMERICAL SOLUTION OF INTEGRAL EQUATIONS

The singular integral equation of the problem of a crack in an orthotropic strip subjected to uniform tension can simply be written as (see equation 55b);

$$\frac{E}{\pi\sqrt{8(K+1)}} \int_b^c f(t) \left[\frac{1}{t-x} + k(x,t) \right] dt = -\sigma(x) \quad (71)$$

$b < x < c$

together with the single valuedness condition of the displacements across the plane $y=0$,

$$\int_b^c f(t) dt = 0 \quad (72)$$

Applying the following variable transformation to convert the limits b and c to -1 and 1 (See Ref.18);

$$\zeta = \frac{2t}{c-b} - \frac{c+b}{c-b}$$

$$\xi = \frac{2x}{c-b} - \frac{c+b}{c-b}$$

$$w = \alpha H \quad (73a-c)$$

and defining,

$$g(\zeta) = \frac{E}{\sqrt{8(K+1)}} \frac{f(t)}{\sigma(x)} \quad (74)$$

the normalized singular integral equation takes the form:

$$\int_{-1}^{+1} \left[\frac{1}{\zeta - \xi} + \frac{c-b}{2} k(\xi, \zeta) \right] g(\zeta) d\zeta = -1 \quad (75)$$

$-1 < \xi < +1$

$$\int_{-1}^{+1} g(\zeta) d\zeta = 0 \quad (76)$$

A. Case of an Internal Crack

Following the procedure given in references (18) or (26), the solution of the singular integral equation (75) together with the single valuedness condition (76) will be as follows:

Since $g(z)$ has a power singularity $1/2$ at the end points, the solution will be sought in the form:

$$g(z) = \frac{F(z)}{\sqrt{1-z^2}} \quad (77)$$

where $F(z)$ is Hölder continuous in the interval $-1 < z < 1$ (See Ref.26). Using the Gauss-Chebyshev integration formula ;

$$\sum_{k=1}^n W_k F(z_k) \left[\frac{1}{z_k - \xi_i} + \frac{c-b}{2H} k(\xi_i, z_k) \right] = -1, \quad i=1, \dots, n-1$$

$$\sum_{k=1}^n W_k F(z_k) = 0 \quad (78a-b)$$

one may obtain an algebraic system of equations where:

$$W_1 = W_n = \frac{1}{2(n-1)}, \quad W_k = \frac{1}{n-1}, \quad k=2, \dots, n-1$$

$$z_k = \cos\left(\pi \frac{k-1}{n-1}\right), \quad k=1, \dots, n$$

$$\xi_i = \cos\left(\pi \frac{2i-1}{2n-2}\right), \quad i=1, \dots, n-1 \quad (79a-c)$$

From (78a-b) and (79a-c), n unknowns $F(z_k)$, $k=1, \dots, n$ can be solved.

For an internal crack, defining the stress intensity factors as⁽¹¹⁾,

$$k(b) = \lim_{x \rightarrow b} \sqrt{2(b-x)} \sigma_{yy}(x,0)$$

$$k(c) = \lim_{x \rightarrow c} \sqrt{2(x-c)} \sigma_{yy}(x,0) \quad (80a-b)$$

one may obtain the following expressions(see Ref.15):

$$\begin{aligned} k(b) &= \frac{E}{\sqrt{8(K+1)}} \lim_{x \rightarrow b} \sqrt{2(x-b)} f(x) \\ &= \frac{E}{\sqrt{8(K+1)}} F(-1) \sqrt{(c-b)/2} \end{aligned}$$

$$\begin{aligned} k(c) &= \frac{-E}{\sqrt{8(K+1)}} \lim_{x \rightarrow c} \sqrt{2(c-x)} f(x) \\ &= \frac{-E}{\sqrt{8(K+1)}} F(1) \sqrt{(c-b)/2} \end{aligned}$$

thus the final form of the normalized stress intensity factors are:

$$\frac{k(b)}{\sigma \sqrt{l}} = F(-1)$$

$$\frac{k(c)}{\sigma \sqrt{l}} = -F(1)$$

(81a-b)

where $l = (c-b)/2$

B. Case of an Edge crack

For the case of an edge crack, the normalized integral equation (75) will be the same but the single valuedness condition will not be valid any more.

When $b=0$ in the integral equation (55b), the first four terms, which are called generalized Cauchy kernels, blow up. In this case, at the end $x=c$, $g(z)$ will have a power singularity $1/2$ but at $x=b=0$ there will not be any singularity.

The only singular point is when $z=1$ and it has been shown⁽¹¹⁾ that, this time the solution will be sought in the form:

$$g(z) = \frac{R(z)}{\sqrt{1-z}} \quad (82)$$

Furthermore it is proposed to consider another form which gives better convergence⁽¹⁵⁾ as,

$$g(z) = \frac{N(z)}{(1-z)^{1/2}(1+z)^{1/2}} \quad (83)$$

and instead of equation (76), the following condition will be used:

$$N(-1) = 0 \quad (84)$$

Substituting equations (83) and (84) into equation (75) and applying the Gauss-Chebyshev formula, the following system of algebraic equations can be obtained:

$$\sum_{k=1}^n W_k N(z_k) \left[\frac{1}{z_k - \xi_i} + \frac{c-b}{2H} k(\xi_i, z_k) \right]_{i=1, \dots, n-1} = -1$$

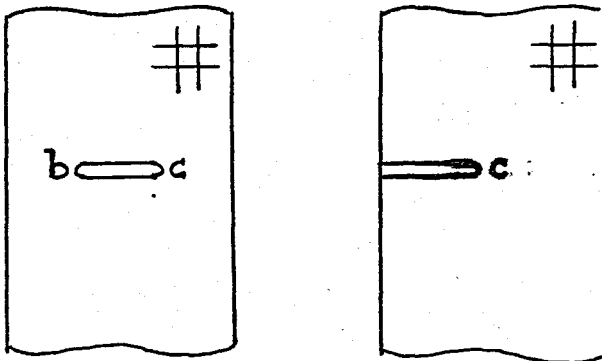
$$N(z_n) = 0 \quad (85a-b)$$

where W_k and z_k , $k=1, \dots, n$ and ξ_i , $i=1, \dots, n-1$ are the same as they are in equations (79a-c).

From the above system of equations, the unknowns $N(Z_k)$, $k=1, \dots, n$ can be found and the stress intensity coefficient is given by (see Ref.15):

$$\frac{k(c)}{\sigma\sqrt{c}} = -\frac{N(1)}{\sqrt{2}} \quad (86)$$

Stress intensity factors for an internal and an edge crack in an orthotropic strip in terms of the functions F and N are shown in Figure 14.



$$\frac{k(b)}{\sigma\sqrt{\ell}} = F(-1)$$

$$\frac{k(c)}{\sigma\sqrt{\ell}} = -F(1)$$

$$\frac{k(c)}{\sigma\sqrt{c}} = -\frac{N(1)}{\sqrt{2}}$$

Figure 14. Stress intensity factors for an internal and an edge crack in an orthotropic strip, obtained from the algebraic system of equations (78a-b) and (85a-b), respectively.

$$\ell = (c-b)/2$$

The computer programs used for the numerical calculation of the stress intensity factors are presented in Appendix K.

The first program is used to calculate the stress intensity factors for a transverse crack in an orthotropic strip subjected to uniform tension at crack faces. For the uniform shear case it is necessary—and sufficient—to change subroutine XKERH.

The second program gives the stress intensity factor values for a rectangular orthotropic plate containing an edge crack and subjected to uniform tension at crack faces.

For both programs, the material elastic constants $E_{11}, E_{22}, G_{12}, \mu_{12}$ and the geometry of the crack (crack length b, c for the strip; b, c, d, e for the plate) are given as data and the stress intensity factors are found as some specific values of the functions F or N (see Figure 14).

VII. RESULTS AND DISCUSSION

The singular integral equations (55b) and (58b) of the strip problem and the system of integral equations (70a-c) of the plate problem is solved numerically by normalizing the interval (b,c) or (d,e) to $(-1,1)$ and then using the numerical solution procedure outlined in Section VI. Stress intensity factors are obtained and tabulated for various crack geometries and compared with isotropic values.

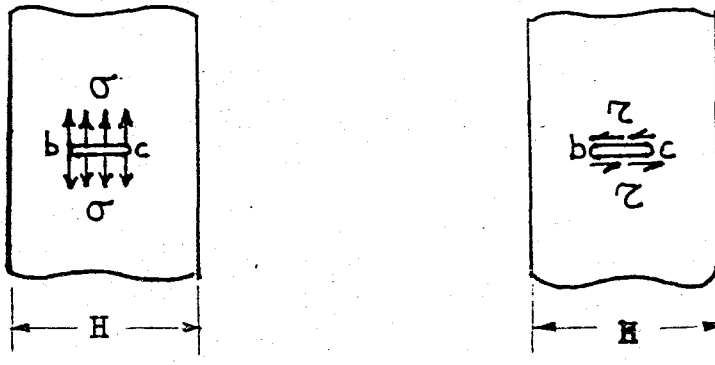
As a specific case of the plate problem, numerical results for a double cantilever beam (DCB) specimen is obtained and compared with that of a finite element solution given by Mandel et.al.⁽³²⁾. Finally the standard compact tension specimen (CTS) is simulated and after the verification of isotropic results given by Civelek and Erdoğan⁽²⁵⁾, stress intensity factors for the orthotropic case are obtained for various crack lengths within a practically useful range.

Table 1 shows the different elastic material constants used throughout the analysis similar to those used by Kaya and Erdoğan⁽¹⁸⁾. As it is the case in references (16) and (18), the present formulation is also done only for orthotropic materials of type I (see Appendix I). Just for comparison purposes which will be discussed later (Figures 18 and 19, Table 3), a material of type II is also included in Table 1.

Although the computations are done for generalized plane stress case only, the results for plane strain case can be obtained by redefining the elastic constants.

Figure 15 shows the two loading conditions considered for the cracked strip and plate. These are uniform tension and uniform shear applied at crack faces.

For each loading condition, stress intensity factors are normalized with respect to an appropriate term, $(\text{stress})\sqrt{\ell}$, where ℓ is the half crack length for internal cracks and crack length for edge cracks. Stress is σ for uniform tension and τ for uniform shear applied at crack faces. Throughout the analysis H is assumed to be constant.



(a) Uniform tension

(b) Uniform shear

Figure 15. Loading conditions considered in the analysis.

(a) Strip containing an internal crack

Table 2 gives the stress intensity factors in an orthotropic strip of material I for different lengths and location of an internal crack subjected to uniform tension and uniform shear. Four different b/H values are taken (0.1, 0.2, 0.3, 0.4) and c/H is varied up to 0.9. Referring to Figure 15, it is seen that the crack extends from b to c in a strip of width H where $k_1(b)$ and $k_1(c)$ are the stress intensity factors at the corresponding crack tips, the subscripts 1 and 2 denoting the normalization with respect to $\sigma\sqrt{\ell}$ and $\zeta\sqrt{\ell}$, respectively, where ℓ is the half crack length given by $(c-b)/2$. As seen in the table, $k_1(b)$ and $k_1(c)$ corresponding to uniform tension are in good agreement with those given in reference (18), while $k_2(b)$ and $k_2(c)$ corresponding to uniform shear are not available in literature.

Figures 16 and 17 shows the dependence of the stress intensity factors on c/H for a fixed b/H value. Thus, one end of the crack is fixed at $b/H=0.2$ and the length is changed by varying c/H . The figures are drawn only for $b/H=0.2$ but one may obtain similar figures for various b/H values. As seen in both figures, in general, $k_1(b), k_1(c)$ corresponding to uniform tension and $k_2(b), k_2(c)$ corresponding to uniform shear increase with increasing c/H values. The values of $k_1(b)$ and $k_2(b)$ are higher than $k_1(c)$ and $k_2(c)$ up to a certain value

of c/H where the crack becomes symmetric and stress intensity factors at both ends become equal to each other. Increasing c/H further reverses the situation and this time $k_1(c)$ and $k_2(c)$ become greater than the others. Thus the crack tip which is closer to the strip boundary has the greater stress intensity factor (SIF) value. Also note that for an infinitely small crack, which means in the limit when $c/H \rightarrow 0.2 (=b/H)$, the SIF value tends to 1.0 which corresponds to the case of 'no crack' as expected.

Three different materials are compared in Table 3 to obtain some idea about the degree of influence of the material orthotropy on the stress intensity factors and SIF for a symmetric internal crack of various lengths subjected to uniform tension and uniform shear are tabulated. Material II is an orthotropic material of type I ($K^2 > 1$) with $K=9.98$ and $\delta=0.75$, material III is isotropic with $K=\delta=1$, the column taken from Delale and Erdogan⁽¹⁷⁾ represents an orthotropic material of type II ($K^2 < 1$) with $K=0.70$ and $\delta=0.75$ and elastic constants of all three are given in Table 1. SIF values given in Table 3 indicate that the results for the orthotropic strip are different than the isotropic results. For approximately the same stiffness ratios, $\delta = (E_{11}/E_{22})^{1/4} = 0.75$, depending on the remaining material constants, the materials may be of different type and SIF may be greater (in this case, in material type II) or smaller (in material type I) than the isotropic values. In orthotropic materials there are four independent material constants; E_{11}, E_{22}, G_{12} and ν_{12} . But when the new material parameters, namely, E, ν, δ, K proposed by Krenk⁽²⁴⁾ are used, the resulting field equation (23) contains only the shear parameter K , which includes E and ν by definition, and it is independent of the stiffness ratio δ .

On the other hand, it is known that if the crack is perpendicular to the boundaries of an infinite orthotropic strip and if the external loads are independent of the coordinate axis parallel to the boundaries, then the SIF values turn out to be invariant with respect to a 90-degree material rotation⁽¹⁷⁾. That's why the SIF related to Material II ($\delta=0.75$) in Table 3 are identical

with that of Material I ($\delta = 1/0.75 = 1.33$) given in Table 2 for similar crack geometries.

In Figure 18, values for a symmetric internal crack subjected to uniform tension are graphed as a function of half crack length-to-width ratio, l/H . As seen, SIF for a material of type II is slightly greater but for a material of type I significantly smaller than that of the isotropic values and the difference increases as the crack length increases. In the limit when $l/H \rightarrow 0$, SIF for all the three materials tend to 1.0 which corresponds to the case 'strip with no cracks'.

In Figure 19, crack face is assumed to be subjected to uniform shear and one may make a similar comparison between the isotropic and orthotropic SIF values but this time there exist a single type of orthotropic material (only type I) since the results for the other type are not available in literature.

In general, it seems that for an orthotropic material depending on the material constants, if the shear parameter K is so that, $K^2 > 1$, then stress intensity factors are smaller than the isotropic ones, while they increase a little bit when $K^2 < 1$. At this stage it will be interesting to examine the effect of K on the SIF values of a specific type of an orthotropic material (either I or II) and this is done for a material of type I containing an edge crack for two different crack lengths and will be discussed later (Table 6, Figure 22).

(b) Strip containing an edge crack

The case of an edge crack is a more important problem than the internal crack due to the fact that for experimental applications an edge-cracked specimen is more practical.

An edge crack is considered in an isotropic strip in Table 4 and in an orthotropic strip in Table 5, under the loading conditions of uniform tension and uniform shear. For $b/H = 0$, SIF are tabulated for increasing c/H values. As seen in the tables, the values found are in good agreement with the previously found values but the case of uniform shear applied to a crack in an ortho-

pic strip (Table 5) is not available in literature.

Figures 20 and 21 shows this relation between the SIF values and crack length c/H for a strip containing an edge crack, for Material III (Isotropic) and Material I (Orthotropic), respectively. As a general rule for an edge crack perpendicular to the sides of the strip subjected to either uniform tension or uniform shear, one may say that, k_1 is always greater than k_2 and as crack length increases k_1 is highly increased whereas k_2 increases slightly. In the limit when $c/H \rightarrow 0$ both k_1 and k_2 tend to infinite plane values given in reference (33). As discussed in the internal crack case, since $K^2 > 1$ for a material of type I, both k_1 and k_2 values given in Table 4 are slightly smaller than that of the isotropic ones given in Table 5.

In Table 6 a comparison is made for an edge crack of $b/H = 0.0$ and $c/H = 0.001$ or 0.5 for five different materials given in Table 1. As seen in Figure 22, for a very small crack of length 0.001 , k_1 and k_2 values coincide but for a crack of length 0.5 , k_1 is highly increased when compared to k_2 . But no matter what the crack length is, the effect of K on the stress intensity factors does not seem to be of significant importance. Thus, one may conclude that, it is not K but K^2 's being smaller or greater than one is the characteristic property in affecting the stress intensity factors. If $K^2 > 1$ the material is of type I and the SIF values are smaller than the isotropic ones, but if $K^2 < 1$ then it is of type II and the SIF values are slightly greater, but for a specific type, K has no significant effect.

(c) Plates containing edge cracks

The problems of the rectangular or square plate and the compact tension specimen (CTS) are solved by taking three line cracks in a strip under uniform tension. The middle crack is kept (from b to c) while the outer cracks are extended to meet the boundaries of the strip ($d=0, e=H$). In this case, both ends of the outer cracks are treated as if they are free ends of an edge crack.

In all the problems considered for this geometry, it is assumed that the tractions p_2 and p_3 on the surfaces of the outer cracks are zero.

In Table 7, SIF values versus the crack length c/H are given for an edge crack in an orthotropic square plate of Material I with a fixed half length-to-width ratio, $B/H=0.5$, subjected to uniform tension. As seen in Figure 23, the relation between k_1 and c/H is similar to that discussed in the strip case of Figure 21. SIF values increase as the crack length increases but for a specific crack length they are greater for the plate case than the strip case. In the limit when $c/H \rightarrow 0$ they tend to the infinite plane value given in reference (33).

In Table 8, the effect of half length-to-width ratio, B/H , on the stress intensity factors for an orthotropic plate of Material I containing an edge crack of a fixed length, $c/H=0.1$, is considered. As seen in Figure 24, for $B/H > 2$ the resulting SIF value is practically the same as that found for an infinite strip with an edge crack (see Table 5). As expected, when the length of the plate is decreased the existence of the crack becomes more and more effective and in the limit when $B/H \rightarrow 0$ the stress intensity factor value become unbounded.

(d) Double Centilever Beam specimen(DCB)

The geometry of the double centilever beam specimen and the elastic material constants used in the finite element solution by Mandel et.al.⁽³²⁾ are given in Appendix J. Taking into consideration the difference in the normalization procedures (see Appendix J), the stress intensity factors are given in Table 9 for various crack lengths. As seen in Figure 25, the data from experimental compliance calibration and the finite element solution given by Mandel et. al. are compared with the SIF values obtained in the present study. The figure indicates that the present formulation covers a wider range of crack lengths and it seems to be more reliable since in the finite element solution mesh size requirements and especially the crack tip mesh dimensions are important

(e) Compact tension specimen(CTS)

The remaining results in this study concern an edge cracked rectangular plate having the dimensions of a compact tension specimen subjected to a pair of concentrated forces. The standard geometry of the CTS is given in Figure 26.

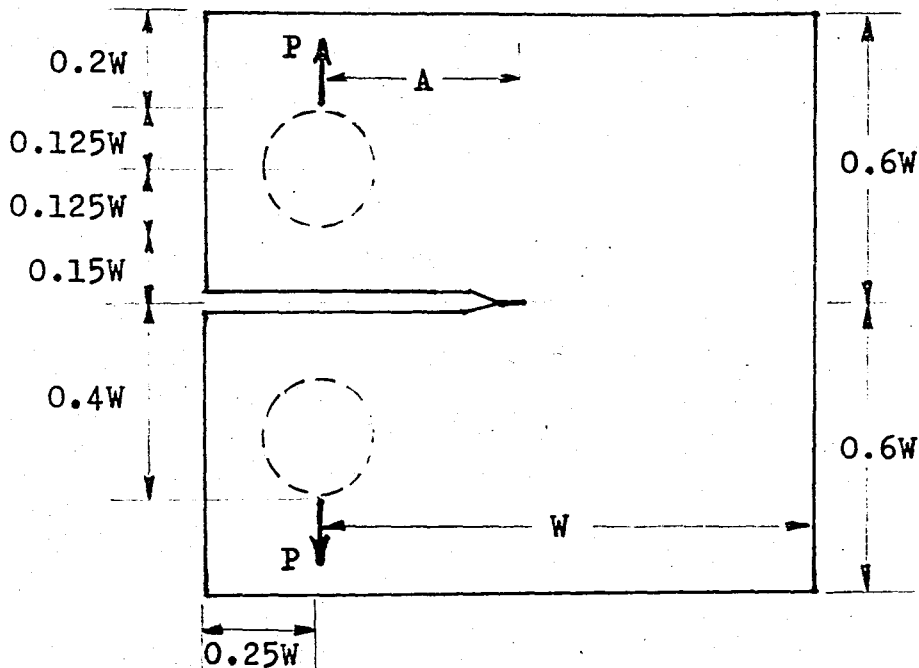


Figure 26. Notation for the compact tension specimen(CTS).

Note that $W=0.8H$, $B=0.48H$, the load distance in y direction $n=0.32H$ and the load distance in x direction $m=0.2H$. As it is stated in the study of Civelek and Erdogan⁽²⁵⁾ for the isotropic case, the effect of the load distance in y direction(n) on the stress intensity factors is rather insignificant but it is not the case for the load distance in x direction(m). Thus, an approximation to the CTS problem in an orthotropic medium by treating the forces as if they act at crack faces do not change the stress intensity factors significantly.

Table 10 gives a comparison with isotropic CTS values given in reference (25). As seen the agreement is quite good. Finally in table 11 and Figure 27, stress intensity factors for an orthotropic CTS are given for various crack lengths within a practically useful range which are not available in literature.

Table 1: The Material Elastic Constants

MATERIAL	E_x (N/m ²)	E_y (N/m ²)	G_{xy} (N/m ²)	μ_{xy}
I	170.65×10^9	55.16×10^9	4.83×10^9	0.1114
II	55.16×10^9	170.65×10^9	4.83×10^9	0.036
III (Iso)	154.77×10^9	155.83×10^9	59.68×10^9	0.3
IV	223.40×10^9	24.13×10^9	8.48×10^9	0.23
V	37.92×10^9	187.54×10^9	4.83×10^9	0.022
VI	4.55×10^9	17.38×10^9	2.00×10^9	0.0838
Ref. (II) (type II)	21.37×10^9	66.88×10^9	17.93×10^9	0.2

Table 2: The stress intensity factors in an orthotropic strip of material I subjected to uniform tension and uniform shear.

$$l = (c-b)/2 \quad a) \frac{b}{H} = 0.1$$

$\frac{c}{H}$	Uniform Tension				Uniform Shear	
	$\frac{k_1(b)}{\sigma\sqrt{l}}$	Ref.(18)	$\frac{k_1(c)}{\sigma\sqrt{l}}$	Ref.(18)	$\frac{k_2(b)}{\tau\sqrt{l}}$	$\frac{k_2(c)}{\tau\sqrt{l}}$
0.1001	1.0000	1.0000	1.0000	1.0000	1.0000	1.0000
0.2	1.0385	1.0385	1.0295	1.0296	1.0225	1.0166
0.3	1.1170	1.1172	1.0757	1.0758	1.0648	1.0422
0.4	1.2119	1.2122	1.1181	1.1183	1.1165	1.0726
0.5	1.3101	1.3106	1.1509	1.1512	1.1772	1.1112
0.6	1.4020	1.4027	1.1772	1.1775	1.2501	1.1637
0.7	1.4816	1.4826	1.2129	1.2133	1.3413	1.2408
0.8	1.5498	1.5510	1.3033	1.3040	1.4640	1.3696
0.9	1.6224	1.6241	1.6224	1.6241	1.6550	1.6550

Table 2: (cont.)

b) $\frac{b}{H} = 0.2$

$\frac{c}{H}$	Uniform Tension				Uniform Shear	
	$\frac{k_1(b)}{\sigma\sqrt{l}}$	Ref.(18)	$\frac{k_1(c)}{\sigma\sqrt{l}}$	Ref.(18)	$\frac{k_2(b)}{\tau\sqrt{l}}$	$\frac{k_2(c)}{\tau\sqrt{l}}$
0.2001	1.0000	1.0000	1.0000	1.0000	1.0000	1.0000
0.3	1.0154	1.0154	1.0128	1.0129	1.0089	1.0078
0.4	1.0493	1.0494	1.0355	1.0355	1.0306	1.0254
0.5	1.0907	1.0909	1.0684	1.0584	1.0626	1.0515
0.6	1.1340	1.1342	1.0835	1.0836	1.1056	1.0891
0.7	1.1774	1.1778	1.1253	1.1255	1.1630	1.1460
0.8	1.2259	1.2264	1.2259	1.2264	1.2431	1.2431
0.9	1.3033	1.3040	1.5498	1.5510	1.3696	1.4640

Table 2: (cont.)

c) $\frac{b}{H} = 0.3$

$\frac{c}{H}$	Uniform Tension				Uniform Shear	
	$\frac{k_1(b)}{\sigma\sqrt{l}}$	Ref.(18)	$\frac{k_1(c)}{\sigma\sqrt{l}}$	Ref.(18)	$\frac{k_2(b)}{\tau\sqrt{l}}$	$\frac{k_2(c)}{\tau\sqrt{l}}$
0.3001	1.0000	1.0000	1.0000	1.0000	1.0000	1.0000
0.4	1.0078	1.0079	1.0068	1.0068	1.0059	1.0056
0.5	1.0260	1.0261	1.0208	1.0208	1.0223	1.0207
0.6	1.0503	1.0504	1.0414	1.0415	1.0489	1.0463
0.7	1.0810	1.0811	1.0810	1.0811	1.0882	1.0882
0.8	1.1253	1.1255	1.1774	1.1778	1.1460	1.1630
0.9	1.2129	1.2133	1.4816	1.4826	1.2408	1.3413

Table 2: (cont.)

d) $\frac{b}{H} = 0.4$

$\frac{c}{H}$	Uniform Tension				Uniform shear	
	$\frac{k_1(b)}{\sigma\sqrt{L}}$	Ref.(18)	$\frac{k_1(c)}{\sigma\sqrt{L}}$	Ref.(18)	$\frac{k_2(b)}{\tau\sqrt{L}}$	$\frac{k_2(c)}{\tau\sqrt{L}}$
0.4001	1.0000	1.0000	1.0000	1.0000	1.0000	1.0000
0.5	1.0049	1.0049	1.0046	1.0046	1.0050	1.0049
0.6	1.0182	1.0182	1.0182	1.0182	1.0199	1.0199
0.7	1.0414	1.0415	1.0503	1.0504	1.0463	1.0489
0.8	1.0835	1.0836	1.1340	1.1342	1.0891	1.1056
0.9	1.1772	1.1775	1.4020	1.4027	1.1637	1.2501

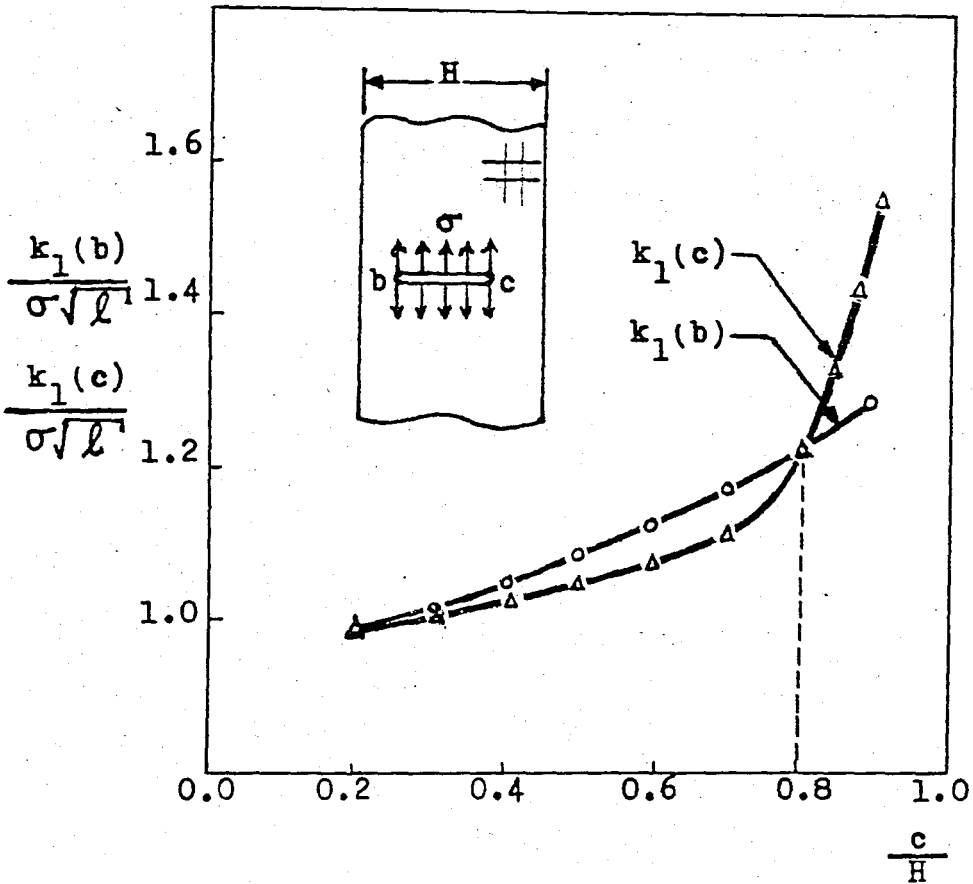


Figure 16. The stress intensity factors for an internal crack in an orthotropic strip of material 1 subjected to uniform tension. $b/H=0.2$, $l=(c-b)/2$

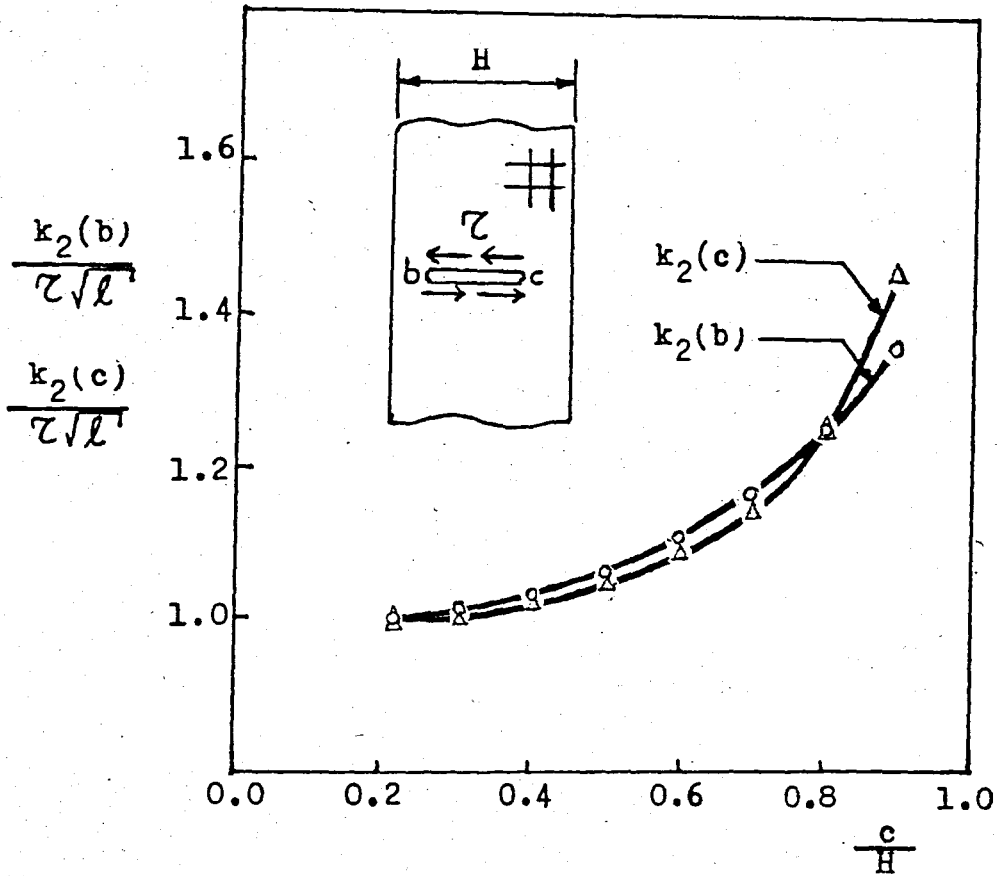


Figure 17. The stress intensity factors for an internal crack in an orthotropic strip of material I subjected to uniform shear. $b/H=0.2$, $l=(c-b)/2$

Table 3: Comparison of the stress intensity factors for a symmetric internal crack subjected to uniform tension or uniform shear for three different materials(see Table 1).

$$l = (c-b)/2$$

	Uniform Tension			uniform Shear		
	$k_1/\sigma\sqrt{l}$			$k_2/\tau\sqrt{l}$		
$\frac{l}{H}$	Mat. II (Type I) $K=9.98$ $\delta=0.75$	Mat. III (Isotr.) $K=1=\delta$	Ref. (17) (Type II) $K=0.70$ $\delta=0.75$	Mat. II (Type I) $K=9.98$ $\delta=0.75$	Mat. III (Isotr.) $K=1=\delta$	Ref. (17) (Type II) $K=0.70$ $\delta=0.75$
0.001	1.0000	1.0000	1.0000	1.0000	1.0000	-
0.1	1.0182	1.0246	1.0261	1.0199	1.0274	-
0.2	1.0810	1.1094	1.1155	1.0882	1.1201	-
0.3	1.2259	1.3033	1.3183	1.2431	1.3245	-
0.4	1.6224	1.8160	1.8471	1.6550	1.8435	-

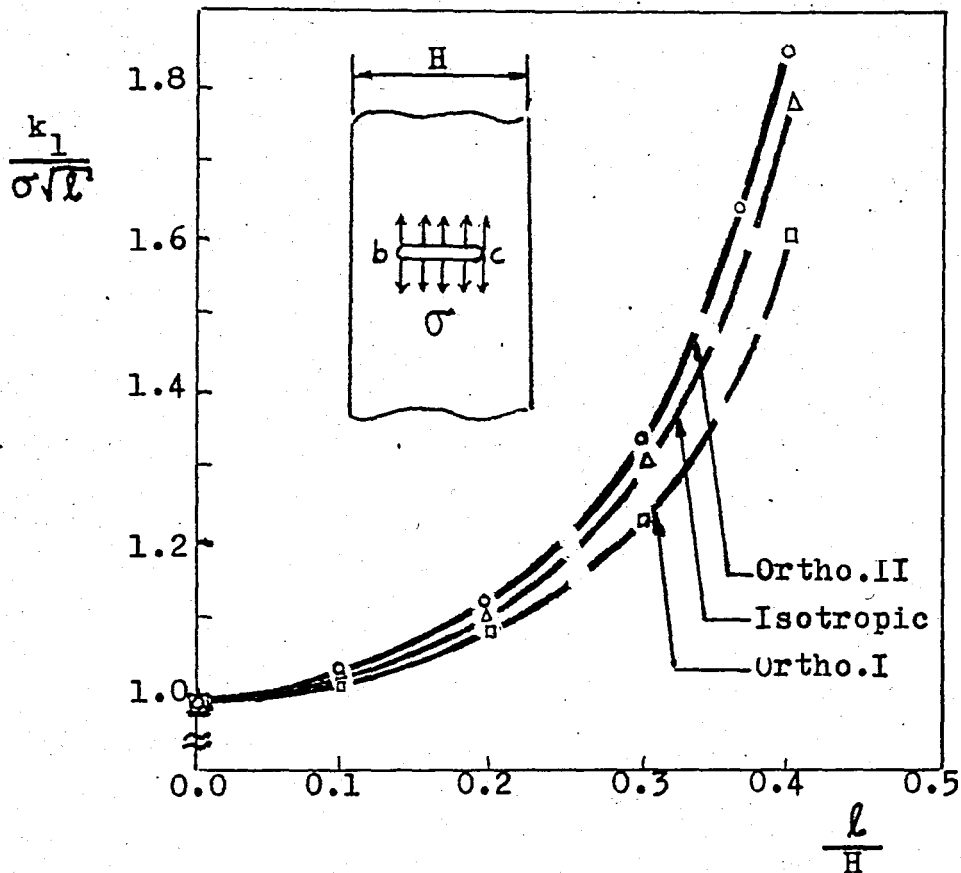


Figure 18. Comparison of the stress intensity factors for a symmetric internal crack subjected to uniform tension for three different materials

$$l = (c-b)/2$$

Ortho.II = Orthotropic, type II

Isotropic = Material III

Ortho.I = Orthotropic, type I, mat. I

See Table 1. for the above materials.

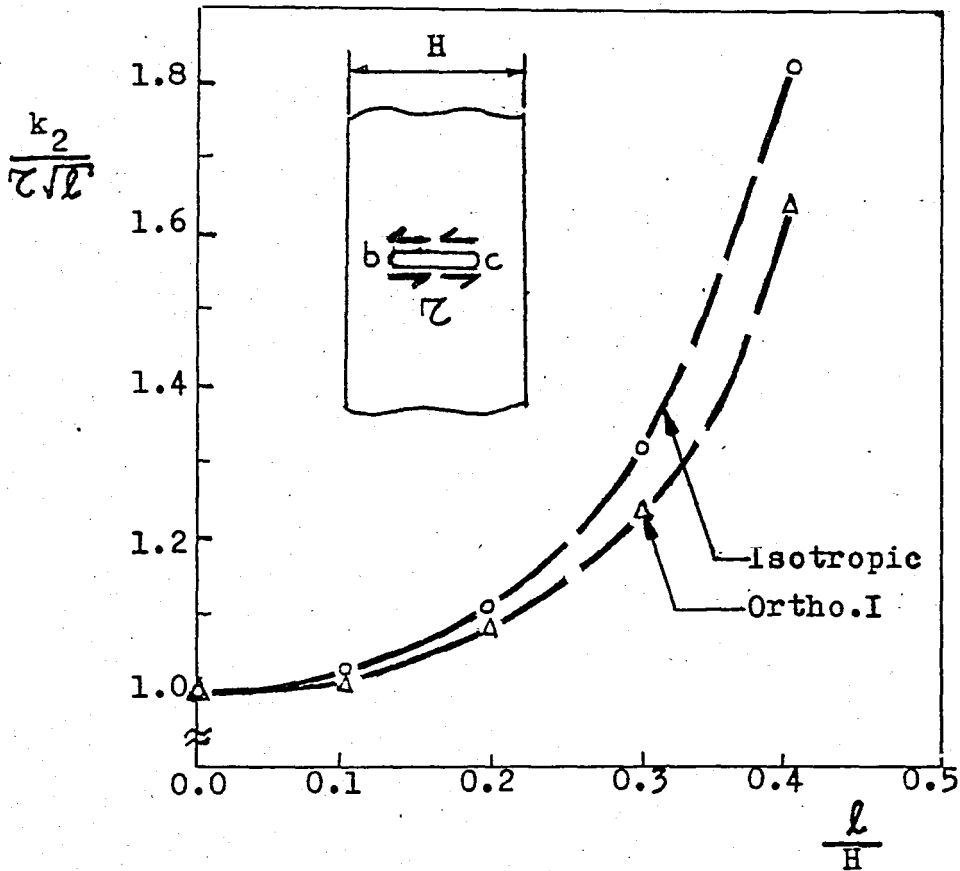


Figure 19. Comparison of the stress intensity factors for a symmetric internal crack subjected to uniform shear for three different materials (Table I)

$$l = (c-b)/2$$

Isotropic = Material III

Ortho.I = Orthotropic, Mat.I, type I

See Table 1. for the above two materials.

Table 4: The stress intensity factors for an edge crack in an isotropic strip of material III subjected to uniform tension and uniform shear.

$$\frac{b}{H} = 0.0$$

$\frac{c}{H}$	Uniform Tension		Uniform Shear	
	$\frac{k_1}{\sigma\sqrt{c}}$	Ref. (18)	$\frac{k_2}{\tau\sqrt{c}}$	Ref. (33)
0.001	1.1220	1.1216	1.1220	—
0.1	1.1897	1.1893	1.1224	1.1221
0.2	1.3682	1.3674	1.1269	1.1266
0.3	1.6615	1.6601	1.1424	1.1420
0.4	2.1151	2.1119	1.1768	1.1765
0.5	2.8339	2.8258	1.2396	1.2394
0.6	3.8871	4.035	1.3456	1.3451
0.7	6.1280	6.361	1.5236	1.5231
0.8	11.7384	11.988	1.8468	1.8463

Table 5: The stress intensity factors for an edge crack in an orthotropic strip of material I subjected to uniform tension and uniform shear.

$$\frac{b}{H} = 0.0$$

$\frac{c}{H}$	Uniform Tension		Uniform shear	
	$\frac{k_1}{\sigma\sqrt{c}}$	Ref. (18)	$\frac{k_2}{\tau\sqrt{c}}$	-
0.001	1.0412	1.0411	1.0412	no data available in the literature
0.1	1.1290	1.1284	1.0425	
0.2	1.3186	1.3172	1.0509	
0.3	1.6095	1.6069	1.0705	
0.4	2.0462	2.0421	1.1051	
0.5	2.7223	2.7199	1.1611	
0.6	3.8656	3.859	1.2494	
0.7	6.0498	6.035	1.3936	
0.8	11.3426	11.274	1.6556	

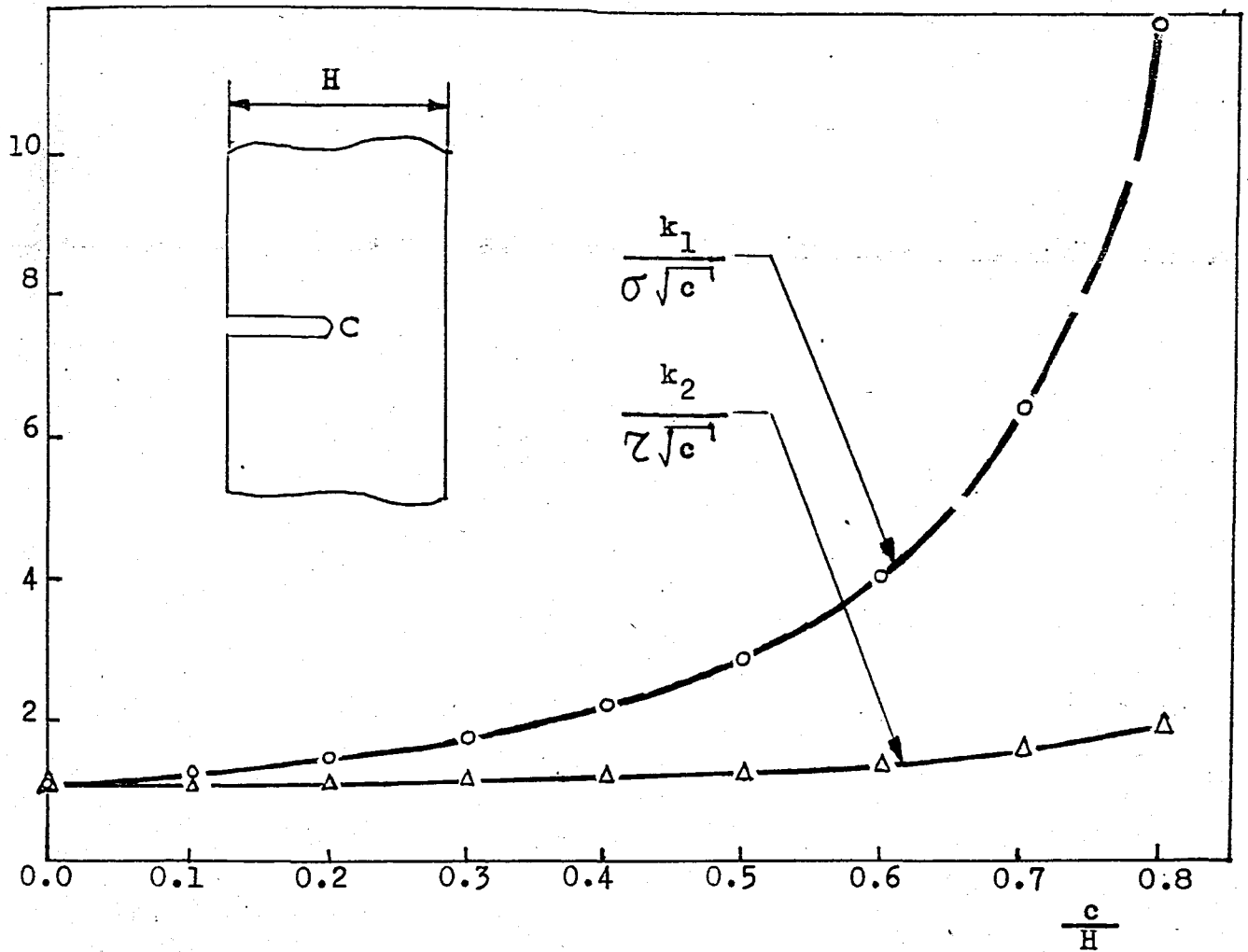


Figure 20. The stress intensity factors for an edge crack in an isotropic strip of material III subjected to uniform tension and uniform shear. $b/H = 0.0$

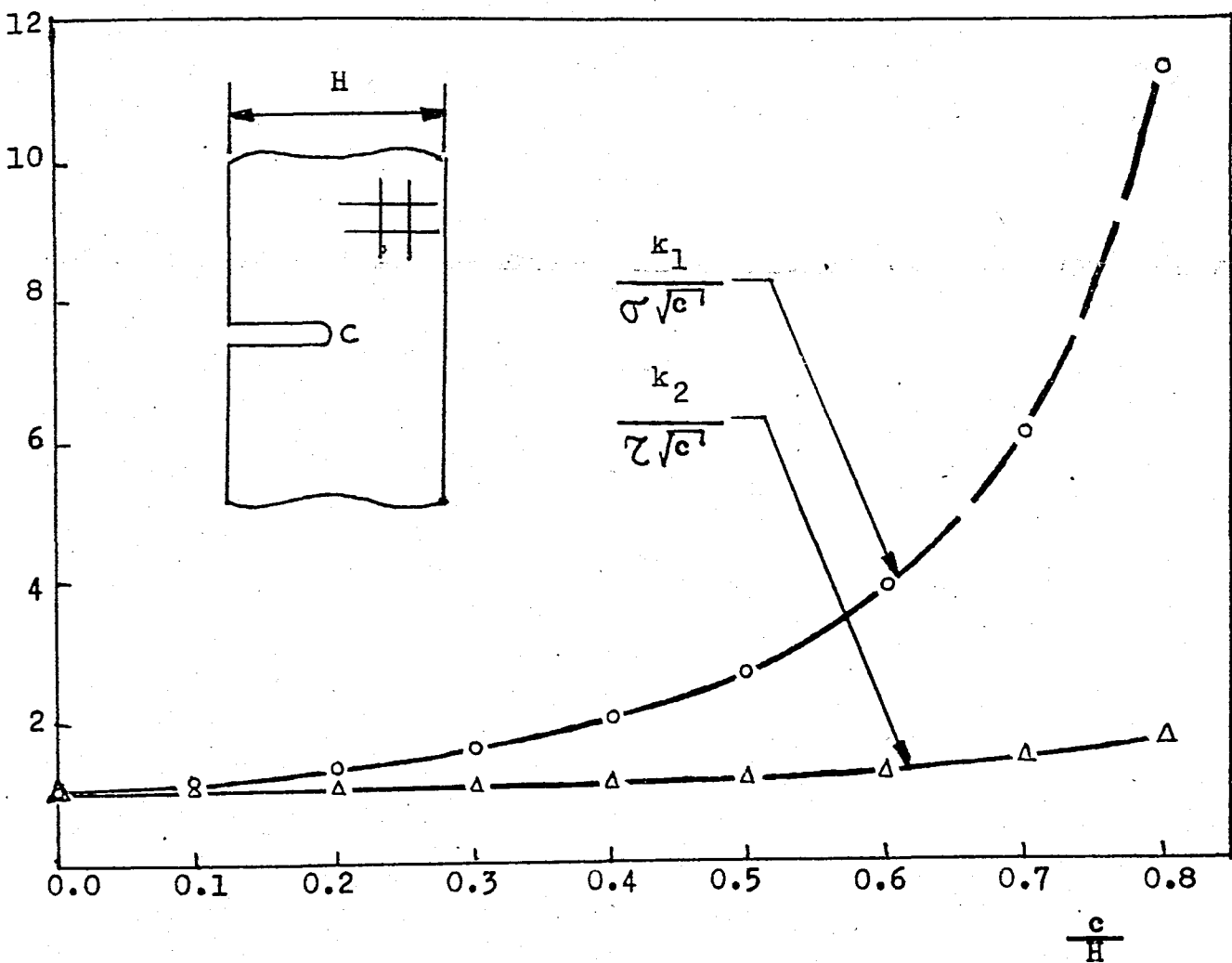


Figure 21. The stress intensity factors for an edge crack in an orthotropic strip of material I subjected to uniform tension and uniform shear. $b/H=0.0$

Table 6: Comparison of the stress intensity factors for an edge crack in a strip of different materials subjected to uniform tension and uniform shear (the effect of K on stress intensity factors).

$$\frac{b}{H} = 0.0$$

MATERIAL	SHEAR PARAMETER K	c/H = 0.001		c/H = 0.5	
		Unif.Tension	Unif.Sheer	Unif.Tension	Unif.Sheer
		$\frac{k_1}{\sigma\sqrt{c}}$	$\frac{k_2}{\tau\sqrt{c}}$	$\frac{k_1}{\sigma\sqrt{c}}$	$\frac{k_2}{\tau\sqrt{c}}$
III(Iso)	1.0001	1.1220	1.1220	2.8339	1.2396
VI	2.0594	1.0944	1.0944	2.7909	1.2108
IV	4.2535	1.0672	1.0672	2.7536	1.1845
V	8.6809	1.0449	1.0449	2.7318	1.1645
I	9.9802	1.0412	1.0412	2.7223	1.1613

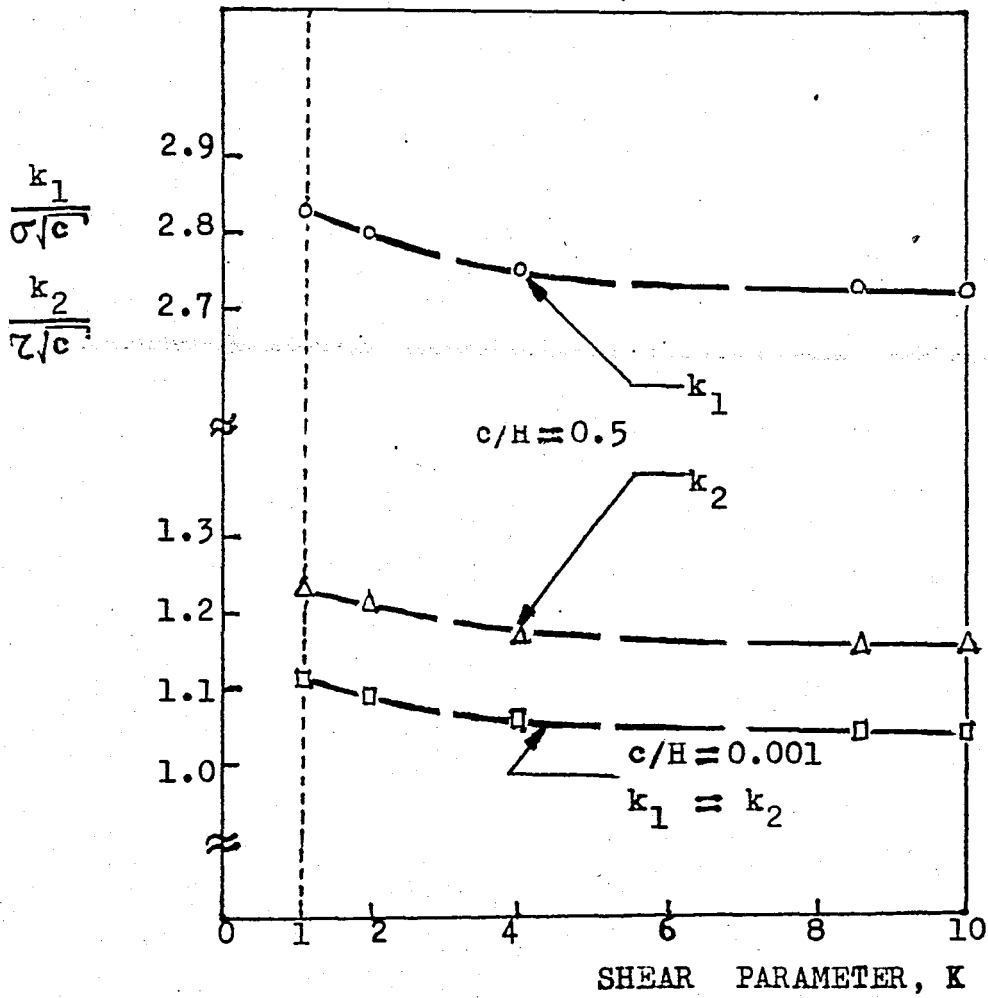


Figure 22. Comparison of the stress intensity factors for an edge crack in a strip of different materials. $b/H=0.0$

Table 7: The stress intensity factors in a uniformly stressed orthotropic plate of material I containing an edge crack.

$$B = 0.5H$$

c/H	0.001	0.1	0.2	0.3	
$\frac{k_1}{\sigma\sqrt{c}}$	1.0413	1.2670	1.6545	2.0962	
c/H	0.4	0.5	0.6	0.7	0.8
$\frac{k_1}{\sigma\sqrt{c}}$	2.6413	3.4450	4.6905	7.0538	13.9104

Table 8: The effect of half length-to-width ratio, B/H, on the stress intensity factors for an orthotropic plate of material I containing an edge crack of length 0.1H .

$$c = 0.1H$$

B/H	0.001	0.05	0.1	0.3	0.5	1	2	∞
$\frac{k_1}{\sigma\sqrt{c}}$	49.7	6.29	2.97	1.48	1.27	1.15	1.14	1.1290

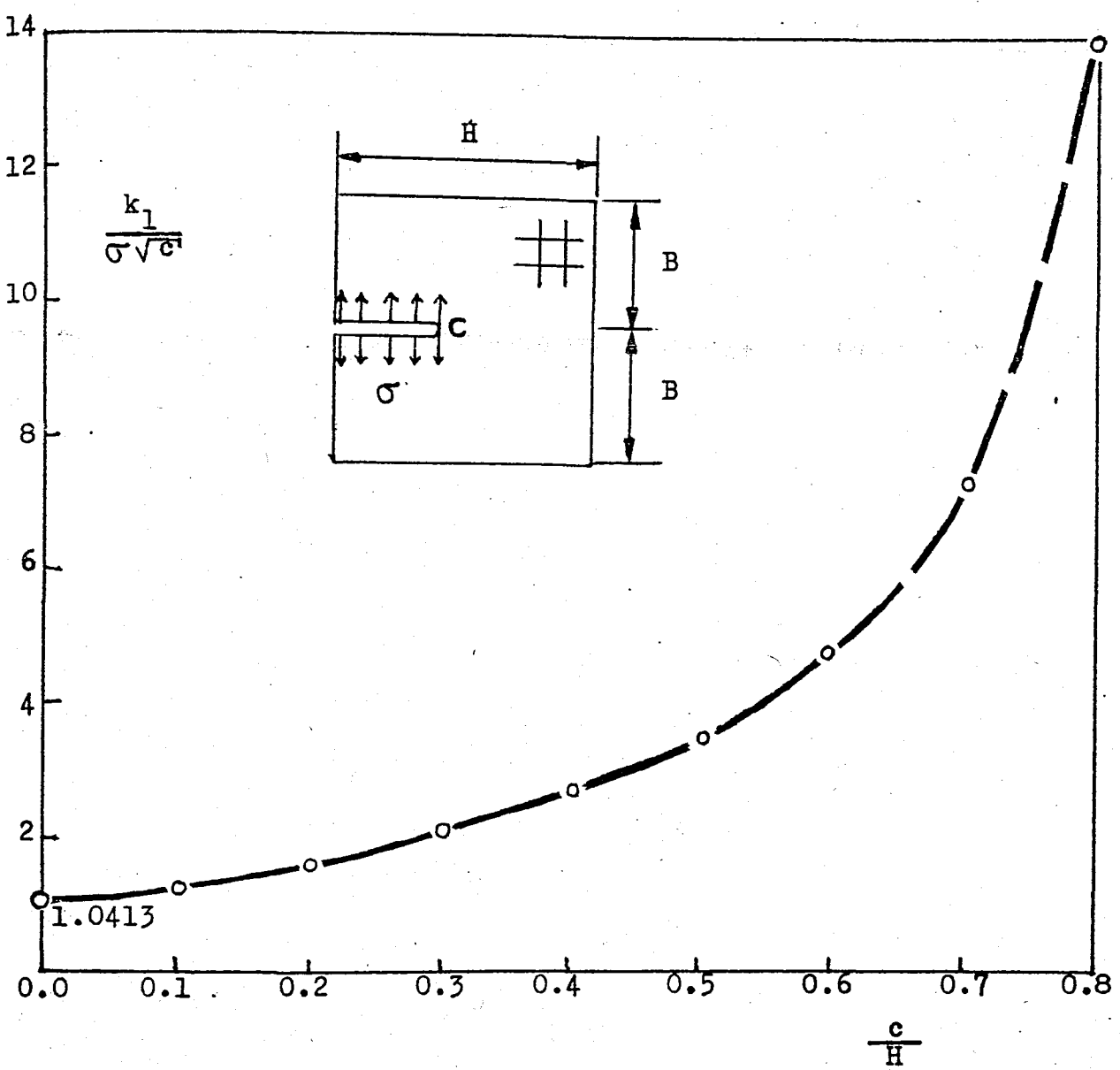


Figure 23. The stress intensity factors in a uniformly stressed orthotropic plate of material I containing an edge crack. $b/H=0.0$, $B/H=0.5$

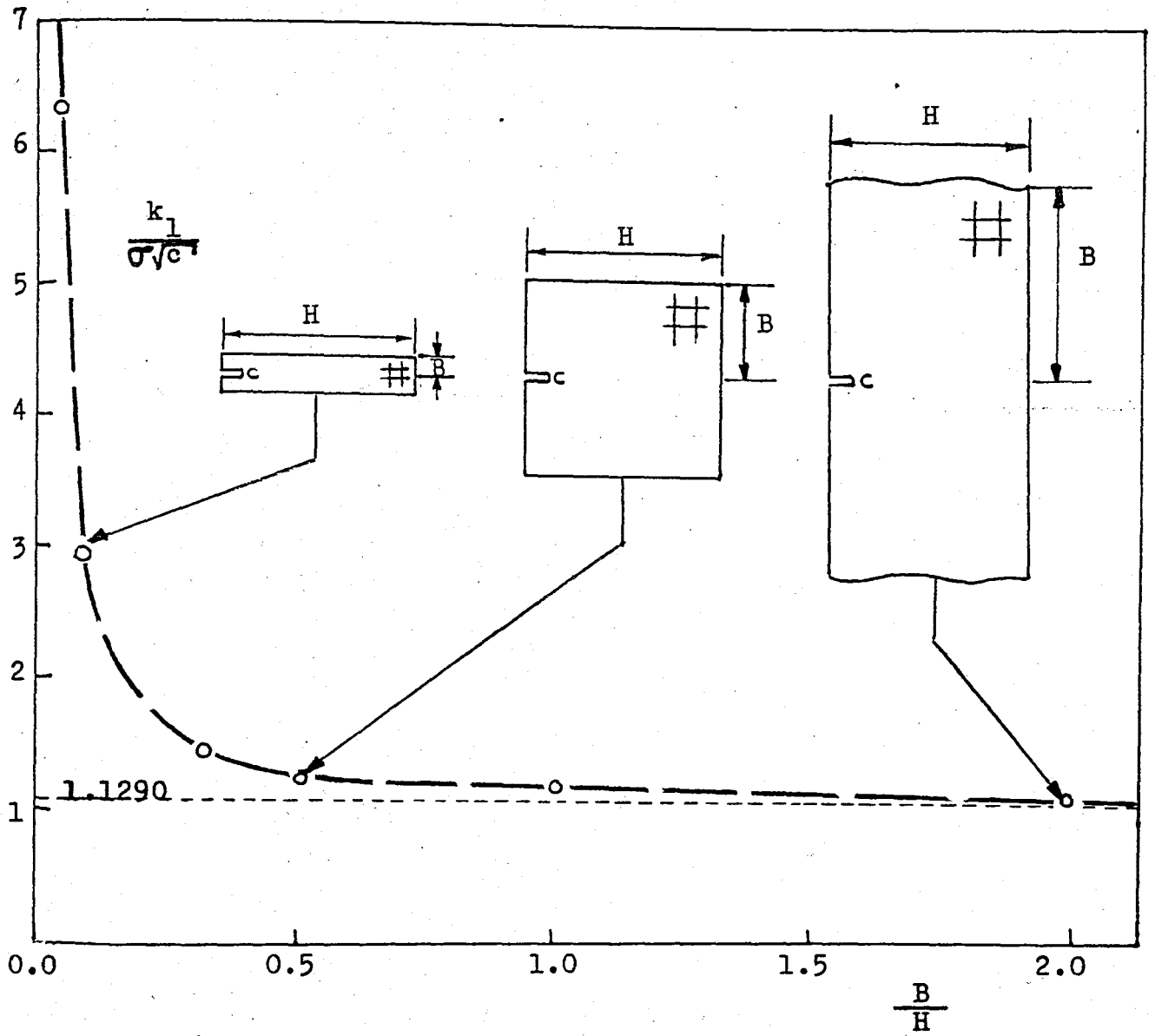


Figure 24. The effect of half length-to-width ratio, B/H , on the stress intensity factors for an orthotropic plate of material I containing an edge crack of length $0.1H$. $b/H=0.0$, $c/H=0.1$

Table 9: stress intensity factors for an orthotropic double cantilever beam (DCB) specimen subjected to concentrated forces P . See Appendix J for the normalization procedure.

c	$\frac{c}{H}$	$\frac{K_I}{P/t}$
0.001w	0.1009	9.31
0.05w	0.145	2.79
0.1w	0.19	2.84
0.2w	0.28	3.34
0.3w	0.37	3.93
0.4w	0.46	4.73
0.5w	0.55	5.88
0.6w	0.64	7.41
0.7w	0.73	10.19
0.8w	0.82	19.04

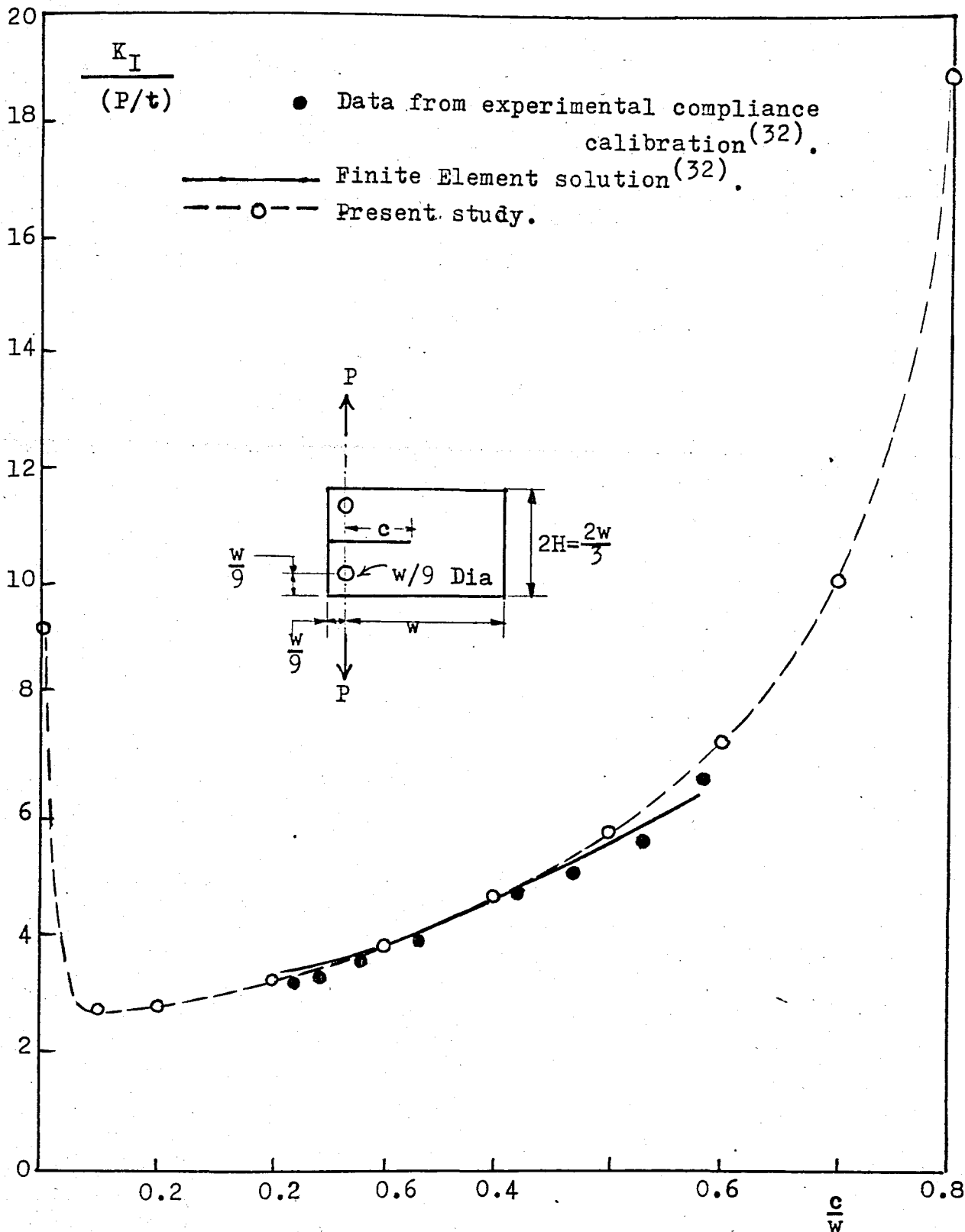


Figure 25. Comparison of the experimental data points and the finite element solution of Mandell et. al. (32) with the present study for the stress intensity factors in a Double Cantilever Beam specimen subjected to a concentrated force P.

Table 10: Comparison of the stress intensity factors in an isotropic compact tension specimen (CTS) with that found by Civelek and Erdogan⁽²⁵⁾ for two crack lengths.

$$k^* = \frac{k_1(c)}{\frac{P}{H}\sqrt{c}}$$

$\frac{c}{H}$	0.5	0.8
k^*	6.1302	22.4450
Ref.(25)	6.1535	20.4519

Table 11: Stress intensity factors for the orthotropic compact tension specimen of material I.

$\frac{c}{H}$	0.5	0.54	0.58	0.62	
k^*	7.25	7.85	8.59	9.55	
$\frac{c}{H}$	0.66	0.70	0.74	0.78	0.80
k^*	10.86	12.76	15.65	20.47	24.23

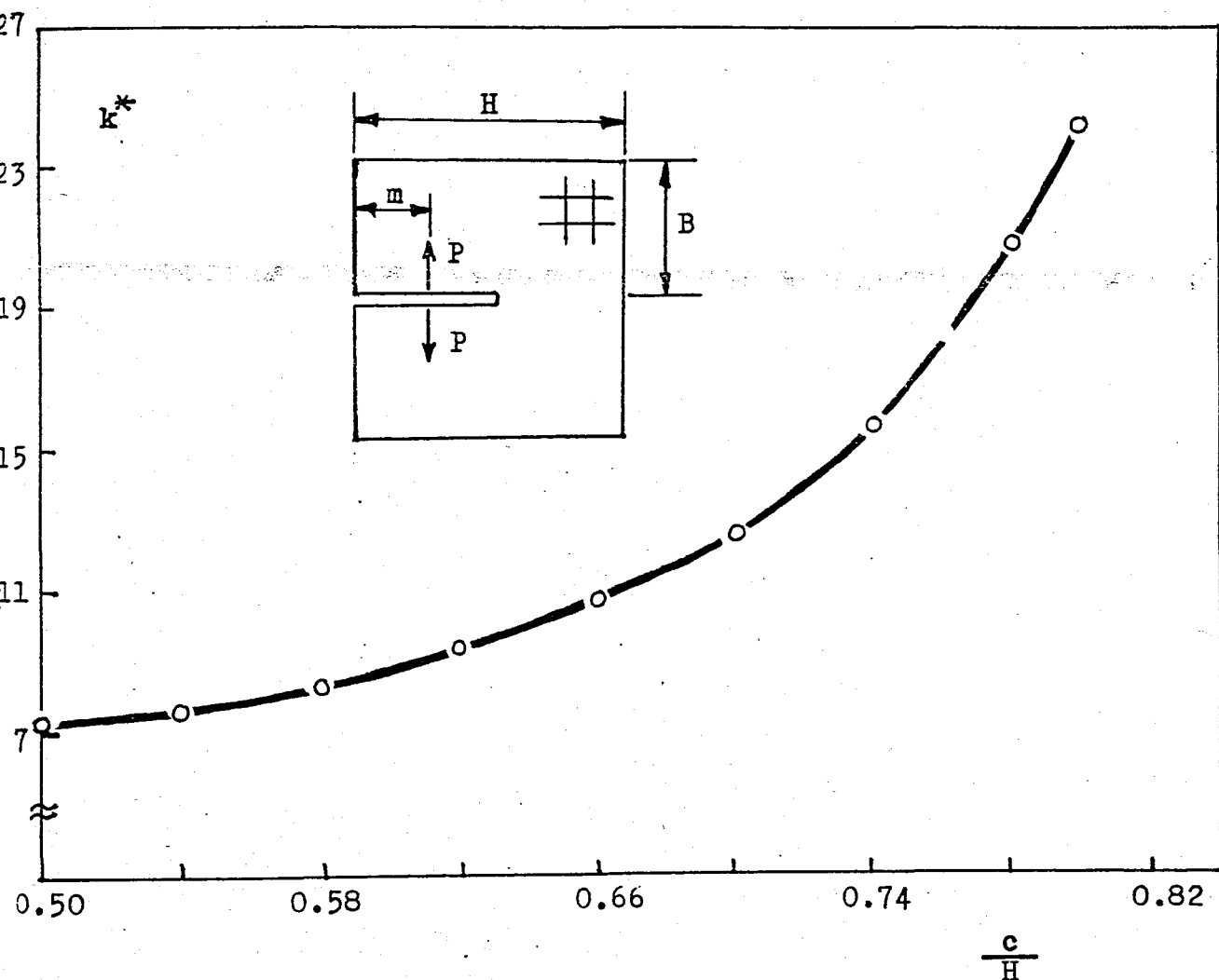


Figure 27. The stress intensity factors for the orthotropic compact tension specimen of Material I.

$$k^* = \frac{k_1(c)}{\frac{P}{H}\sqrt{c}}, \quad m=0.2H, \quad B=0.48H$$

VIII.

CONCLUSIONS

The problems of a single transverse crack in an orthotropic strip subjected to uniform tension or uniform shear and an edge crack in an orthotropic plate subjected to uniform tension are studied and the following results are obtained:

1) In plane problems of orthotropic materials, if the medium is infinite containing a line crack; orthotropy does not affect the stress intensity factor (SIF) and the results are identical to the isotropic case with the same crack geometry. However, if the medium is bounded, SIF is highly dependent on material orthotropy and it is smaller or greater than the corresponding isotropic values.

2) Instead of a direct use of the four independent elastic constants, introducing the new material parameters proposed by Krenk⁽²⁴⁾ not only simplifies the solution procedure but also enables a straightforward transition from orthotropic to isotropic problems depending upon a single parameter, namely the shear parameter K .

3) Depending on the elastic constants, orthotropic materials are classified in two groups: Materials of type I and of type II. A different formulation is needed for each combination. In terms of the new material parameters, the material is of type I if $K^2 > 1$ and of type II if $K^2 < 1$.

4) The solution procedure for various crack problems in infinite or finite orthotropic mediums is greatly simplified by the use of the stress field solutions of a pair of edge dislocations.

5) For an internal crack in an orthotropic strip:

- Stress intensity factors increase as crack length increases.

- The crack tip which is closer to the strip boundary has the greater SIF.

- The loading condition (uniform tension or uniform shear) does not have a significant effect on the range of the SIF values.

6) For an edge crack in an orthotropic strip:

- The loading condition does have a significant effect on the SIF values and k_1 corresponding to uniform tension is always greater than k_2 corresponding to uniform shear.

- As crack length increases k_1 is highly increased whereas k_2 increases slightly.

7) The effect of material orthotropy on the stress intensity factors seems to depend upon the type of the material which is characterized by the shear parameter K . For approximately the same stiffness ratios, SIF values may be greater or smaller than the corresponding isotropic values. From the results obtained in the present analysis for materials of type I compared with that obtained in Ref.(17) for a material of type II; it seems that SIF values for type I materials are always greater than the isotropic ones whereas for type II materials reverse is true.

8) Although K^2 's being smaller or greater than one characterizes the type of an orthotropic material, a somewhat interesting result is that within a specific type (only type I is considered here), no matter what the crack length is, the effect of K on the stress intensity factors does not seem to be of significant importance.

9) Orthotropic plate problems can successfully be solved by taking multiple cracks in an infinite orthotropic strip and superimposing the stress distributions due to each, keeping the inner crack(s) and extending the outer ones to meet the boundaries of the strip. In this case, both ends of the outer cracks are treated as if they are the free ends of an edge crack. In the present analysis this procedure is applied to formulate the problem of an orthotropic rectangular or square plate containing an edge crack, subjected to uniform tension.

10) For an edge crack in an orthotropic square plate subjected to uniform tension; SIF values increase as the crack length increases, but for a specific crack length they are greater for the plate case when compared with the infinite strip case. However, for half length-to-width ratios of $b/h > 2$, the resulting values are practically the same as that found for the infinite strip case (see Fig.24).

11) Formulation of the crack problems using singular integral equations and especially the stress fields of edge dislocations and the new material parameters, seems to be much more reliable than the finite element solutions which are applicable only to a restricted range of crack lengths.

APPENDIX A

The terms $r_i(\alpha)$ in equations (35a-d) and (41a-d):

Taking $z_1 = e^{\alpha h(w_1 - w_2)}$, $z_2 = e^{\alpha h(w_1 - w_2)}$, $z_3 = e^{-\alpha h(w_1 - w_2)}$ and $z_4 = e^{-\alpha h(w_1 - w_2)}$ as they are expressed in the computer program,

$$D(\alpha) = -z_1 + c_1^2 z_2 - z_3 + c_1^2 z_4 + 2c_2 c_3$$

$$r_1(\alpha) = c_1 [z_1 - z_2]$$

$$r_9(\alpha) = -r_3(\alpha)$$

$$r_2(\alpha) = c_2 [-z_1 + 1]$$

$$r_{10}(\alpha) = c_1 c_2 [z_4 - 1]$$

$$r_3(\alpha) = c_1^2 [-(1/c_1^2)z_3 + z_4 + 1/c_1^2 - 1]$$

$$r_{11}(\alpha) = -c_1 [z_4 - z_3]$$

$$r_4(\alpha) = c_1 c_2 [z_2 - 1]$$

$$r_{12}(\alpha) = -c_2 [z_3 - 1]$$

$$r_5(\alpha) = c_1 [z_1 - z_4]$$

$$r_{13}(\alpha) = -r_7(\alpha)$$

$$r_6(\alpha) = c_3 [z_1 - 1]$$

$$r_{14}(\alpha) = c_1 c_3 [z_2 - 1]$$

$$r_7(\alpha) = c_1^2 [-z_2 + (1/c_1^2)z_3 - 1/c_1^2 + 1]$$

$$r_{15}(\alpha) = -c_1 [z_2 - z_3]$$

$$r_8(\alpha) = c_1 c_3 [z_4 - 1]$$

$$r_{16}(\alpha) = c_3 [z_3 - 1]$$

where $c_1 = \frac{-(w_1 + w_2)}{(w_1 - w_2)}$, $c_2 = \frac{-2w_2}{(w_1 - w_2)}$, $c_3 = \frac{+2w_1}{(w_1 - w_2)}$

In the above expressions for r , as discussed in Appendix D, following terms blow up when :

Four z_1 in the first eight terms when $x, t \rightarrow 0$, and their exponential symmetries in the last eight terms when $x, t \rightarrow h$ (first terms in r_{11} and r_{15} and the second terms in r_{12} and r_{16}).

After separating the singular parts, these eight r_i expressions become: $r_{1f}(\alpha) = c_1 [-c_2 c_3 z_2 - z_3 + c_1^2 z_4 + 2c_2 c_3]$

$$r_{2f}(\alpha) = c_2 [-c_1^2 z_2 + z_3 - c_1^2 z_4 - 2c_2 c_3 + 1]$$

$$r_{5f}(\alpha) = c_1 [c_1^2 z_2 - z_3 - c_2 c_3 z_4 + 2c_2 c_3]$$

$$r_{6f}(\alpha) = c_3 [c_1^2 z_2 - z_3 + c_1^2 z_4 + 2c_2 c_3 - 1]$$

but there is no need to define r_{11f} , r_{12f} , r_{15f} and r_{16f} (see Appendix C).

APPENDIX B

Kernels in the expressions (36a-b):

$$\bar{k}_{11}(x, y, t) = \int_0^{\infty} \frac{1}{D(\alpha)} \left\{ \begin{aligned} &w_1 r_1 e^{-\alpha w_1(t+x)} + w_1^3 r_2 e^{-\alpha(w_2 t + w_1 x)} \\ &-w_1 r_3 e^{+\alpha w_1(t-x)} - w_1^3 r_4 e^{+\alpha(w_2 t - w_1 x)} \\ &+w_2 r_5 e^{-\alpha w_2(t+x)} + w_2^3 r_6 e^{-\alpha(w_1 t + w_2 x)} \\ &-w_2 r_7 e^{+\alpha w_2(t-x)} - w_2^3 r_8 e^{+\alpha(w_1 t - w_2 x)} \\ &+w_1 r_9 e^{-\alpha w_1(t-x)} + w_1^3 r_{10} e^{-\alpha(w_2 t - w_1 x)} \\ &-w_1 r_{11} e^{+\alpha w_1(t+x)} - w_1^3 r_{12} e^{+\alpha(w_2 t + w_1 x)} \\ &+w_2 r_{13} e^{-\alpha w_2(t-x)} + w_2^3 r_{14} e^{-\alpha(w_1 t - w_2 x)} \\ &-w_2 r_{15} e^{+\alpha w_2(t+x)} - w_2^3 r_{16} e^{+\alpha(w_1 t + w_2 x)} \end{aligned} \right\} \sin \alpha y d\alpha$$

$$\bar{k}_{12}(x, y, t) = \int_0^{\infty} \frac{1}{D(\alpha)} \left\{ \begin{aligned} &r_1 e^{-\alpha w_1(t+x)} + w_1^2 r_2 e^{-\alpha(w_2 t + w_1 x)} \\ &-r_3 e^{+\alpha w_1(t-x)} - w_1^2 r_4 e^{+\alpha(w_2 t - w_1 x)} \\ &+r_5 e^{-\alpha w_2(t+x)} + w_2^2 r_6 e^{-\alpha(w_1 t + w_2 x)} \\ &-r_7 e^{+\alpha w_2(t-x)} - w_2^2 r_8 e^{+\alpha(w_1 t - w_2 x)} \\ &-r_9 e^{-\alpha w_1(t-x)} - w_1^2 r_{10} e^{-\alpha(w_2 t - w_1 x)} \\ &+r_{11} e^{+\alpha w_1(t+x)} + w_1^2 r_{12} e^{+\alpha(w_2 t + w_1 x)} \\ &-r_{13} e^{+\alpha w_2(t-x)} - w_2^2 r_{14} e^{+\alpha(w_1 t - w_2 x)} \\ &+r_{15} e^{+\alpha w_2(t+x)} + w_2^2 r_{16} e^{+\alpha(w_1 t + w_2 x)} \end{aligned} \right\} \cos \alpha y d\alpha$$

where $r_i = r_i(\alpha)$, $i=1, \dots, 16$ are defined in Appendix A.

Kernels in the expressions (42 a-b) :

$$\begin{aligned}
 k_{11}(x, y, t) = & \int_0^{\infty} \frac{1}{D(\alpha)} \left\{ w_1^2 \left[r_1 e^{-\alpha w_1(t+x)} + r_2 e^{-\alpha(w_2 t + w_1 x)} \right. \right. \\
 & \left. \left. + r_3 e^{+\alpha w_1(t-x)} + r_4 e^{+\alpha(w_2 t - w_1 x)} \right] \right. \\
 & + w_2^2 \left[r_5 e^{-\alpha w_2(t+x)} + r_6 e^{-\alpha(w_1 t + w_2 x)} \right. \\
 & \left. + r_7 e^{+\alpha w_2(t-x)} + r_8 e^{+\alpha(w_1 t - w_2 x)} \right] \\
 & + w_1^2 \left[r_9 e^{-\alpha w_1(t-x)} + r_{10} e^{-\alpha(w_2 t - w_1 x)} \right. \\
 & \left. + r_{11} e^{+\alpha w_1(t+x)} + r_{12} e^{+\alpha(w_2 t + w_1 x)} \right] \\
 & \left. + w_2^2 \left[r_{13} e^{-\alpha w_2(t-x)} + r_{14} e^{-\alpha(w_1 t - w_2 x)} \right. \right. \\
 & \left. \left. + r_{15} e^{+\alpha w_2(t+x)} + r_{16} e^{+\alpha(w_1 t + w_2 x)} \right] \right\} \cos \alpha y d\alpha
 \end{aligned}$$

$$\begin{aligned}
 k_{12}(x, y, t) = & \int_0^{\infty} \frac{1}{D(\alpha)} \left\{ -w_1 \left[r_1 e^{-\alpha w_1(t+x)} + r_2 e^{-\alpha(w_2 t + w_1 x)} \right. \right. \\
 & \left. \left. + r_3 e^{+\alpha w_1(t-x)} + r_4 e^{+\alpha(w_2 t - w_1 x)} \right] \right. \\
 & - w_2 \left[r_5 e^{-\alpha w_2(t+x)} + r_6 e^{-\alpha(w_1 t + w_2 x)} \right. \\
 & \left. + r_7 e^{+\alpha w_2(t-x)} + r_8 e^{+\alpha(w_1 t - w_2 x)} \right] \\
 & + w_1 \left[r_9 e^{-\alpha w_1(t-x)} + r_{10} e^{-\alpha(w_2 t - w_1 x)} \right. \\
 & \left. + r_{11} e^{+\alpha w_1(t+x)} + r_{12} e^{+\alpha(w_2 t + w_1 x)} \right] \\
 & \left. + w_2 \left[r_{13} e^{-\alpha w_2(t-x)} + r_{14} e^{-\alpha(w_1 t - w_2 x)} \right. \right. \\
 & \left. \left. + r_{15} e^{+\alpha w_2(t+x)} + r_{16} e^{+\alpha(w_1 t + w_2 x)} \right] \right\} \sin \alpha y d\alpha
 \end{aligned}$$

where $r_i = r_i(\alpha)$, $i=1, \dots, 16$ are defined in Appendix A.

APPENDIX C

A discussion on kernel $k_{11}(x,y,t)$ of equation (42a):

It is important to note that in kernel $k_{11}(x,y,t)$, the last eight terms are 'exponentially symmetric' with respect to the first eight terms. This means, by a substitution of $x \rightarrow H-x$ and $t \rightarrow H-t$ in the first eight terms one can obtain the negatives of the last eight. For example, the negative of $r_{11}e^{\alpha w_1(t+x)}$ can be obtained by such a substitution in $r_1 \cdot e^{-\alpha w_1(t+x)}$ as follows:

$$\begin{aligned} r_1 e^{-\alpha w_1 [(H-t)+(H-x)]} &= c_1 [e^{\alpha H(w_1+w_2)} - e^{\alpha H(w_1-w_2)}] e^{-2\alpha H w_1} \cdot e^{\alpha w_1(t+x)} \\ &= c_1 [e^{-\alpha H(w_1-w_2)} - e^{-\alpha H(w_1+w_2)}] e^{\alpha w_1(t+x)} \\ &= -r_{11} e^{\alpha w_1(t+x)} \end{aligned}$$

Therefore, if one defines R_1 and R_{11} as,

$$\begin{aligned} R_1(x,t,\alpha) &= w_1^2 r_1 e^{-\alpha w_1(t+x)} \\ R_{11}(x,t,\alpha) &= w_1^2 r_1 e^{+\alpha w_1(t+x)} \end{aligned}$$

then it will be easier to handle the problem since:

$$R_1(H-x, H-t, \alpha) = -R_{11}(x, t, \alpha)$$

$$\text{Similarly, } R_2(H-x, H-t, \alpha) = -R_{12}(x, t, \alpha)$$

$$R_3(H-x, H-t, \alpha) = -R_9(x, t, \alpha)$$

$$R_4(H-x, H-t, \alpha) = -R_{10}(x, t, \alpha)$$

$$R_5(H-x, H-t, \alpha) = -R_{15}(x, t, \alpha)$$

$$R_6(H-x, H-t, \alpha) = -R_{16}(x, t, \alpha)$$

$$R_7(H-x, H-t, \alpha) = -R_{13}(x, t, \alpha)$$

$$R_8(H-x, H-t, \alpha) = -R_{14}(x, t, \alpha)$$

Thus, the kernel $k_{11}(x, y, t)$ can be expressed in a very compact form as:

$$k_{11}(x, y, t) = \int_0^{\infty} \frac{1}{D(\alpha)} \sum_{i=1}^8 [R_i(x, t, \alpha) - R_i(H-x, H-t, \alpha)] \cos \alpha y d\alpha$$

To prevent confusion, it must be stated that in this Appendix, r_1 is used to define R_1 just to show the principle. However, in the final form of the kernel k_{11} in equation (43a); R_i , $i=1, 8$ are defined after the asymptotic examination of k_{11} . Thus, for example r_{1f} is used in defining R_1 . Also note that R_i , $i=1, 8$ are sufficient to define the kernel because of the symmetry discussed above.

APPENDIX D

Examination of the asymptotic behavior
of the kernel $k_{11}(x,y,t)$:

Asymptotic examination of such a kernel means separating it into two parts:

$$k_{11}(x,y,t) = k_s(x,y,t) + k_b(x,y,t)$$

where k_s is the singular part which will be evaluated in closed form. That means, it concerns the terms which blow up when $\alpha \rightarrow \infty$ and either $x,t \rightarrow 0$ or $x,t \rightarrow H$.

and k_b is the bounded part which will be evaluated by performing the infinite integration.

To make this separation all the terms within the integrand of $k_{11}(x,y,t)$ are divided by $D(\alpha)$ and the following ones are observed to blow up when $\alpha \rightarrow \infty$:

$$\left. \begin{array}{l} \text{Singular} \\ \text{when} \\ x,t \rightarrow 0 \end{array} \right\} \begin{cases} \frac{r_1(\alpha)}{D(\alpha)} e^{-\alpha w_1(t+x)} \cos \alpha y = -w_1^2 c_1 e^{-\alpha w_1(t+x)} \cos \alpha y \\ \quad + \frac{1}{D(\alpha)} r_{1f} e^{-\alpha w_1(t+x)} \cos \alpha y \\ \frac{r_2(\alpha)}{D(\alpha)} e^{-\alpha(w_2 t + w_1 x)} \cos \alpha y = w_1^2 c_2 e^{-\alpha(w_2 t + w_1 x)} \cos \alpha y \\ \quad + \frac{1}{D(\alpha)} r_{2f} e^{-\alpha(w_2 t + w_1 x)} \cos \alpha y \\ \frac{r_5(\alpha)}{D(\alpha)} e^{-\alpha w_2(t+x)} \cos \alpha y = -w_2^2 c_1 e^{-\alpha w_2(t+x)} \cos \alpha y \\ \quad + \frac{1}{D(\alpha)} r_{5f} e^{-\alpha w_2(t+x)} \cos \alpha y \\ \frac{r_6(\alpha)}{D(\alpha)} e^{-\alpha(w_1 t + w_2 x)} \cos \alpha y = -w_2^2 c_3 e^{-\alpha(w_1 t + w_2 x)} \cos \alpha y \\ \quad + \frac{1}{D(\alpha)} r_{6f} e^{-\alpha(w_1 t + w_2 x)} \cos \alpha y \end{cases}$$

and the following ones are singular when $x, t \rightarrow h$:

$$\begin{aligned} \frac{r_{11}(\alpha)}{D(\alpha)} e^{\alpha w_1(t+x)} \cos \alpha y &= w_1^2 c_1 e^{-\alpha w_1 [(H-t)+(H-x)]} \cos \alpha y \\ &+ \frac{1}{D(\alpha)} r_{11f} e^{\alpha w_1(t+x)} \cos \alpha y \end{aligned}$$

$$\begin{aligned} \frac{r_{12}(\alpha)}{D(\alpha)} e^{\alpha(w_2 t + w_1 x)} \cos \alpha y &= -w_1^2 c_2 e^{-\alpha [w_2(H-t) + w_1(H-x)]} \cos \alpha y \\ &+ \frac{1}{D(\alpha)} r_{12f} e^{\alpha(w_2 t + w_1 x)} \cos \alpha y \end{aligned}$$

$$\begin{aligned} \frac{r_{15}(\alpha)}{D(\alpha)} e^{\alpha w_2(t+x)} \cos \alpha y &= w_2^2 c_1 e^{-\alpha w_2 [(H-t)+(H-x)]} \cos \alpha y \\ &+ \frac{1}{D(\alpha)} r_{15f} e^{\alpha w_2(t+x)} \cos \alpha y \end{aligned}$$

$$\begin{aligned} \frac{r_{16}(\alpha)}{D(\alpha)} e^{\alpha(w_1 t + w_2 x)} \cos \alpha y &= w_2^2 c_3 e^{-\alpha [w_1(H-t) + w_2(H-x)]} \cos \alpha y \\ &+ \frac{1}{D(\alpha)} r_{16f} e^{\alpha(w_1 t + w_2 x)} \cos \alpha y \end{aligned}$$

Therefore it is possible to express $k_{11}(x, y, t)$ as follows:

$$\begin{aligned} k_{11}(x, y, t) &= Q_2(x, y, t) - Q_2(H-x, y, H-t) \\ &+ \int_0^{\infty} \frac{1}{D(\alpha)} \sum_{i=1}^8 [R_i(x, t, \alpha) - R_i(H-x, H-t, \alpha)] \cos \alpha y d\alpha \end{aligned}$$

where Q_2 and R_i , $i=1, 8$ are defined in Appendices E and F.

In evaluating the closed form integrations within the singular part of the kernel k_{11} , it is helpful to note that:

$$\int_0^{\infty} e^{-\alpha u} \cos \alpha y d\alpha = \frac{u}{u^2 + y^2}$$

APPENDIX B

$$Q_1(x,y,t) = (t-x) \left[\frac{-1/w_1}{w_1^2 y^2 + (t-x)^2} + \frac{1/w_2}{w_2^2 y^2 + (t-x)^2} \right]$$

$$Q_2(x,y,t) = -c_1(t+x) \left[\frac{w_1^3}{w_1^2(t+x)^2 + y^2} + \frac{w_2^3}{w_2^2(t+x)^2 + y^2} \right] \\ + \frac{w_1^2 c_2 (w_2 t + w_1 x)}{(w_2 t + w_1 x)^2 + y^2} - \frac{w_2^2 c_3 (w_1 t + w_2 x)}{(w_1 t + w_2 x)^2 + y^2}$$

$$Q_3(x,y,t) = y \left[\frac{-w_1}{w_1^2 y^2 + (t-x)^2} + \frac{w_2}{w_2^2 y^2 + (t-x)^2} \right]$$

$$Q_4(x,y,t) = y \left[\frac{-w_1 c_1}{w_1^2(t+x)^2 + y^2} - \frac{w_2 c_1}{w_2^2(t+x)^2 + y^2} \right. \\ \left. + \frac{w_1^3 c_2}{(w_2 t + w_1 x)^2 + y^2} - \frac{w_2^3 c_2}{(w_1 t + w_2 x)^2 + y^2} \right]$$

$$Q_5(x,y,t) = Q_3(x,y,t)$$

$$Q_6(x,y,t) = y \left[\frac{w_1 c_1}{w_1^2(t+x)^2 + y^2} + \frac{w_2 c_1}{w_2^2(t+x)^2 + y^2} \right. \\ \left. - \frac{w_1 c_2}{(w_2 t + w_1 x)^2 + y^2} + \frac{w_2 c_3}{(w_1 t + w_2 x)^2 + y^2} \right]$$

$$Q_7(x,y,t) = (t-x) \left[\frac{w_1}{w_1^2 y^2 + (t-x)^2} - \frac{w_2}{w_2^2 y^2 + (t-x)^2} \right]$$

$$Q_8(x,y,t) = -c_1(t+x) \left[\frac{w_1}{w_1^2(t+x)^2 + y^2} + \frac{w_2}{w_2^2(t+x)^2 + y^2} \right] \\ + \frac{w_1^2 c_2 (w_2 t + w_1 x)}{(w_2 t + w_1 x)^2 + y^2} - \frac{w_2^2 c_3 (w_1 t + w_2 x)}{(w_1 t + w_2 x)^2 + y^2}$$

APPENDIX F

In the following expressions for R_i, T_i, U_i and S_i $i=1, \dots, 8$ see Appendix A for r_{if} , $i=1, 2, 5, 6$ and r_i , $i=3, 4, 7, 8$.

$$R_1(x, t, \alpha) = w_1^2 r_{1f} e^{-\alpha w_1(t+x)}$$

$$R_2(x, t, \alpha) = w_1^2 r_{2f} e^{-\alpha(w_2 t + w_1 x)}$$

$$R_3(x, t, \alpha) = w_1^2 r_3 e^{+\alpha w_1(t-x)}$$

$$R_4(x, t, \alpha) = w_1^2 r_4 e^{+\alpha(w_2 t - w_1 x)}$$

$$R_5(x, t, \alpha) = w_2^2 r_{5f} e^{-\alpha w_2(t+x)}$$

$$R_6(x, t, \alpha) = w_2^2 r_{6f} e^{-\alpha(w_1 t + w_2 x)}$$

$$R_7(x, t, \alpha) = w_2^2 r_7 e^{+\alpha w_2(t-x)}$$

$$R_8(x, t, \alpha) = w_2^2 r_8 e^{+\alpha(w_1 t - w_2 x)}$$

$$T_1(x, t, \alpha) = -w_1 r_{1f} e^{-\alpha w_1(t+x)}$$

$$T_2(x, t, \alpha) = -w_1 r_{2f} e^{-\alpha(w_2 t + w_1 x)}$$

$$T_3(x, t, \alpha) = -w_1 r_3 e^{+\alpha w_1(t-x)}$$

$$T_4(x, t, \alpha) = -w_1 r_4 e^{+\alpha(w_2 t - w_1 x)}$$

$$T_5(x, t, \alpha) = -w_2 r_{5f} e^{-\alpha w_2(t+x)}$$

$$T_6(x, t, \alpha) = -w_2 r_{6f} e^{-\alpha(w_1 t + w_2 x)}$$

$$T_7(x, t, \alpha) = -w_2 r_7 e^{+\alpha w_2(t-x)}$$

$$T_8(x, t, \alpha) = -w_2 r_8 e^{+\alpha(w_1 t - w_2 x)}$$

$$U_1(x, t, \alpha) = r_{1f} e^{-\alpha w_1(t+x)}$$

$$U_2(x, t, \alpha) = w_1^2 r_{2f} e^{-\alpha(w_2 t + w_1 x)}$$

$$U_3(x, t, \alpha) = -r_3 e^{+\alpha w_1(t-x)}$$

$$U_4(x, t, \alpha) = -w_1^2 r_4 e^{+\alpha(w_2 t - w_1 x)}$$

$$U_5(x, t, \alpha) = r_{5f} e^{-\alpha w_2(t+x)}$$

$$U_6(x, t, \alpha) = w_2^2 r_{6f} e^{-\alpha(w_1 t + w_2 x)}$$

$$U_7(x, t, \alpha) = -r_7 e^{+\alpha w_2(t-x)}$$

$$U_8(x, t, \alpha) = -w_2^2 r_8 e^{+\alpha(w_1 t - w_2 x)}$$

$$S_1(x, t, \alpha) = w_1 r_{1f} e^{-\alpha w_1(t+x)}$$

$$S_2(x, t, \alpha) = w_1^3 r_{2f} e^{-\alpha(w_2 t + w_1 x)}$$

$$S_3(x, t, \alpha) = -w_1 r_3 e^{+\alpha w_1(t-x)}$$

$$S_4(x, t, \alpha) = -w_1^3 r_4 e^{+\alpha(w_2 t - w_1 x)}$$

$$S_5(x, t, \alpha) = w_2 r_{5f} e^{-\alpha w_2(t+x)}$$

$$S_6(x, t, \alpha) = w_2^3 r_{6f} e^{-\alpha(w_1 t + w_2 x)}$$

$$S_7(x, t, \alpha) = -w_2 r_7 e^{+\alpha w_2(t-x)}$$

$$S_8(x, t, \alpha) = -w_2^3 r_8 e^{+\alpha(w_1 t - w_2 x)}$$

Note that : $T_i = \frac{-1}{w_1} R_i$ $S_i = w_1 U_i$ for $i=1, 2, 3, 4$
 $T_i = \frac{-1}{w_2} R_i$ $S_i = w_2 U_i$ for $i=5, 6, 7, 8.$

APPENDIX G

$$k_{11}(x, t) = \frac{1}{w_1 - w_2} \left[Q_2(0, x, t) - Q_2(0, H-x, H-t) + k_{f1} \right]$$

$$k_{12}(x, t) = \frac{2}{w_1 - w_2} \left[Q_1(B, x, t) + Q_2(B, x, t) - Q_2(B, H-x, H-t) + k_{g1} \right]$$

$$k_{13}(x, t) = \frac{2}{w_1 - w_2} \left[Q_3(-B, x, t) + Q_4(-B, x, t) + Q_4(-B, H-x, H-t) + k_{h1} \right]$$

$$k_{21}(x, t) = \frac{1}{w_1 - w_2} \left[Q_1(B, x, t) + Q_2(B, x, t) - Q_2(B, H-x, H-t) + k_{f2} \right]$$

$$k_{22}(x, t) = \frac{1}{w_1 - w_2} \left[Q_2(0, x, t) - Q_2(0, H-x, H-t) + Q_1(2B, x, t) \right. \\ \left. + Q_2(2B, x, t) - Q_2(2B, H-x, H-t) + k_{g2} \right]$$

$$k_{23}(x, t) = \frac{-1}{w_1 - w_2} \left[Q_3(2B, x, t) + Q_4(2B, x, t) + Q_4(2B, H-x, H-t) + k_{h2} \right]$$

$$k_{31}(x, t) = \frac{1}{w_1 - w_2} \left[Q_5(B, x, t) + Q_6(B, x, t) + Q_6(B, H-x, H-t) + k_{f3} \right]$$

$$k_{32}(x, t) = \frac{1}{w_1 - w_2} \left[Q_5(2B, x, t) + Q_6(2B, x, t) + Q_6(2B, H-x, H-t) + k_{g3} \right]$$

$$k_{33}(x, t) = \frac{1}{w_1 - w_2} \left[Q_2(0, x, t) - Q_2(0, H-x, H-t) - Q_7(2B, x, t) \right. \\ \left. - Q_8(2B, x, t) + Q_8(2B, H-x, H-t) + k_{h3} \right]$$

where k_{fi} , k_{gi} , k_{hi} $i=1, 2, 3$ are defined in Appendix H.

APPENDIX H

$$k_{f1}(x, t) = \int_0^{\infty} \frac{1}{D(\alpha)} \sum_{i=1}^8 \left[R_i(x, t, \alpha) - R_i(H-x, H-t, \alpha) \right] d\alpha$$

$$k_{g1}(x, t) = \int_0^{\infty} \frac{1}{D(\alpha)} \sum_{i=1}^8 \left[R_i(x, t, \alpha) - R_i(H-x, H-t, \alpha) \right] \cos(\alpha B) d\alpha$$

$$k_{h1}(x, t) = \int_0^{\infty} \frac{1}{D(\alpha)} \sum_{i=1}^8 \left[S_i(x, t, \alpha) + S_i(H-x, H-t, \alpha) \right] \sin(\alpha B) d\alpha$$

$$k_{f2}(x, t) = \int_0^{\infty} \frac{1}{D(\alpha)} \sum_{i=1}^8 \left[R_i(x, t, \alpha) - R_i(H-x, H-t, \alpha) \right] \cos(\alpha B) d\alpha$$

$$k_{g2}(x, t) = 2 \int_0^{\infty} \frac{1}{D(\alpha)} \sum_{i=1}^8 \left[R_i(x, t, \alpha) - R_i(H-x, H-t, \alpha) \right] \cos^2(\alpha B) d\alpha$$

$$k_{h2}(x, t) = \int_0^{\infty} \frac{1}{D(\alpha)} \sum_{i=1}^8 \left[S_i(x, t, \alpha) + S_i(H-x, H-t, \alpha) \right] \sin(2\alpha B) d\alpha$$

$$k_{f3}(x, t) = \int_0^{\infty} \frac{1}{D(\alpha)} \sum_{i=1}^8 \left[T_i(x, t, \alpha) + T_i(H-x, H-t, \alpha) \right] \sin(\alpha B) d\alpha$$

$$k_{g3}(x, t) = \int_0^{\infty} \frac{1}{D(\alpha)} \sum_{i=1}^8 \left[T_i(x, t, \alpha) + T_i(H-x, H-t, \alpha) \right] \sin(2\alpha B) d\alpha$$

$$k_{h3}(x, t) = 2 \int_0^{\infty} \frac{1}{D(\alpha)} \sum_{i=1}^8 \left[U_i(x, t, \alpha) - U_i(H-x, H-t, \alpha) \right] \sin^2(2\alpha B) d\alpha$$

APPENDIX I

Examination of the roots of the transformed field equation (29) shows that:

(i) For $K^2 > 1$, there are four real roots:

$$s_1, s_2, s_3 = -s_1 \text{ and } s_4 = -s_2, (s_1 > 0, s_2 > 0).$$

In this case, the corresponding material is classified as 'type I' ⁽¹⁷⁾.

(ii) For $K^2 < 1$, the roots are complex:

$$s_1 = w_1 - iw_2 = -s_3, \quad s_2 = w_1 + iw_2 = -s_4, \quad (w_1, w_2 > 0).$$

This time the related material is classified as 'type II'.

Just for a comparison purpose results for a symmetric internal crack of various crack lengths obtained by Delale and Erdoğan ⁽¹⁷⁾ where the material is assumed to be of type II are included in Table 3 and Figure 17.

Solution of the transformed field equation (29) for a material of type I is as follows:

The characteristic equation may be expressed as,

$$s^4 - (2K\alpha^2)s^2 + \alpha^4 = 0$$

where K is the shear parameter defined in Section II.B.

Taking $p = s^2$,

$$p^2 - (2K\alpha^2)p + \alpha^4 = 0$$

$$p_{1,2} = \frac{2K\alpha^2 \mp \sqrt{4K^2\alpha^4 - 4\alpha^4}}{2} = \alpha^2 [K \mp \sqrt{K^2 - 1}]$$

Since $s = \pm\sqrt{p}$, it follows that:

$$s_{1,2,3,4} = \mp |\alpha| \left[K \pm \sqrt{K^2 - 1} \right]^{1/2}$$

Defining w_1 and w_2 as;

$$w_1 = \left[K + \sqrt{K^2 - 1} \right]^{1/2}$$

$$w_2 = \left[K - \sqrt{K^2 - 1} \right]^{1/2}$$

the roots of the characteristic equation may finally be expressed as:

$$s_1 = -w_1 |\alpha| = -s_3$$

$$s_2 = -w_2 |\alpha| = -s_4$$

where w_1 and w_2 are,

Real if $K^2 > 1$

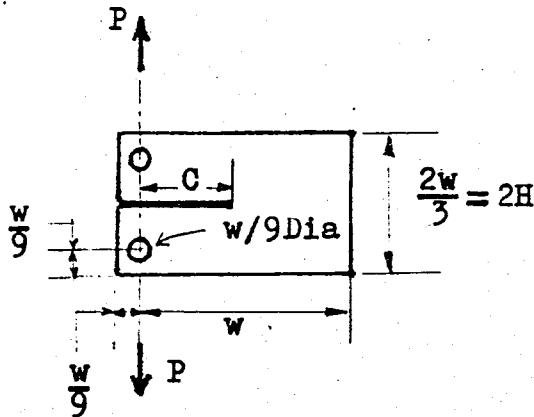
Complex Conjugates if $K^2 < 1$

Orthotropic materials are denoted as type I when w_1 and w_2 are Real, and as type II when they are Complex conjugates. A different formulation is needed for each type. In our analysis all the materials are of type I, thus the general solution of the field equation may be expressed as:

$$\Phi(x, \alpha) = A_1 e^{-w_1 |\alpha| x} + B_1 e^{-w_2 |\alpha| x} + A_2 e^{+w_1 |\alpha| x} + B_2 e^{+w_2 |\alpha| x}$$

APPENDIX J

Geometry of the Double Centilever Beam specimen:



Material properties used in the finite element solution of Mandel et.al. (32):

Material; E-glass/polyester

$$E_{xx} = 1.79 \times 10^6 \text{ psi}$$

$$E_{yy} = 2.66 \times 10^6 \text{ psi}$$

$$G_{xy} = 0.48 \times 10^6 \text{ psi}$$

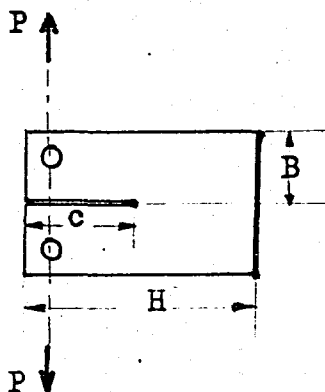
$$\nu_{xy} = 0.19$$

Average thickness, $t = 0.216$ in.

$w = 4.5$ in.

Difference in the normalization procedures:

In terms of the notation used throughout this analysis, the geometry of the DCB specimen is,



where $B = w/3$, $H = (10/9)w = 5in.$, P is per unit thickness .

It should be noted that, K_I which appears in Table 9 and Figure 25 is the standard Mode I stress intensity factor used in fracture mechanics and is related to the stress intensity factor $k(c)$ by

$$K_I = k(c)\sqrt{\pi}$$

When the force P is not considered as being per unit thickness and the thickness t is included explicitly, then the present normalization of the stress intensity factor may be expressed as

$$\frac{k(c)}{\frac{P}{H}\sqrt{c}}$$

Denoting this term by A , the normalization made by Mandell et.al may be expressed as:

$$\frac{K_I}{\frac{P}{t}} = \frac{A}{H} \sqrt{\pi c}$$

AND WEI CORRESPONDS TO w_k WHICH ARE DEFINED IN SECTION VI .

```
S(1)=1.
S(N)=-1.
R(1)=COS(PI/(2.*XN-2.))
WEI(1)=1./2./(XN-1.)
WEI(N)=WEI(1)
```

```
DO 20 I=2,N11
XI=I
S(I)=COS((XI-1.)*PI/(XN-1.))
R(I)=COS((2.*XI-1.)*PI/(2.*XN-2.))
WEI(I)=1./(XN-1.)
```

20 CONTINUE

```
CM=(C-B)/2.
CP=(C+B)/2.
DO 30 I=1,N11
```

X1 CORRESPONDS TO γ .

```
X1=CM*R(I)+CP
```

RIGHT HAND SIDE OF THE NORMALIZED SINGULAR INTEGRAL EQN. BECOMES CONSTANT (-1) FOR UNIFORM TENSION CASE.

```
RR(I)=-1.
DO 30 J=1,N
```

X2 CORRESPONDS TO τ

```
X2=CM*S(J)+CP
CALL XKFRH(X1,X2,WEI,XX,W1,W2,KAP,EXPWP,EXPWM,EXPNWP,EXPNWM,DEN,N
*1,C1,C2,C3,CM,XH1)
NJ=(J-1)*N+I
```

XH1 IS THE VALUE OF THE INFINITE INTEGRAL.

```
A(NJ)=WEI(J)*CM*XH1
```

30 CONTINUE

```
DO 40 J=1,N
NJ=(J-1)*N+N
IF(B.NE.U.0)GO TO 44
```

SINGLE VALUEDNESS CONDITION FOR AN EDGE CRACK.

```
A(NJ)=0.U
IF(J.EQ.N) A(NJ)=1.
GO TO 40
```

SINGLE VALUEDNESS CONDITION FOR AN INTERNAL CRACK.

```
A(NJ)=WEI(J)
40 CONTINUE
RR(N)=0.
EPS=1.E-14
CALL GELG(RR,A,N,1,EPS,IER)
```

XK2 DENOTES THE STRESS INTENSITY FACTOR $K(C)$ WHEREAS XK1 CORRESPONDS TO $K(B)$.

```
XK2=-RR(1)
IF(B.EQ.U.0) GO TO 55
XK1=RR(N)
WRITE(6,16)B,C,XK1,XK2
FORMAT(//,17X,F10.4,13X,F10.4,13X,G14.7,10X,G14.7)
GO TO 98
```

FOR THE CASE OF AN EDGE CRACK, A DIFFERENT SOLUTION IS PROPOSED FOR BETTER CONVERGENCE.

```
XK2=XK2/SQRT(2.)
WRITE(6,17)B,C,XK2
FORMAT(//,17X,F10.4,13X,F10.4,17X,****,14X,G14.7)
GO TO 98
STOP
END
```

SUBROUTINE LAGUER(NN,X,A)
 CALCULATES THE ZEROS X(I) OF THE NN-TH ORDER
 LAGUERRE POLYNOMIAL LN(ALF) FOR THE SEGMENT (0,INF)
 ALF IS TAKEN ZERO. THE SMALLEST ZERO WILL BE STORED IN X(1).
 ALSO CALCULATES THE CORRESPONDING COEFFICIENTS A(I) OF THE
 NN-TH ORDER LAGUERRE QUADRATURE FORMULA OF DEGREE 2*NN-1.

```

  IMPLICIT REAL*8 (A-H,O-Z)
  DIMENSION X(NN),A(NN),B(15),C(151)
  EPS=1.E-9
  FN=NN
  DO 8 I=1,NN
    B(I)=2*I-1
  8 C(I)=(I-1)**2
  CC=1.
  DO 1 J=2,NN
  1 CC=CC*C(J)
  DO 7 I=1,NN
    IF(I-1) 6,2,3
      SMALLEST ZERO
  2 XT=3./(1.+2.4*FN)
    GO TO 6
  3 IF(I-2) 6,4,5
      SECOND ZERO
  4 XF=XT+15./(1.+2.5*FN)
    GO TO 6
      ALL OTHER ZEROS
  5 FI=I-2
    RI=(1.+2.55*FI)/(1.9+FI)
    XI=XT+RI*(XT-X(I-2))
  6 CALL LGROOT(XT,NN,DPN,PN1,B,C,EPS)
    X(I)=XI
    A(I)=CC/DPN/PN1
  7 CONTINUE
  RETURN
  END

```

SUBROUTINE LGROOT(X,NN,DPN,PN1,B,C,EPS)
 IMPROVES THE APPROXIMATE ROOT X.
 DPN=DERIVATIVE OF P(N) AT X.
 PN1=VALUE OF P(N-1) AT X.

```

  IMPLICIT REAL*8 (A-H,O-Z)
  DIMENSION B(NN),C(NN)
  ITER=0
  1 ITER=ITER+1
  CALL LGRECR(P,DP,PN1,X,NN,B,C)
  U=P/DP
  X=X-U
  IF(ABS(U/X)-EPS) 3,3,2
  2 IF(ITER-10) 1,3,3
  3 DPN=DP
  RETURN
  END

```

SUBROUTINE LGRECR(PN,DPN,P-1,X,NN,B,C)

```

  IMPLICIT REAL*8 (A-H,O-Z)
  DIMENSION B(NN),C(NN)
  P1=1.
  P=X-1.
  DP1=0.
  DP=1.
  DO 1 J=2,NN
    Q=(X-B(J))*P-C(J)*P1
    DQ=(X-B(J))*DP+D-C(J)*DP1
  1 P1=P
    P=Q
    DP1=DP
    DP=DQ
  PN=P
  DPN=DP
  PN1=P1
  RETURN
  END

```


C
C
C
C
C
C
C

IN THE FOLLOWING SUBROUTINE THE INTEGRAND OF THE SINGULAR INTEGRAL
EQN. OF THE PROBLEM (EQN. 55b) IS CONSIDERED AND SOLVED NUMERICALLY.
X1 AND X2 CORRESPONDS TO THE SINGULAR PARTS WITHIN THE KERNEL AND
USING THE DO LOOP, THE INFINITE INTEGRATION (BOUNDED PART) IS PER-
FORMED THROUGH THE USE OF THE WEIGHTS A OF THE LAGUERRE QUADRA-
TURE FORMULA.

```

SUBROUTINE XKERH (X,T,A,W,W1,W2,K,Z1,Z2,Z3,Z4,C,N,C1,C2,C3,CM,XH1)
IMPLICIT REAL*8 (A-H,O-Z)
DIMENSION A(20),W(20),Z2(20),Z3(20),Z4(20),U(20)
X1= 1./(1-X)+(1./ (W1-W2))*(-W1*C1/(T+X)+W1*C2/(X+(W2/W1)*T)
      -W2*C1/(T+X)-W2*C3/(X+(W1/W2)*T))
X2=- (1./ (W1-W2))* (-W1*C1/(1.-T-X)+W1*C2/((1.-X)+(W2/W1)*(1.-T))
      -W2*C1/(1.-T-X)-W2*C3/((1.-X)+(W1/W2)*(1.-T)))
XH1=X1+X2
DO 1 I=1,N
R1=W1**2.*C1      * (-C2*C3*Z2(I)-Z3(I)+C1**2.*Z4(I)+2.*C2*C3)
R2=W1**2.*C2      * (-C1**2.*Z2(I)+Z3(I)-C1**2.*Z4(I)-2.*C2*C3+1.)
R3=W1**2.*C1**2.* * (-1./C1**2.) * Z3(I)+Z4(I)+1./C1**2.-1.)
R4=W1**2.*C1*C2   * (Z2(I)-1.)
R5=W2**2.*C1      * (C1**2.*Z2(I)-Z3(I)-C2*C3*Z4(I)+2.*C2*C3)
R6=W2**2.*C3      * (C1**2.*Z2(I)-Z3(I)+C1**2.*Z4(I)+2.*C2*C3-1.)
R7=W2**2.*C1**2.* * (-Z2(I)+(1./C1**2.) * Z3(I)-1./C1**2.+1.)
R8=W2**2.*C1*C3   * (Z4(I)-1.)
S1 = R1*DEXP(-W(T)*W1*(T+X)) /D(T)
S2 = R2*DEXP(-W(T)*(W2*T+W1*X)) /D(T)
S3 = R3*DEXP(+W(T)*W1*(T-X)) /D(T)
S4 = R4*DEXP(+W(T)*(W2*T-W1*X)) /D(T)
S5 = R5*DEXP(-W(T)*W2*(T+X)) /D(T)
S6 = R6*DEXP(-W(T)*(W1*T+W2*X)) /D(T)
S7 = R7*DEXP(+W(T)*W2*(T-X)) /D(T)
S8 = R8*DEXP(+W(T)*(W1*T-W2*X)) /D(T)
S9 =-R1*DEXP(-W(T)*W1*((1.-T)+(1.-X))) /D(I)
S10=-R2*DEXP(-W(T)*(W2*(1.-T)+W1*(1.-X))) /D(I)
S11=-R3*DEXP(+W(T)*W1*((1.-T)-(1.-X))) /D(I)
S12=-R4*DEXP(+W(T)*(W2*(1.-T)-W1*(1.-X))) /D(I)
S13=-R5*DEXP(-W(T)*W2*((1.-T)+(1.-X))) /D(I)
S14=-R6*DEXP(-W(T)*(W1*(1.-T)+W2*(1.-X))) /D(I)
S15=-R7*DEXP(+W(T)*W2*((1.-T)-(1.-X))) /D(I)
S16=-R8*DEXP(+W(T)*(W1*(1.-T)-W2*(1.-X))) /D(I)
XH1=XH1+A(I)*(S1+S2+S3+S4+S5+S6+S7+S8+S9+S10+S11+S12+S13+S14+S15+
R S16)/(W1-W2)
1 CONTINUE
RETURN
END

```

C
C
C
C

C
C
C
C

```

SUBROUTINE GELG(N,A,M,N,EPS,IER)
IMPLICIT REAL*8 (A-H,O-Z)
DIMENSION A(1),R(1)
IF(N)23,23,1
SEARCH FOR GREATEST ELEMENT IN MATRIX A
1 IER=0
PIV=0.
MM=M*M
NM=N*M
DO 3 L=1,MM
TB=ABS(A(L))
IF(TB-PIV)3,3,2
2 PIV=TB
I=L
3 CONTINUE
TOL=EPS*PIV
A(I) IS PIVOT ELEMENT. PIV CONTAINS THE ABSOLUTE VALUE OF A(I).
START ELIMINATION LOOP
LST=1
DO 17 K=1,M
TEST ON SINGULARITY
4 IF(PIV)23,23,4
5 IF(IER)7,5,7
6 IER=K-1
7 PIVI=1./A(I)
J=(I-1)/M
I=I-J*M-K

```

```

      J=J+1-K
C   I+K IS ROW INDEX, J+K COLUMN INDEX OF PIVOT ELEMENT
C   PIVOT ROW REDUCTION AND ROW INTERCHANGE IN RIGHT HAND SIDE R
      DO 8 L=K, NM, M
          LL=L+I
          TB=PIVI*R(LL)
          R(LL)=R(L)
8     R(L)=TB
C   IS ELIMINATION TERMINATED ?
      IF(K-M)9,18,18
C   COLUMN INTERCHANGE IN MATRIX A.
      9 LEND=LST+M-K
      IF(J)12,12,10
      10 II=J+M
      DO 11 L=LST, LEND
          TB=A(L)
          LL=L+II
          A(L)=A(LL)
      11 A(LL)=TB
C   ROW INTERCHANGE AND PIVOT ROW REDUCTION IN MATRIX A.
      12 DO 13 L=LST, MM, M
          LL=L+I
          TB=PIVI*A(LL)
          A(LL)=A(L)
      13 A(L)=TB
C   SAVE COLUMN INTERCHANGE INFORMATION
      A(LST)=J
C   ELEMENT REDUCTION AND NEXT PIVOT SEARCH
      PIV=0.
      LST=LST+1
      J=0
      DO 16 II=LST, LEND
          PIVI=-A(II)
          IST=II+M
          J=J+1
          DO 15 L=IST, MM, M
              LL=L-J
              A(L)=A(L)+PIVI*A(LL)
              TB=ABS(A(L))
              IF(TB-PIV)15,15,14
      14 PIV=TB
          I=L
      15 CONTINUE
          DO 16 L=K, NM, M
              LL=L+J
              16 R(LL)=R(LL)+PIVI*R(L)
      17 LST=LST+M
C   END OF ELIMINATION LOOP
C   BACK SUBSTITUTION AND BACK INTERCHANGE
      18 IF(M-1)23,22,19
      19 IST=MM+M
          LST=M+1
          DO 21 I=2, M
              II=LST-I
              IST=IST-LST
              L=IST-M
              L=A(L)+.5
              DO 21 J=II, NM, M
                  TB=R(J)
                  LL=J
                  DO 20 K=IST, MM, M
                      LL=LL+1
                      20 TB=TB-A(K)*R(LL)
                      K=J+L
                      R(J)=R(K)
                      R(K)=TB
      21
      22 RETURN
C   ERPR RETURN
      23 IER=-1
          RETURN
      END

```

```

*****
*****
*****
*****
***** THIS PROGRAM CALCULATES THE STRESS INTENSITY FACTORS
***** AT CRACK TIPS FOR A RECTANGULAR, ORTHOTROPIC PLATE
***** CONTAINING AN EDGE CRACK
***** AND SUBJECTED TO UNIFORM TENSION AT CRACK FACES.
*****
***** THE PROBLEM IS FORMULATED SUPERIMPOSING THE STRESS DISTRIBUTIONS
***** DUE TO THREE TRANSVERSE EDGE CRACKS IN A STRIP, KEEPING THE MIDDLE ONE
***** AND LETTING THE OUTER ONES MEET THE EDGES (SEE SECTION VC AND THE SYSTEM
***** OF SINGULAR INTEGRAL EQUATIONS (70A-C)
*****
***** THE KERNELS XKER11, XKER12, ..., XKER33 ARE DEFINED IN APPENDIX G,
***** FUNCTIONS G1, G2, ..., G6 MAY BE FOUND IN APPENDIX E,
***** FUNCTIONS FHN, GN, GS, FHS CORRESPONDS TO THE SUMMATIONS OVER R, S, U, T,
***** RESPECTIVELY, WHICH ARE DEFINED IN APPENDIX F, AND TAKE PLACE WITHIN
***** THE BOUNDED KERNELS GIVEN IN APPENDIX H.
***** FUNCTION GENC CORRESPONDS TO THE SINGULAR PARTS OF THE KERNELS
***** XKER11, XKER12, XKER33.
*****
*****
***** IMPLICIT REAL*8 (A-H,O-Z)
***** REAL*8 M1, L, KAP
***** DIMENSION XX(10), AL(10), EXPWP(10), EXPWM(10), EXPNWP(10), EXPNWM(10),
***** RDEN(10), WEIL(10), S(20), R(20), WEI(20), U(20), V(20), WE(20), A(3600),
***** RSS(1800)
***** READ(5,*)E1,E2,G12,V12
***** READ(5,*)A1,B,C,E,D
***** READ(5,*)M,N,N1
***** V21=V12*(E2/E1)
***** KAP=SQRT(E1+E2)*1./G12-V12/(E1-V21/E2)/2.
***** WRITE(6,1)E1,E2,G12,V12,KAP,M,N,N1
***** FORMAT(1H1,22X, 'MATERIAL CONSTANTS ', E1 =, E15.6,/,46X, E2 =,
***** RE15.6,/,45X, G12 =, E15.6,/,45X, V12 =, F6.4,/,/,23X, 'SHEAR PARA
***** RMETER ', KAP =, F10.4,/,/,45X, M =, I3,/,45X, N =, I3,/,
***** &45X, N1 =, I3)
***** WRITE(6,2)A1,B,C,E,D
***** FORMAT(///,45X, 'A1 =, F8.4,/,45X, B =, F8.4,/,45X, C =,
***** RF8.4,/,45X, E =, F8.4,/,45X, D =, F8.4)
***** PI=4.*ATAN(1.)
***** W1=SQRT(KAP+SQRT(KAP**2.-1.))
***** W2=SQRT(KAP-SQRT(KAP**2.-1.))
***** C1=-(W1+W2)/(W1-W2)
***** C2=-2.*W2/(W1-W2)
***** C3=+2.*W1/(W1-W2)
***** CALL LAGUER(N1,XY,AL)
***** DO 10 I=1,N1
***** EXPWP(I)=DEXP(XY(I)*(W1+W2))
***** EXPWM(I)=DEXP(XY(I)*(W1-W2))
***** EXPNWP(I)=1./EXPWP(I)
***** EXPNWM(I)=1./EXPWM(I)
***** DEN(I)=-EXPWP(I)+C1**2.*EXPWM(I)+C1**2.*EXPNWM(I)-EXPNWP(I)
***** R+2.*C2*C3
***** WEIL(I)=AL(I)*DEXP(XX(I))
10 CONTINUE
***** XN=N
***** N11=N-1
***** S(1)=1.
***** S(N)=-1.
***** R(1)=COS(PI/(2.*XN-2.))
***** WEI(1)=1./2./((XN-1.))
***** WEI(N)=WEI(1)
***** DO 11 I=2,N11
***** XI=I
***** S(I)=COS((XI-1.)*PI/(XN-1.))
***** R(I)=COS((2.*XI-1.)*PI/(2.*XN-2.))
***** WEI(I)=1./((XN-1.))
11 CONTINUE
***** XM=M
***** M11=M-1
***** U(1)=1.
***** U(M)=-1.

```

```

V(1)=COS(PI/(2.*XM-2.))
WE(1)=1./2./(XM-1.)
WE(M)=WE(1)
DO 12 I=2,M11
XI=I
U(I)=COS((XI-1.)*PI/(XM-1.))
V(I)=COS((2.*XI-1.)*PI/(2.*XM-2.))
WE(I)=1./(XM-1.)
12 CONTINUE
MM=2*M+N
H1=(B-A1)/2.
H2=(B+A1)/2.
E1=(E-C)/2.
E2=(F+C)/2.
DO 13 I=1,N11
X=H1*H(I)+H2
DO 14 J=1,N
NJ11=(J-1)*MM+I
T=H1*S(J)+H2
CALL XKER11(T,X,WEIL,XX,EX=WP,EXPWM,EXPNWP,EXPNWM,DEN,N1,XK11,
RW1,W2,C1,C2,C3)
A(NJ11)=WEI(J)*H1*XK11
14 CONTINUE
DO 15 J=1,M
T=E1*U(J)+E2
JJ1=J+N
JJ2=J+M+N
NJ12=(JJ1-1)*MM+T
NJ13=(JJ2-1)*MM+T
CALL XKER12(T,X,WEIL,XX,EX=WP,EXPWM,EXPNWP,EXPNWM,DEN,N1,D,XK12,
RW1,W2,C1,C2,C3)
CALL XKER13(T,X,WEIL,XX,EX=WP,EXPWM,EXPNWP,EXPNWM,DEN,N1,D,XK13,
RW1,W2,C1,C2,C3)
A(NJ12)=WE(J)*E1*XK12
A(NJ13)=WE(J)*E1*XK13
15 CONTINUE
13 CONTINUE
DO 16 J=1,N
NJ11=(J-1)*MM+N
A(NJ11)=0.
16 CONTINUE
DO 17 J=1,M
JJ1=J+N
JJ2=J+M+N
NJ12=(JJ1-1)*MM+N
NJ13=(JJ2-1)*MM+N
A(NJ12)=0.
A(NJ13)=0.
17 CONTINUE
M12=V/2
DO 18 I=1,M11
II1=I+N
II2=I+M+N
X=E1*V(I)+E2
IF(I.EQ.M12)GO TO 30
DO 19 J=1,N
T=H1*S(J)+H2
NJ21=(J-1)*MM+II1
NJ31=(J-1)*MM+II2
CALL XKER21(T,X,WEIL,XX,EX=WP,EXPWM,EXPNWP,EXPNWM,DEN,N1,D,XK21,
RW1,W2,C1,C2,C3)
CALL XKER31(T,X,WEIL,XX,EX=WP,EXPWM,EXPNWP,EXPNWM,DEN,N1,D,XK31,
RW1,W2,C1,C2,C3)
A(NJ21)=WEI(J)*H1*XK21
A(NJ31)=WEI(J)*H1*XK31
19 CONTINUE
DO 20 J=1,M
JJ1=J+N
JJ2=J+M+N
NJ22=(JJ1-1)*MM+II1
NJ23=(JJ2-1)*MM+II1
NJ32=(JJ1-1)*MM+II2
NJ33=(JJ2-1)*MM+II2
CALL XKER22(T,X,WEIL,XX,EX=WP,EXPWM,EXPNWP,EXPNWM,DEN,N1,D,XK22,
RW1,W2,C1,C2,C3)
CALL XKER23(T,X,WEIL,XX,EX=WP,EXPWM,EXPNWP,EXPNWM,DEN,N1,D,XK23,
RW1,W2,C1,C2,C3)

```

```

CALL XKER32(T,X,W,EIL,XX,EXPWP,EXPWM,EXPNWP,EXPNWM,DEN,N1,D,XK32,
&W1,W2,C1,C2,C3)
CALL XKER33(T,X,W,EIL,XX,EXPWP,EXPWM,EXPNWP,EXPNWM,DEN,N1,D,XK33,
&W1,W2,C1,C2,C3)
A(NJ22)=WE(J)*E1*XK22
A(NJ23)=WE(J)*E1*XK23
A(NJ32)=WE(J)*E1*XK32
A(NJ33)=WE(J)*E1*XK33
20 CONTINUE
GO TO 19
30 DO 31 J=1,N
NJ21=(J-1)*MM+II1
NJ31=(J-1)*MM+II2
A(NJ21)=0.
A(NJ31)=0.
31 CONTINUE
DO 32 J=1,M
JJ1=J+N
JJ2=J+M+N
NJ22=(JJ1-1)*MM+II1
NJ23=(JJ2-1)*MM+II1
NJ32=(JJ1-1)*MM+II2
NJ33=(JJ2-1)*MM+II2
A(NJ22)=0.
A(NJ23)=0.
A(NJ32)=0.
A(NJ33)=0.
32 CONTINUE
18 CONTINUE
DO 21 J=1,N
NJ21=(J-1)*MM+M+N
NJ31=(J-1)*MM+2*M+N
A(NJ21)=0.
A(NJ31)=0.
21 CONTINUE
DO 22 J=1,M
JJ1=J+N
JJ2=J+M+N
NJ22=(JJ1-1)*MM+M+N
NJ23=(JJ2-1)*MM+M+N
NJ32=(JJ1-1)*MM+2*M+N
NJ33=(JJ2-1)*MM+2*M+N
A(NJ22)=0.
A(NJ23)=0.
A(NJ32)=0.
A(NJ33)=0.
22 CONTINUE
L1=(N-1)*MM+N
L2=N*MM+N+M12
L3=(M+N)*MM+M+N+12
L4=(M+N-1)*MM+M+N
L5=(MM-1)*MM+MM
A(L1)=1.
A(L2)=1.
A(L3)=1.
A(L4)=1.
A(L5)=1.
DO 23 I=1,N
DO 23 J=1,N11
NJ11=(J-1)*MM+I
SS(NJ11)=0.
IF(I.EQ.J) SS(NJ11)=-1.
23 CONTINUE
DO 24 I=1,M
II1=I+N
II2=I+M+N
DO 24 J=1,N11
NJ21=(J-1)*MM+II1
NJ31=(J-1)*MM+II2
SS(NJ21)=0.
SS(NJ31)=0.
24 CONTINUE
EPS=1.E-14
CALL GELG(SS,A,MM,N11,EPS,IER)
SUM=0.
DO 25 I=1,N11
NJ=(I-1)*MM+1
SUM=SUM-SS(NJ)

```

```

X1=B1*R(I)+B2
WRITE(6,26)X1,SS,NJ)
FORMAT(2X,,X=,,G14.7,3X,,G6EENS FUNC=,,G14.7)
CONTINUE
SUM=SUM/SQRT(2.)
WRITE(6,27)SUM
FORMAT(2X,,K(UNIFORM PRESSURE)=,,G14.7)
N112=N11-1
DO 28 I=2,N112
  NJ=(I-1)*MM+1
  X11=B1*R(I-1)+B2
  X12=B1*R(I+1)+B2
  XX1=(X11+X12)/2.
  X1=B1*R(I)+B2
  XX2=XX1-X1
  X1=XX1-XX2/3.
  XKK1=2.*SS(NJ)/B1/(R(I-1)-R(I+1))
  XKK1=XKK1/SQRT(2.)
  WRITE(6,29)X1,XKK1
  FORMAT(2X,,X=,,G14.7,3X,,K(B)=,,G14.7)
CONTINUE
STOP
END

```

SUBROUTINE LAGUER(NN,X,A)

CALCULATES THE ZEROS $X(I)$ OF THE NN-TH ORDER LAGUERRE POLYNOMIAL $LN(ALF)$ FOR THE SEGMENT $(0,INF)$. ALF IS TAKEN ZERO. THE SMALLEST ZERO WILL BE STOPPED IN $X(1)$. ALSO CALCULATES THE CORRESPONDING COEFFICIENTS $A(I)$ OF THE NN-TH ORDER LAGUERRE QUADRATURE FORMULA OF DEGREE $2*NN-1$.

```

IMPLICIT REAL*8 (A-H,O-Z)
DIMENSION X(NN),A(NN),B(15),C(151)
EPS=.00000001
FN=NN
DO 8 I=1,NN
  B(I)=2*I-1
  C(I)=(I-1)**2
  CC=1.
  DO 1 J=2,NN
    1 CC=CC*C(J)
  DO 7 I=1,NN
    IF(I-1) 6,2,3
    2 XT=3./(1.+2.4*FN)
    GO TO 6
    3 IF(I-2) 6,4,5
    4 XI=XT+15./(1.+2.5*FN)
    GO TO 6
    5 FI=I-2
    R1=(1.+2.55*FI)/(1.9*FI)
    XI=XT+R1*(XT-X(I-2))
    6 CALL LGROOT(XT,NN,DPN,PN1,n,C,EPS)
    X(I)=XI
    A(I)=CC/DPN/PN1
  7 CONTINUE
  RETURN
END

```

SUBROUTINE LGROOT(X,NN,DPN,PN1,B,C,EPS)

IMPROVES THE APPROXIMATE ROOT X.
 DPN=DERIVATIVE OF P(N) AT X
 PN1=VALUE OF P(N-1) AT X

```

IMPLICIT REAL*8 (A-H,O-Z)
DIMENSION B(NN),C(NN)
ITER=0
1 ITER=ITER+1
CALL LGRECR(P,DP,PN1,X,NN,n,C)
U=P/DP

```

```

X=X-D
IF (ABS(D/X)-EPS) 3,3,2
2 IF (ITER-10) 1,3,3
3 OPN=DP
RETURN
END

```

```

SUBROUTINE LGHECR(PN,DPN,PN1,X,NN,R,C)
IMPLICIT REAL*8 (A-H,O-Z)
DIMENSION R(NN),C(NN)
P1 = 1.
P = X-1.
DP1=0.
DP = 1.
DO 1 J=2,NN
Q = (X-R(J))*P-C(J)*P1
DQ = (X-R(J))*DP+P-C(J)*DP1
P1 = P
P = Q
DP1=DP
1 DP = DQ
PN = P
DPN=DP
PN1=P1
RETURN
END

```

```

FUNCTION Q1(D,T,X,W1,W2)
IMPLICIT REAL*8 (A-H,O-Z)
Q1=(T-X)*(-1./W1/(W1**2.*D**2.+(T-X)**2.)
+1./W2/(W2**2.*D**2.+(T-X)**2.))
RETURN
END

```

```

FUNCTION Q3(D,T,X,W1,W2)
IMPLICIT REAL*8 (A-H,O-Z)
Q3=D*(-W1/(W1**2.*D**2.+(T-X)**2.)+W2/(W2**2.*D**2.+(T-X)**2.))
RETURN
END

```

```

FUNCTION Q7(D,T,X,W1,W2)
IMPLICIT REAL*8 (A-H,O-Z)
Q7=(T-X)*( W1/(W1**2.*D**2.+(T-X)**2.)
-W2/(W2**2.*D**2.+(T-X)**2.))
RETURN
END

```

```

FUNCTION Q5(D,T,X,W1,W2)
IMPLICIT REAL*8 (A-H,O-Z)
Q5=D*(-W1/(W1**2.*D**2.+(T-X)**2.)+W2/(W2**2.*D**2.+(T-X)**2.))
RETURN
END

```

```

FUNCTION Q2(D,T,X,W1,W2,C1,C2,C3)
IMPLICIT REAL*8 (A-H,O-Z)
X1=W1**3./((W1*(T+X))**2.+D**2.)
X2=W2**3./((W2*(T+X))**2.+D**2.)
X3=-(W1**2.*C2*(W2*T+W1*X))/(W2*T+W1*X)**2.+D**2.)
X4=-(W2**2.*C3*(W1*T+W2*X))/(W1*T+W2*X)**2.+D**2.)
Q2=-C1*(T+X)*(X1+X2)+X3+X4
RETURN
END

```

```

FUNCTION Q4(D,T,X,W1,W2,C1,C2,C3)
IMPLICIT REAL*8 (A-H,O-Z)

```

```

X1=-W1*C1/((W1*(T+X))**2.+D**2.)
X2=-W2*C1/((W2*(T+X))**2.+D**2.)
X3= W1**3.*C2/((W2*T+W1*X)**2.+D**2.)
X4=-W2**3.*C3/((W1*T+W2*X)**2.+D**2.)
Q4=D*(X1+X2+X3+X4)
RETURN
END

```

C
C
C

```

FUNCTION Q8(D,T,X,W1,W2,C1,C2,C3)
IMPLICIT REAL*8 (A-H,O-Z)
X1= W1/((W1*(T+X))**2.+D**2.)
X2= W2/((W2*(T+X))**2.+D**2.)
X3= W1**2.*C2*(W2*T+W1*X)/((W2*T+W1*X)**2.+U**2.)
X4=-W2**2.*C3*(W1*T+W2*X)/((W1*T+W2*X)**2.+U**2.)
Q8=-C1*(T+X)*(X1+X2)+X3+X4
RETURN
END

```

C
C
C

```

FUNCTION Q6(D,T,X,W1,W2,C1,C2,C3)
IMPLICIT REAL*8 (A-H,O-Z)
X1= W1*C1/((W1*(T+X))**2.+D**2.)
X2= W2*C1/((W2*(T+X))**2.+D**2.)
X3=-W1*C2/((W2*T+W1*X)**2.+D**2.)
X4= W2*C3/((W1*T+W2*X)**2.+D**2.)
Q6=D*(X1+X2+X3+X4)
RETURN
END

```

C
C
C

```

FUNCTION FHN(T,X,W1,W2,C1,C2,C3,Z2,Z3,Z4,W)
IMPLICIT REAL*8 (A-H,O-Z)
R1=W1**2.*C1 *(-C2*C3*Z2-Z3+C1**2.*Z4+2.*C2*C3)
R2=W1**2.*C2 *(-C1**2.*Z2+Z3-C1**2.*Z4-2.*C2*C3+1.)
R3=W1**2.*C1**2.*(-(1./C1**2.)*Z3+Z4+1./C1**2.-1.)
R4=W1**2.*C1*C2 *(Z2-1.)
R5=W2**2.*C1 *(C1**2.*Z2-Z3-C2*C3*Z4+2.*C2*C3)
R6=W2**2.*C3 *(C1**2.*Z2-Z3+C1**2.*Z4+2.*C2*C3-1.)
R7=W2**2.*C1**2.*(-Z2+(1./C1**2.)*Z3-1./C1**2.+1.)
R8=W2**2.*C1*C3 *(Z4-1.)
FHN=R1*DEXP(-W*W1*(T+X))+R2*DEXP(-W*(W2*T+W1*X))
+R3*DEXP(+W*W1*(T-X))+R4*DEXP(+W*(W2*T-W1*X))
+R5*DEXP(-W*W2*(T+X))+R6*DEXP(-W*(W1*T+W2*X))
+R7*DEXP(+W*W2*(T-X))+R8*DEXP(+W*(W1*T-W2*X))
RETURN
END

```

C
C
C

```

FUNCTION GN(T,X,W1,W2,C1,C2,C3,Z2,Z3,Z4,W)
IMPLICIT REAL*8 (A-H,O-Z)
S1= W1 *C1 *(-C2*C3*Z2-Z3+C1**2.*Z4+2.*C2*C3)
S2= W1*W1**2.*C2 *(-C1**2.*Z2+Z3-C1**2.*Z4-2.*C2*C3+1.)
S3=-W1 *C1**2.*(-(1./C1**2.)*Z3+Z4+1./C1**2.-1.)
S4=-W1**3.*C1*C2 *(Z2-1.)
S5= W2* C1 *(C1**2.*Z2-Z3-C2*C3*Z4+2.*C2*C3)
S6= W2*W2**2.*C3 *(C1**2.*Z2-Z3+C1**2.*Z4+2.*C2*C3-1.)
S7=-W2* C1**2.*(-Z2+(1./C1**2.)*Z3-1./C1**2.+1.)
S8=-W2**3.*C1*C3 *(Z4-1.)
GN=S1*DEXP(-W*W1*(T+X))+S2*DEXP(-W*(W2*T+W1*X))
+S3*DEXP(+W*W1*(T-X))+S4*DEXP(+W*(W2*T-W1*X))
+S5*DEXP(-W*W2*(T+X))+S6*DEXP(-W*(W1*T+W2*X))
+S7*DEXP(+W*W2*(T-X))+S8*DEXP(+W*(W1*T-W2*X))
RETURN
END

```

C
C
C

```

FUNCTION GS(T,X,W1,W2,C1,C2,C3,Z2,Z3,Z4,W)
IMPLICIT REAL*8 (A-H,O-Z)
U1= C1 *(-C2*C3*Z2-Z3+C1**2.*Z4+2.*C2*C3)
U2= W1**2.*C2 *(-C1**2.*Z2+Z3-C1**2.*Z4-2.*C2*C3+1.)
U3= -C1**2.*(-(1./C1**2.)*Z3+Z4+1./C1**2.-1.)
U4=-W1**2.*C1*C2 *(Z2-1.)

```



```

U5= C1 *(C1**2.*Z2-Z3-C2*C3*Z4+2.*C2*C3)
U6= W2**2.*C3 *(C1**2.*Z2-Z3+C1**2.*Z4+2.*C2*C3-1.)
U7= -C1**2.*(-Z2+(1./C1**2.)*Z3-1./C1**2.+1.)
U8=-W2**2.*C1*C3*(Z4-1.)
GS=U1*DEXP(-W*W1*(T+X))+U2*DEXP(-W*(W2*T+W1*X))
+U3*DEXP(+W*W1*(T-X))+U4*DEXP(+W*(W2*T-W1*X))
+U5*DEXP(-W*W2*(T+X))+U6*DEXP(-W*(W1*T+W2*X))
+U7*DEXP(+W*W2*(T-X))+U8*DEXP(+W*(W1*T-W2*X))
RETURN
END

```

```

FUNCTION FHS(T,X,W1,W2,C1,C2,C3,Z2,Z3,Z4,W)
IMPLICIT REAL*8 (A-H,O-Z)
I1=-W1 *C1 *(-C2*C3*Z2-Z3+C1**2.*Z4+2.*C2*C3)
I2=-W1 *C2 *(-C1**2.*Z2+Z3-C1**2.*Z4-2.*C2*C3+1.)
I3=-W1 *C1**2.*(-(1./C1**2.)*Z3+Z4+1./C1**2.-1.)
I4=-W1 *C1*C2*(Z2-1.)
I5=-W2 *C1 *(C1**2.*Z2-Z3-C2*C3*Z4+2.*C2*C3)
I6=-W2 *C3 *(C1**2.*Z2-Z3+C1**2.*Z4+2.*C2*C3-1.)
I7=-W2 *C1**2.*(-Z2+(1./C1**2.)*Z3-1./C1**2.+1.)
I8=-W2 *C1*C3*(Z4-1.)
FHS=I1*DEXP(-W*W1*(T+X))+I2*DEXP(-W*(W2*T+W1*X))
+I3*DEXP(+W*W1*(T-X))+I4*DEXP(+W*(W2*T-W1*X))
+I5*DEXP(-W*W2*(T+X))+I6*DEXP(-W*(W1*T+W2*X))
+I7*DEXP(+W*W2*(T-X))+I8*DEXP(+W*(W1*T-W2*X))
RETURN
END

```

```

FUNCTION GENC(T,X,W1,W2,C1,C2,C3)
IMPLICIT REAL*8 (A-H,O-Z)
X1=1./(T-X)+(1./W1-W2)*(-W1*C1/(T+X)+W1**2.*C2/(W1*X+W2*T)
-W2*C1/(T+X)-W2**2.*C3/(W2*X+W1*T))
X2=(1./(W1-W2))*(+W1*C1/(2.-T-X)-W1**2.*C2/(W1*(1.-X)+W2*(1.-T))
+W2*C1/(2.-T-X)+W2**2.*C3/(W2*(1.-X)+W1*(1.-T)))
GENC=X1+X2
RETURN
END

```

```

SUBROUTINE XKER1(T,X,A,XI,EXPWP,EXPWM,EXPNWP,EXPNWM,DEN,N,XK11,
W1,W2,C1,C2,C3)
IMPLICIT REAL*8 (A-H,O-Z)
DIMENSION A(1),XT(1),EXPWM(1),EXPNWP(1),EXPNWM(1),DEN(1)
XK11=GENC(T,X,W1,W2,C1,C2,C3)
DO 1 I=1,N
W=XI(I)
Z2=EXPWM(I)
Z3=EXPNWP(I)
Z4=EXPNWM(I)
X1=FHN(T,X,W1,W2,C1,C2,C3,Z2,Z3,Z4,W)
X2=FHN(1.-T,1.-X,W1,W2,C1,C2,C3,Z2,Z3,Z4,W)
XK11=XK11+A(I)*(X1-X2)/DEN(I)/(W1-W2)
1 CONTINUE
RETURN
END

```

```

SUBROUTINE XKER2(T,X,A,XI,EXPWP,EXPWM,EXPNWP,EXPNWM,DEN,N,D,XK12,
W1,W2,C1,C2,C3)
IMPLICIT REAL*8 (A-H,O-Z)
DIMENSION A(1),XT(1),EXPWM(1),EXPNWP(1),EXPNWM(1),DEN(1)
XK12=2.*Q1(D,T,X,W1,W2)
X1=Q2(D,1,X,W1,W2,C1,C2,C3)
X2=Q2(D,1.-T,1.-X,W1,W2,C1,C2,C3)
XK12=(XK12+2.*(X1-X2))/(W1-W2)
DO 1 I=1,N
W=XI(I)
Z2=EXPWM(I)
Z3=EXPNWP(I)
Z4=EXPNWM(I)
X3=FHN(T,X,W1,W2,C1,C2,C3,Z2,Z3,Z4,W)
X4=FHN(1.-T,1.-X,W1,W2,C1,C2,C3,Z2,Z3,Z4,W)

```

XK12=XK12+2.*A(I)*(X3-X4)*COS(W*D)/DEN(I)/(W1-W2)

1 CONTINUE
RETURN
END

```

SUBROUTINE XKER13(T,X,A,XI,EXPWP,EXPWM,EXPNWP,EXPNWM,DEN,N,D,XK13,
R W1,W2,C1,C2,C3)
IMPLICIT REAL*8 (A-H,O-Z)
DIMENSION A(1),X_T(1),EXPWM(1),EXPNWP(1),EXPNWM(1),DEN(1)
XK13=2.*Q3(-D,T,X,W1,W2)
X1=Q4(-D,T,X,W1,W2,C1,C2,C3)
X2=Q4(-D,1.-T,1.-X,W1,W2,C1,C2,C3)
XK13=(XK13+2.*(X1+X2))/(W1-W2)
DO 1 I=1,N
Z2=EXPWM(I)
Z3=EXPNWP(I)
Z4=EXPNWM(I)
W=XI(I)
X3=GN(T,X,W1,W2,C1,C2,C3,Z2,Z3,Z4,W)
X4=GN(1.-T,1.-X,W1,W2,C1,C2,C3,Z2,Z3,Z4,W)
XK13=XK13-2.*A(I)*(X3+X4)*SIN(W*D)/DEN(I)/(W1-W2)
1 CONTINUE
RETURN
END

```

```

SUBROUTINE XKER21(T,X,A,XI,EXPWP,EXPWM,EXPNWP,EXPNWM,DEN,N,D,XK21,
R W1,W2,C1,C2,C3)
IMPLICIT REAL*8 (A-H,O-Z)
DIMENSION A(1),X_T(1),EXPWM(1),EXPNWP(1),EXPNWM(1),DEN(1)
XK21=G1(D,T,X,W1,W2)
X1=Q2(D,T,X,W1,W2,C1,C2,C3)
X2=Q2(D,1.-T,1.-X,W1,W2,C1,C2,C3)
XK21=(XK21+X1-X2)/(W1-W2)
DO 1 I=1,N
W=XI(I)
Z2=EXPWM(I)
Z3=EXPNWP(I)
Z4=EXPNWM(I)
X3=FHN(T,X,W1,W2,C1,C2,C3,Z2,Z3,Z4,W)
X4=FHN(1.-T,1.-X,W1,W2,C1,C2,C3,Z2,Z3,Z4,W)
XK21=XK21+A(I)*(X3-X4)*COS(W*D)/DEN(I)/(W1-W2)
1 CONTINUE
RETURN
END

```

```

SUBROUTINE XKER22(T,X,A,XI,EXPWP,EXPWM,EXPNWP,EXPNWM,DEN,N,D,XK22,
R W1,W2,C1,C2,C3)
IMPLICIT REAL*8 (A-H,O-Z)
DIMENSION A(1),X_T(1),EXPWM(1),EXPNWP(1),EXPNWM(1),DEN(1)
XK22=GENC(D,T,X,W1,W2,C1,C2,C3)+Q1(2.*D,T,X,W1,W2)/(W1-W2)
X1=Q2(2.*D,T,X,W1,W2,C1,C2,C3)
X2=Q2(2.*D,1.-T,1.-X,W1,W2,C1,C2,C3)
XK22=XK22+(X1-X2)/(W1-W2)
DO 1 I=1,N
W=XI(I)
Z2=EXPWM(I)
Z3=EXPNWP(I)
Z4=EXPNWM(I)
X3=FHN(T,X,W1,W2,C1,C2,C3,Z2,Z3,Z4,W)
X4=FHN(1.-T,1.-X,W1,W2,C1,C2,C3,Z2,Z3,Z4,W)
XK22=XK22+2.*A(I)*(X3-X4)*COS(W*D)**2/DEN(I)/(W1-W2)
1 CONTINUE
RETURN
END

```

```

SUBROUTINE XKER23(T,X,A,XI,EXPWP,EXPWM,EXPNWP,EXPNWM,DEN,N,D,XK23,
R W1,W2,C1,C2,C3)
IMPLICIT REAL*8 (A-H,O-Z)
DIMENSION A(1),X_T(1),EXPWM(1),EXPNWP(1),EXPNWM(1),DEN(1)
XK23=Q3(2.*D,T,X,W1,W2)

```

```

X1=G4(2.*D,T,X,W1,W2,C1,C2,C3)
X2=G4(2.*D,1.-T,1.-X,W1,W2,C1,C2,C3)
XK23=(XK23+X1+X2)/(W1-W2)
DO 1 I=1,N
W=XI(I)
Z2=EXPWM(I)
Z3=EXPNWP(I)
Z4=EXPNWM(I)
X3=GN(I,X,W1,W2,C1,C2,C3,Z2,Z3,Z4,W)
X4=GN(1.-T,1.-X,W1,W2,C1,C2,C3,Z2,Z3,Z4,W)
XK23=(XK23+A(I))*(X3+X4)*S+N(2.*W*D)/DEN(I)/(W1-W2)
1 CONTINUE
RETURN
END

```

C
C
C

```

SUBROUTINE XKER31(T,X,A,XI,EXPWP,EXPWM,EXPNWP,EXPNWM,DEN,N,C,XK31,
W1,W2,C1,C2,C3)
IMPLICIT REAL*8 (A-H,O-Z)
DIMENSION A(1),XT(1),EXPWM(1),EXPNWP(1),EXPNWM(1),DEN(1)
XK31=G5(U,T,X,W1,W2)
X1=G6(U,T,X,W1,W2,C1,C2,C3)
X2=G6(U,1.-T,1.-X,W1,W2,C1,C2,C3)
XK31=(XK31+X1+X2)/(W1-W2)
DO 1 I=1,N
W=XI(I)
Z2=EXPWM(I)
Z3=EXPNWP(I)
Z4=EXPNWM(I)
X3=FHS(T,X,W1,W2,C1,C2,C3,Z2,Z3,Z4,W)
X4=FHS(1.-T,1.-X,W1,W2,C1,C2,C3,Z2,Z3,Z4,W)
XK31=XK31+A(I)*(X3+X4)*SIN(W*U)/DEN(I)/(W1-W2)
1 CONTINUE
RETURN
END

```

C
C
C

```

SUBROUTINE XKER32(T,X,A,XI,EXPWP,EXPWM,EXPNWP,EXPNWM,DEN,N,C,XK32,
W1,W2,C1,C2,C3)
IMPLICIT REAL*8 (A-H,O-Z)
DIMENSION A(1),XT(1),EXPWM(1),EXPNWP(1),EXPNWM(1),DEN(1)
XK32=G5(2.*D,T,X,W1,W2)
X1=G6(2.*D,T,X,W1,W2,C1,C2,C3)
X2=G6(2.*D,1.-T,1.-X,W1,W2,C1,C2,C3)
XK32=(XK32+X1+X2)/(W1-W2)
DO 1 I=1,N
W=XI(I)
Z2=EXPWM(I)
Z3=EXPNWP(I)
Z4=EXPNWM(I)
X3=FHS(T,X,W1,W2,C1,C2,C3,Z2,Z3,Z4,W)
X4=FHS(1.-T,1.-X,W1,W2,C1,C2,C3,Z2,Z3,Z4,W)
XK32=XK32+A(I)*(X3+X4)*SIN(2.*W*D)/DEN(I)/(W1-W2)
1 CONTINUE
RETURN
END

```

C
C
C

```

SUBROUTINE XKER33(T,X,A,XI,EXPWP,EXPWM,EXPNWP,EXPNWM,DEN,N,C,XK33,
W1,W2,C1,C2,C3)
IMPLICIT REAL*8 (A-H,O-Z)
DIMENSION A(1),XT(1),EXPWM(1),EXPNWP(1),EXPNWM(1),DEN(1)
XK33=GENC(T,X,W1,W2,C1,C2,C3)-G7(2.*D,T,X,W1,W2)/(W1-W2)
X1=G8(2.*D,T,X,W1,W2,C1,C2,C3)
X2=G8(2.*D,1.-T,1.-X,W1,W2,C1,C2,C3)
XK33=XK33-(X1-X2)/(W1-W2)
DO 1 I=1,N
W=XI(I)
Z2=EXPWM(I)
Z3=EXPNWP(I)
Z4=EXPNWM(I)
X3=GS(I,X,W1,W2,C1,C2,C3,Z2,Z3,Z4,W)
X4=GS(1.-T,1.-X,W1,W2,C1,C2,C3,Z2,Z3,Z4,W)
XK33=XK33+2.*A(I)*(X3-X4)*CIN(W*D)**2/DEN(I)/(W1-W2)
1 CONTINUE

```

RETURN
END

SUBROUTINE GELG(Q,A,M,N,EPS,IER)

IMPLICIT REAL*8 (A-H,O-Z)
DIMENSION A(1),R(1)
IF(M)23,23,1

1 SEARCH FOR GREAT_EST ELEMENT IN MATRIX A

IER=0

PIV=0.

MM=M*M

NN=N*N

DO 3 L=1,MM

IR=ABS(A(L))

IF(IR-PIV)3,3,2

2 PIV=IR

I=L

3 CONTINUE

TOL=EPS*PIV

A(I) IS PIVOT ELEMENT. PIV CONTAINS THE ABSOLUTE VALUE OF A(I).

START ELIMINATION LOOP

LST=1

DO 17 K=1,N

TEST ON SINGULARITY

IF(PIV)23,23,4

4 IF(IER)7,5,7

5 IF(PIV-TOL)6,6,7

6 IER=K-1

7 PIVI=1./A(I)

J=(I-1)/M

I=I-J*M-K

J=J+1-K

I+K IS ROW-INDEX, J+K COLUMN-INDEX OF PIVOT ELEMENT

PIVOT ROW REDUCTION AND ROW INTERCHANGE IN RIGHT HAND SIDE R

DO 8 L=K,MM,M

LL=L+I

TR=PIVI*A(LL)

R(LL)=R(L)

8 R(L)=TR

IS ELIMINATION TERMINATED

IF(K=N)9,18,18

COLUMN INTERCHANGE IN MATRIX A

9 LEND=LST+M-K

IF(J)12,12,10

10 II=J*M

DO 11 L=LST,LEND

IR=A(L)

LL=L+II

A(L)=A(LL)

11 A(LL)=IR

ROW INTERCHANGE AND PIVOT ROW REDUCTION IN MATRIX A

12 DO 13 L=LST,MM,M

LL=L+I

TR=PIVI*A(LL)

A(LL)=A(L)

13 A(L)=TR

SAVE COLUMN INTERCHANGE INFORMATION

A(LST)=J

ELEMENT REDUCTION AND NEXT PIVOT SEARCH

PIV=0.

LST=LST+1

J=0

DO 16 II=LST,LEND

PIVI=-A(II)

```

IST=I+M
J=J+1
DO 15 L=IST,MM,M
LL=L-J
A(L)=A(L)+PIV1*A(LL)
TH=ABS(A(L))
IF (TH-PIV) 15,15,14
14 PIV=TH
I=L
15 CONTINUE
DO 16 L=K,MM,M
LL=L+J
16 R(LL)=R(LL)+PIV1*R(L)
17 LST=LST+M
END OF ELIMINATION LOOP

```

C
C
C

```

BACK SUBSTITUTION AND BACK INTERCHANGE
18 IF (M-1) 23,22,19
19 IST=MM+M
LST=M+1
DO 21 I=2,M
II=LST-I
IST=IST-LST
L=IST-M
L=A(L)+.5
DO 21 J=II,MM,M
TH=R(J)
LL=J
DO 20 K=IST,MM,M
LL=LL+1
20 TH=TH-A(K)*R(LL)
K=J+L
R(J)=R(K)
21 R(K)=TH
22 RETURN

```

C
C
C

```

ERROR RETURN
23 IER=-1
RETURN
END

```

REFERENCES

1. Bilby, B.A. and Eshelby, J.D., Fracture (ed. Liebowitz, M.), Academic Press, New York, vol.1, p.100, 1968.
2. Koiter, W.T., "On the Flexural rigidity of a Beam Weakened by Transverse Sawcuts", Proc. Roy. Neth. Akad. of Sci., B59, p.354, 1956.
3. Koiter, W.T., "Rectangular Tensile Sheet with Symmetric Edge Cracks", J. of Applied Mechanics, Vol.32, p.237, 1965.
4. Isida, M., "Stress Intensity Factors for the Tension of an Eccentrically Cracked Strip", J. of Applied Mechanics, Vol.33, p.674, 1966.
5. Sneddon, I.N. and Tweed, J., "The Stress Intensity Factor for a Griffith Crack in an Elastic Body in which Body Forces are Acting", Int. J. of Frac. Mech., Vol.3, No.4, pp.317-331, 1967.
6. Sneddon, I.N., Das, S.C., "The Stress Intensity Factor at the Tip of an Edge Crack in an Elastic Half Plane", Int. J. Engng. Sci., Vol.9, pp.25-36, 1971.
7. Sneddon, I.N. and Srivastav, R.P., "The Stress Field in the vicinity of a Griffith Crack in a Strip of Finite Width", Int. J. Engng. Sci., Vol.9, p.479, 1971.
8. Hilton, P.D. and Sih, G.C., "A Laminate Composite with a Crack Normal to the Interfaces", Int. J. of Solids and Str., Vol.7, p.913, 1971.
9. Bogy, D.B., "The Plane Elastostatic Solution for a symmetrically Loaded Crack in a Strip Composite", Int. J. Engng. Sci., vol.11, p.985, 1973.
10. Ejike, U.B.C.O., "Edge Crack in a Strip of an Elastic Solid", Int. J. Engng. Sci., Vol.11, p.109, 1973.
11. Gupta, G.D. and Erdoğan, F., "The Problem of Edge Cracks in an Infinite Strip", J. of Applied Mechanics, vol.41, p.1001, 1974.
12. Erdoğan, F. and Arın, K., "A Half Plane and a strip with an Arbitrarily Located Crack", Lehigh University, Report IFSM-73-39, 1974.
13. Erdoğan, F. and Aksoğan, U., "Bonded Half Planes containing an Arbitrarily Oriented Crack", Int. J. Solids and Str., vol.10, p.569, 1974.

14. Krenk, S., "On the Elastic Strip with an Internal Crack", Int. J. Solids and Str., Vol. 11, p. 693, 1975.
15. Civelek, M. B., "Simetrik Tekil Kuvvetlerle Yüklü Sonsuz Şeritte Çatlak Problemi", Doçentlik Tezi, Boğaziçi Üniversitesi, Mart 1978.
16. Delale, F. and Erdoğan, F., "Fracture of Composite Orthotropic Plates Containing Periodic Buffer Strips", Technical Report, NASA Grant NGR 39-007-011, Jan. 1976.
17. Delale, F. and Erdoğan, F., "The Problem of Internal And Edge Cracks in an Orthotropic Strip", J. of Applied Mechanics, Vol. 44, p. 237, 1977.
18. Kaya, A. C. and Erdoğan, F., "Stress Intensity Factors in an orthotropic Strip under General Loading conditions", Technical Report, NASA Grant NGR 39-007-011, June 1978.
19. Ang, D. D. and Williams, M. L., "Combined Stresses in an orthotropic Plate having a Finite crack", J. of Applied Mechanics, vol. 28, p. 372, 1962.
20. Savin, G. N., Stress Concentration Around Holes, Pergamon Press, New York, 1961.
21. Sih, G. C., Paris, P. C. and Irwin G. R., "On Cracks in Rectilinearly anisotropic Bodies", Int. J. Frac. Mech., vol. 1, p. 189, 1965.
22. Krenk, S., "Stress Distribution in an infinite anisotropic Plate with collinear cracks", Int. J. Solids and Str., vol. 11, p. 449, 1975.
23. Delale, F., Bakırtaş, İ. and Erdoğan, F., "The problem of an inclined crack in an Orthotropic strip", Technical Report, NASA Grant NGR 39-007-011, April 1978.
24. Krenk, S., "On the Elastic Constants of Plane Orthotropic Elasticity", J. Compos. Mat., vol. 13, p. 108, 1979.
25. Civelek, M. B. and Erdoğan, F., "Crack Problems for a Rectangular Plate and an Infinite Strip", Technical Report, NASA Grant NGR 39-007-011, July 1980.
26. Ioakimidis, N. I., "Some Remarks on the Numerical Solution of Cauchy Type Singular Integral Equations with Index Equal to -1", Int. J. Solids and Str., Vol 14, pp. 403-407, 1981.
27. Tupholme, G. E., "A Study of Cracks in Orthotropic Crystals using Dislocation Layers", J. Engng. Math., Vol. 8, p. 57, 1974.

28. Zener, C., Fracturing of Metals, Cleveland Symposium, A.S.M., 1948.
29. Friedel, J., Dislocations, Pergamon Press, Oxford, 1964.
30. Eshelby, J.D., Read, W.T. and Shockley, W., "Anisotropic Elasticity with Applications to Dislocation Theory", Acta Met., vol.1, pp.251-259, 1953.
31. Stroh, A.N., "Dislocations and Cracks in Anisotropic Elasticity", Phil.Mag., vol.3, pp.625-646, 1958.
32. Mandell, J.F., McGarry, F.J., Wang, S.S. and Im, J., "Stress Intensity Factors for anisotropic Fracture Test Specimens of Several Geometries", J.Compos.Mat., Vol.8, p.106, April 1974.
33. Civelek, M.B., Private Communication, Boğaziçi University, Civil Engineering Dept., 1983.